

نموذج رقم (1)

إقرار

أنا الموقع أدناه مقدم الرسالة التي تحمل العنوان:

تصميم جهاز انفيرتر عالي الاداء باستخدام انظمة التحكم الضبابي لتقليل الشوائب

Designing Power Inverter with Minimum Harmonic

Distortion Using Fuzzy Logic Control

أقر بأن ما اشتملت عليه هذه الرسالة إنما هو نتاج جهدي الخاص، باستثناء ما تمت الإشارة إليه حيثما ورد، وإن هذه الرسالة ككل أو أي جزء منها لم يقدم من قبل لنيل درجة أو لقب علمي أو بحثي لدى أي مؤسسة تعليمية أو بحثية أخرى.

#### DECLARATION

The work provided in this thesis, unless otherwise referenced, is the researcher's own work, and has not been submitted elsewhere for any other degree or qualification

Student's name:

اسم الطالب: فاروق يوسف شرف

Signature:

التوقيع: 

Date:

التاريخ: 2014 / 03 / 24

The Islamic University of Gaza  
Research and Graduate Affairs  
Faculty of Engineering  
Electrical Engineering Department



الجامعة الإسلامية - غزة  
شؤون البحث العلمي و الدراسات العليا  
كلية الهندسة  
قسم الهندسة الكهربائية

## Designing Power Inverter with Minimum Harmonic Distortion Using Fuzzy Logic Control

By  
**Farok Y. Sharaf**

**Supervisor**  
**Prof. Dr. Mohammed Hussein**

This thesis is submitted in Partial Fulfillment of the  
Requirements for the Degree of Master of Science in  
Electrical Engineering

2014 م - 1435 هـ

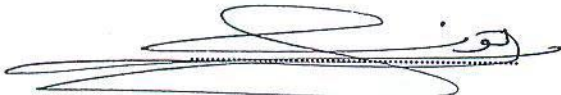




## نتيجة الحكم على أطروحة ماجستير

بناءً على موافقة شئون البحث العلمي والدراسات العليا بالجامعة الإسلامية بغزة على تشكيل لجنة الحكم على أطروحة الباحث/ فاروق يوسف رباح شرف لنيل درجة الماجستير في كلية الهندسة قسم الهندسة الكهربائية - أنظمة التحكم وموضوعها:

تصميم جهاز انفيرتر عالي الأداء باستخدام أنظمة التحكم الضبابي لتقليل الشوائب  
Designing Power Inverter with Minimum Harmonic Distortion Using  
Fuzzy Logic Control

وبعد المناقشة العلنية التي تمت اليوم الأحد 15 جمادى الأولى 1435هـ، الموافق 2014/03/16م الساعة الواحدة والنصف ظهراً بمبنى طيبة، اجتمعت لجنة الحكم على الأطروحة والمكونة من:

	مشرفاً ورئيساً	أ.د. محمد توفيق حسين
	مناقشاً داخلياً	د. حاتم علي العايدي
	مناقشاً خارجياً	د. أنور محمد موسى

وبعد المداولة أوصت اللجنة بمنح الباحث درجة الماجستير في كلية الهندسة / قسم الهندسة الكهربائية -

أنظمة التحكم.

واللجنة إذ تمنحه هذه الدرجة فإنها توصيه بتقوى الله ولزوم طاعته وأن يسخر علمه في خدمة دينه ووطنه.

والله ولي التوفيق،،،

مساعد نائب الرئيس للبحث العلمي والدراسات العليا

٢٠١٤  
أ.د. فؤاد علي العاجز  


## إقرار

أنا الموقع أدناه مقدم الرسالة التي تحمل العنوان:

تصميم جهاز انفيرتر عالي الاداء باستخدام انظمة التحكم الضبابي لتقليل الشوائب .  
أقر بأن ما اشتملت عليه هذه الرسالة إنما هي نتاج جهدي الخاص، باستثناء ما تمت الإشارة إليه حيثما ورد، وإن هذه الرسالة ككل، أو أي جزء منها لم يقدم من قبل لنيل درجة أو لقب علمي أو بحثي لدى أية مؤسسة تعليمية أو بحثية أخرى.

## DECLARATION

The work provided in this thesis, unless otherwise referenced, is the researcher's own work, and has not been submitted elsewhere for any other degree or qualification.

Student's name:

اسم الطالب:

Signature:

التوقيع:

Date:

التاريخ:

صفحة نتيجة الحكم على البحث (نتيجة الحكم من قبل لجنة المناقشة)

## **DEDICATION**

*I would like to dedicate the outcomes of this research thesis to my beloved father and mother. There is no doubt in my mind that without their continued support and counsel I could not have completed this process. I also dedicate this work to all my lovely family members” brothers, sisters, wife, and lovely kids” who have been a constant source of motivation, inspiration, and support.*

## **Acknowledgement**

*I thank Allah, the lord of the worlds, for His mercy and limitless help and guidance. May peace and blessings be upon Mohammed the last of the messengers.*

*I would like to express my deep appreciation to my advisor Prof. Dr. Mohammed Hussein for providing advice, support and excellent guidance.*

*Special thanks go Dr. Hatem A. Elaydi and Dr. Anwar Mousa-thesis examiners- for their patience, guidance, and generous support during this research.*

*My thanks go to Islamic University for their help and support, not only during this research but also during the entire period of my Master study.*

*Special thanks go to the faculty of engineering staff at all levels and positions for their help and assistance that they provided me during my study.*

*My deep thanks go to my wife for her support and encouragement.*

*Words will not be enough to thank my Father and mother for their patience and encouragement during my thesis.*

*Finally, thanks for everyone who has raised his hands and prayed ALLAH for my success.*

## *Abstract*

In recent years, there has been a rapidly growing demand for high quality power inverter. The inverter performs the opposite function of a rectifier, where it is a high-power electronic oscillator, which converts DC to AC in different shapes.

In light of this fact, this thesis will present the analysis and design of fuzzy logic control (FLC) of a single-phase voltage source inverter with the utilization of an L-C filter and voltage sensor. It also presents a comparative study between classical PI (proportional integral) controller and the fuzzy logic controller implemented by Matlab simulation. The research simulation results show that the proposed FLC can reduce the total harmonic distortion (THD) under linear loading condition.

Hardware design experiment is presented for a 1kVA, 50Hz power inverter under various loading conditions to demonstrate and validate the proposed research study.

## **ملخص**

في السنوات الأخيرة، كان هناك طلب متزايد على اجهزة الانفيرتر عالية الاداء. الذي يؤدي وظيفة تحويل التيار الثابت من مصادر ثابتة وغيرها كالبطاريات الى تيار متردد بشكل معين بحيث يتناسب مع اجهزة المنازل والمصانع .

في ضوء هذا الواقع، فإن هذه الرسالة سوف تعمل على تصميم جهاز الانفيرتر ونستخدم نوع جديد من انظمة التحكم وهي انظمة التحكم الضبابية حيث يعمل هذا المتحكم على معايرة الفولتية الخارجة من هذا الجهاز بحيث تكون مناسبة للأحمال وايضا سوف نتناول تصميم الفلتر المناسب لهذا الجهاز . هذه الدراسة سوف تستخدم مقارنة بين انظمة التحكم الكلاسيكية وانظمة التحكم الضبابية حيث ان هذه المقارنة سوف تكون مبنية على مقارنة التشوه في الاشارة الخارجة من الانفيرتر تحت احمال خطية . سوف يتم تطبيق هذا المشروع عمليا وذلك بتصميم جهاز بقدرة 1000 واط بتردد 50 هيرتز .



## TABLE OF CONTENT

<b>CHAPTER 1: INTRODUCTION.....</b>	<b>1</b>
1.1 Genral Introduction .....	1
1.2 Previous Study .....	3
1.3 Statement Of The Problem.....	5
1.4 Research Objective And Methodology.....	6
1.4.1 Research Methodology .....	6
1.4.2 Research Contribution .....	7
1.5 Thesis Organization.....	7
<b>CHAPTER 2: BACKGROUND &amp; BASIC CONCEPTS.....</b>	<b>9</b>
2.1 Introduction .....	9
2.2 Type Of Inverter Output.....	10
2.2.1 Square Wave Inverter.....	10
2.2.2 Modified Sine Wave Inverter.....	11
2.2.3 Pure Sine Wave Inverter .....	11
2.3 Voltage Source & Current Source Inverter .....	12
2.3.1 Voltage Source Inverter.....	12
2.3.2 Current Source Inverter.....	12
2.4 Single Phase Half Bridge & Full Bridge VSI Inverter .....	13
2.4.1 Single Phase Half Bridge Inverter.....	13
2.4.2 Single Phase Full Bridge Inverter.....	14
2.5 Pulse Width Modulation (PWM).....	15
2.5.1 Single PWM .....	15
2.5.2 Multiple PWM.....	17
2.5.3 Sinusoidal PWM (SPWM).....	18
2.5.4 Fuzzy Sinusoidal PWM .....	19
2.6 Harmonics .....	19
2.6.1 History Of Harmonics .....	19

2.6.2 Source Of Harmonics.....	20
2.6.3 Effects Of Harmonic Distortions In Power System.....	20
2.6.4 Harmonic Distortion Of Inverter.....	21
<b>CHAPTER 3: FUZZY LOGIC CONTROL.....</b>	<b>24</b>
3.1 History OF Fuzzy Logic .....	24
3.2 Introduction.....	25
3.3 Classical Sets Versus Fuzzy Sets.....	26
3.4 Fuzzy Set Operations.....	27
3.5 Fuzzy Logic Control Component.....	29
3.5.1 Fuzzification component.....	30
3.5.2 Fuzzy processing components (Mamdani method)....	32
3.5.3 Defuzzification.....	35
3.6 Advantages And Disadvantages Of Mamdani Method.....	37
<b>CHAPTER 4: CONTROLLER DESIGN &amp; SIMULATION RESULT.....</b>	<b>38</b>
4.1 Introduction.....	38
4.2 System Description For Single Phase DC-AC PWM Inverter.....	39
4.3 Component Selection.....	40
4.4 Filter Design.....	41
4.5 The Mathematical Model For Single Phase Inverter.....	42
4.6 Designing Controller.....	44
4.6.1 Designing PI Controller.....	45
4.6.2 Selection of PI Controller Parameter.....	46
4.6.3 Closed loop Control Design.....	46
4.7 Design Of Fuzzy Logic Controller.....	48
4.8 Simulation Result.....	51
4.8.1 PI Controller Simulink.....	51
4.8.2 Fuzzy Controller Simulink.....	53

<b>CHAPTER 5: HARDWARE IMPLEMENTATION FOR PROPOSED SYSTEM.....</b>	<b>57</b>
5.1 Introduction .....	57
5.2 Push Pull Converter.....	57
5.3 SPWM Generators.....	59
5.3.1 Bubba Oscillator .....	59
5.3.2 Carrier Wave Generator.....	60
5.3.3 The Comparator Circuit.....	61
5.4 H-Bridge And Driver Circuit .....	63
5.5 Design Fuzzy Controller.....	64
5.5.1 How To Build Program In Microcontroller.....	65
5.5.2 The Operation of Fuzzy Controller.....	66
5.6 Actual Hardware Implementation.....	67
5.7 Hardware Result.....	71
 <b>CHAPTER 6: CONCLUSIONS AND FUTURE WORKS .....</b>	 <b>73</b>
 <b>REFERENCES.....</b>	 <b>75</b>
<b>VITA.....</b>	<b>77</b>
<b>APPENDICES.....</b>	<b>78</b>

## LIST OF FIGURE

Figure 1.1: Square, Modified, and Pure Sine Wave.....	2
Figure 1.2: The block diagram for power inverter with FLC.....	6
Figure 2.1: square wave signal.....	10
Figure 2.2: Modified sine wave.....	11
Figure 2.3: Pure sine wave.....	12
Figure 2.4: Single phase half bridge inverter.....	13
Figure 2.5: Single phase full bridge inverter.....	14
Figure 2.6: Output voltage of single phase width modulation.....	16
Figure 2.7: Multiple pulse width modulation.....	17
Figure 2.8: Sinusoidal pulse width modulation.....	18
Figure 2.9: Harmonic waves for square wave.....	22
Figure 2.10: Square wave harmonic analysis.....	23
Figure 3.1: Binary logic representation of discrete temperature valve.....	25
Figure 3.2: Cool air temperature range.....	26
Figure 3.3: Complement of fuzzy sets A.....	27
Figure 3.4: Intersection of fuzzy sets A and B.....	28
Figure 3.5: Union of fuzzy sets A and B.....	28
Figure 3.6: Fuzzy logic controller operation.....	29
Figure 3.7: Membership function chart.....	30
Figure 3.8: Membership function shapes.....	31
Figure 3.9: Fuzzy logic input seven membership function labels.....	32
Figure 3.10: Fuzzification stage.....	33
Figure 3.11: Rule evaluation in Mamdani method.....	34
Figure 3.12: Fuzzy outcome evaluations.....	35
Figure 3.13: COG approach in defuzzification stage.....	36
Figure 4.1: Single phase full bridge inverter.....	39

Figure 4.2: Unipolar PWM scheme.....	40
Figure 4.3: Inductor ripple current.....	41
Figure 4.4: Schematic diagram for inverter with LC filter.....	42
Figure 4.5: Block diagram of the linear model for PWM inverter.....	43
Figure 4.6: Block diagram for the system with controller.....	44
Figure 4.7: An approximate linearized control model.....	46
Figure 4.8: Closed loop design by MATLAB SISO TOOLS.....	47
Figure 4.9: Root locus design for closed loop system.....	47
Figure 4.10: Step response for the system.....	48
Figure 4.11: Schematic diagram for the system with fuzzy controller.....	49
Figure 4.12: Fuzzy membership for input and output.....	49
Figure 4.13: Input output relationship surface.....	50
Figure 4.14: Matlab Simulink for PWM inverter under PI controller.....	51
Figure 4.15: Load voltage and spectrum analyzer for full load PWM inverter under PI controller.....	52
Figure 4.16: Load current and spectrum analyzer for full load PWM inverter.....	53
Figure 4.17: Input and output membership by Matlab fuzzy logic control tool.....	54
Figure 4.18: Matlab simulations for PWM inverter under fuzzy controller.....	54
Figure 4.19: Load voltage and spectrum analyzer for full load PWM inverter under fuzzy logic controller.....	55
Figure 4.20: Load current and spectrum analyzer for full load PWM inverter under fuzzy logic controller.....	56
Figure 5.1: Schematic circuit for push pull converter.....	58
Figure 5.2: Schematic circuit for bubba oscillator.....	59
Figure 5.3: Schematic circuit for triangular generator.....	61
Figure 5.4: Schematic circuits for comparator circuit.....	62

Figure 5.5: The output waves for PWM generator.....	62
Figure 5.6: Typical connections for IR2110 driver.....	63
Figure 5.7: schematic circuit for full bridge inverter with driver.....	64
Figure 5.8: The actual hardware for push pull converter.....	67
Figure 5.9: The AC output signal for the push pull converter.....	68
Figure 5.10: The actual hardware for SPWM generator with FLC.....	68
Figure 5.11: The result output from Bubba oscillator.....	69
Figure 5.12: The result output from triangular generator.....	69
Figure 5.13: The generated pulses for SPWM generator.....	70
Figure 5.14: H-Bridge and driver circuit.....	70
Figure 5.15: SPWM full bridge inverter.....	71
Figure 5.16: The result output signal for full load inverter.....	72

## **LIST OF TABLES**

Table 4.1: Parameters of PWM inverter.....	40
Table 4.2: Fuzzy rules.....	50
Table 5.1: Key features of PIC16F877A.....	65

## **Abbreviations**

A voltage-source inverter	VSI
A current-source inverter	CSI
Fuzzy Logic Control	FLC
Center of Gravity	COG
Sine Pulse Width Modulation	SPWM
Total Harmonic Distortion	THD
Electromagnetic Interference	EMI
Pulse Width Modulation	PWM
Resonant Snubber Inverter	RSI
Single Input Single Output	SISO
Proportional Integral	PI
Printed Circuit Board	PCB
Adjustable Speed Drives	ASD
Uniform Pulse Width Modulation	UPWM





# CHAPTER 1

---

## INTRODUCTION

### 1.1 General Introduction

DC/AC inverters are electronic devices used to produce AC power at a desired output voltage or current and frequency. Inverters are used for many applications, as in situations where low voltage DC sources such as batteries, solar panels or fuel cells must be converted so that devices can run off AC power. One example of such a situation would be converting electrical power from a car battery to run a laptop, TV or cell phone.

Most inverters do their job by performing two methods: the first method is converting the incoming DC into AC, then they step up the resulting AC to main voltage level using a transformer. The second method is converting the low voltage DC power to a high voltage DC source, then convert high DC source to an AC waveform by using H-bridge driver.

The terms voltage-fed and current-fed are used in connection with the output from inverter circuits. A voltage-source inverter (VSI) is one in which the DC input voltage is essentially constant and independent of the load current drawn. The inverter specifies the load voltage while the load dictates the drawn current shape.

A current-source inverter (CSI) is one in which the source input is DC current hence, the output current is constant and the load impedance determines the output voltage.

There are many types of inverters that are different in the output sources such as: square wave, modified sine wave and pure sine wave as shown in figure (1.1) [1]. The square wave output has a high harmonic content, not suitable to AC loads such as motors or transformers; therefore, square wave units are considered as the pioneers of inverter development. A modified square wave

or modified sine wave inverter is similar to a square wave output except that the output goes to zero volts for a time before switching positive or negative. It is simple, low cost and is compatible with most electronic devices.

A pure sine wave inverter produces a nearly perfect sine wave output (less than 5% total harmonic distortion) that is essentially the same as utility-supplied grid power [2]. Thus, it is compatible with all AC electronic devices. The mathematical model used for calculating output voltage of inverter is

$$U(\omega t) = \sum_{n=1}^{\infty} U_h \cdot \sin(n\omega t) \quad 1.1$$

Where,  $\omega = 2\pi f$  ,  $f$  is the frequency in Hz,  $t$  is the continuous time signal  $0 \leq t \leq T$  and  $U_h$  is the amplitude of harmonics.

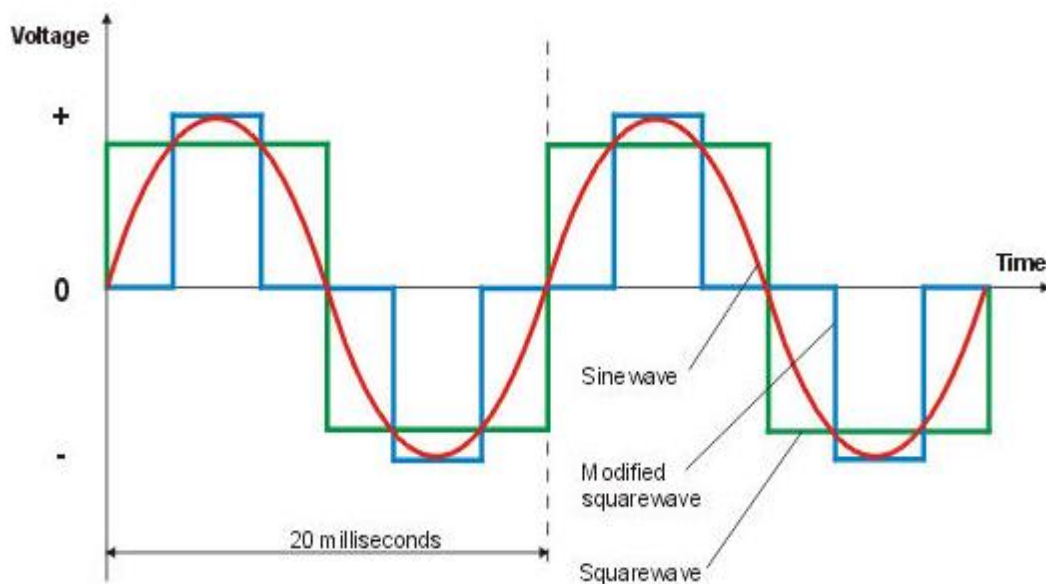


Figure 1.1: Square, Modified, and Pure Sine Wave

Most inverters have classical controllers such as proportional-integral, these controllers are not compatible for some application because the output signal is not pure sine wave.

However the total harmonic distortion influence in the loads causing high power dissipation. Fuzzy logic controllers [3] have become the most popular controller compared with conventional controller, since FLC can work with imprecise inputs, handle nonlinearity and it is more robust.

Actually, power inverters that are used in Gaza strip have high THD so the qualities of inverters are very low. Therefore, the thesis outcomes focus on the performance of an inverter output waveform by proposing the fuzzy logic control as a new strategy of the controller; hence, the new technique is used to keep the output distortion at acceptable level, as the desired output of an inverter must be pure sine wave.

## **1.2 Previous Studies**

**In 2010**, Aleksey Trubitsyn [4] proposed high efficiency DC/AC power converter for photovoltaic application, he presented the development of a micro inverter for single-phase photovoltaic application. A multidimensional control technique was utilize to achieve high efficiency, encompassing frequency control, inverter and cycloconverter by phase shift control.

This work provided modified sine wave so the output have a little harmonic distortions, which it is not compatible with all devices like motors.

**In 2009**, Rickard Ekström [5] presented inverter system design and control for a wave power substation, he investigated the design of the inverter, gate drive, filter, control system and protections for this substation. In addition, extensive market research was done, resulting in decisions of what components to be merchandise.

This work used SPWM without feedback controller; therefore, the output display high drop voltage when a load is applied.

**In 2004**, Keith Jeremy McKenzie [6] proposed eliminating harmonics in a cascaded H-Bridges multilevel inverter using resultant theory, symmetric polynomials, and power sums. This work studied a multilevel converter with assumed equal dc sources. The multilevel fundamental switching scheme was used to control the needed power electronics switches. In addition, a method presented where switching angles computed such that a desired fundamental sinusoidal voltage produced while at the same time certain higher order harmonics are eliminated.

This work used multilevel DC sources to generate sine wave signal so in practical design the cost of this type inverter is very high.

**In 2001**, Robert A. Gannett [7] proposed control strategies for high power four-leg voltages source inverter where it addressed some of the causes of poor power quality and control strategies to ensure a high performance level in inverter fed power systems.

This work used conventional controllers; therefore, the harmonic distortion influence in some devices like fans and sound devices.

**In 1998**, Obasohan I. Omozusi [8] proposed the operation of a single-phase induction generator with a PWM inverter as a source of excitation. The simulation of the single-phase induction generator, and PWM inverter was done using device model. Matlab/Simulink was found to be a great tool in modeling the PWM inverter and the single-phase induction generator.

This work used the inverter only to control in a single-phase induction generator.

**In 1998**, Yuqing Tang [9] proposed high power inverter EMI characterization and improvement using an auxiliary resonant snubber inverter. This work deals with electromagnetic interference where it was identified as high

switching (dv/dt) and (di/dt) rates interacting with inverter parasitic components. The relation between the (dv/dt), ( di/dt ) and the EMI generation were discussed. The EMI sources of a hard-switching single-phase PWM inverter were identified and measured with separation of common-mode and differential-mode noises. The noise reduction in an auxiliary resonant snubber inverter (RSI) was presented.

### 1.3 Statement of the Problem:

The conventional controllers that used for power inverter are inaccurate in some applications; therefore, the motivation was to research into new technologies to address this problems by reducing the distortion harmonics. The proportional-integral controller, PI which is commonly used in power inverter as power output, is not accurate in some applications such as transformer, fans and sound devices where the total harmonic distortion influences the behavior of this devices also may damage this devices for long time. Therefore, this study will focus on this problem by presenting new technique of fuzzy logic controller to improve the performance of the inverter, the system block diagram of the inverter is shown in figure (1.2). Assuming  $V_o$  be the load voltage,  $V_{ref}$  be the desired sinusoidal waveform, and  $V_e = V_o - V_{ref}$  be the voltage error.

Choosing  $x_1 = i_l$ ,  $x_2 = v_o$  the resulting error dynamic state equation can be derived as [5]:

$$\begin{bmatrix} \dot{x}_1 \\ \dot{x}_2 \end{bmatrix} = \overbrace{\begin{bmatrix} 0 & -\frac{1}{L} \\ \frac{1}{C} & -\frac{1}{RC} \end{bmatrix}}^A \cdot \begin{bmatrix} x_1 \\ x_2 \end{bmatrix} + \overbrace{\begin{bmatrix} \frac{V_{dc}}{L} \\ 0 \end{bmatrix}}^B U$$

$$y = [0 \quad 1] \cdot \begin{bmatrix} x_1 \\ x_2 \end{bmatrix} \tag{1.2}$$

Where  $\tilde{x}$  is the state vector,  $u$  is the control input,  $A$  is the system matrix,  $B$  is the control matrix. The control objective is to make the output voltage equals to a reference input.

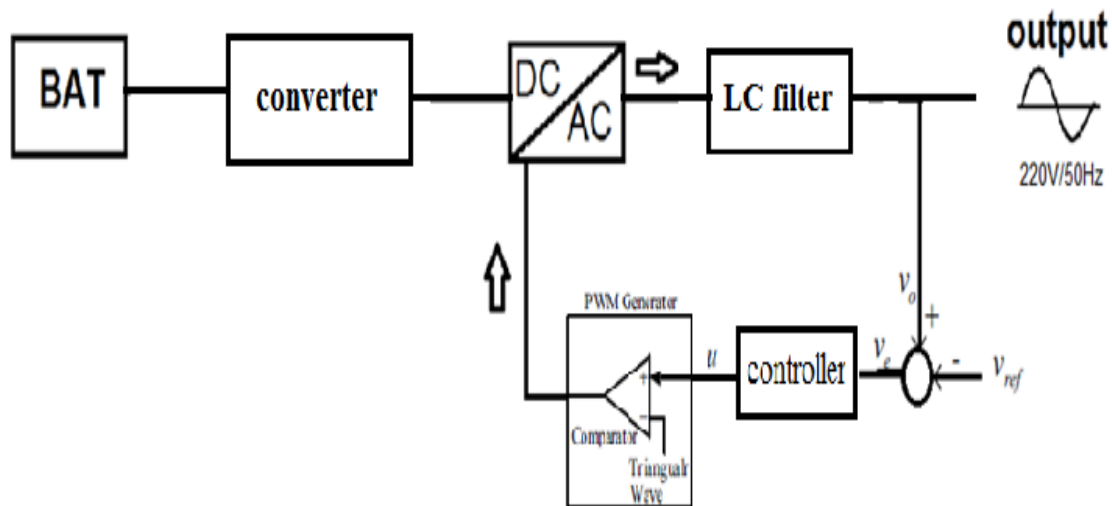


Figure 1.2: The block diagram for power inverter with FLC

## 1.4 Research Objective and Methodology

### 1.4.1 Research Methodology

The research will be implementing as follow

1. Collecting data on the inverters types, application and schematic circuits.
2. Designing PI controller using Matlab SISO Tool for the close loop system.
3. Using Mamdani method to design the proposed fuzzy logic controller with the utilization of Matlab fuzzy tools and identifying the membership functions.

4. Simulating the system using Matlab and studying the behavior of the inverter.
5. Comparing the performance of the PI controller and FL controller and discussing the THD for the inverter system.
6. Analyzing the system and designing the schematic circuit that contained power drivers and control system using Protuse program.
7. Building up the actual hardware inverter circuit.

### **1.4.2 Research Contributions**

It is a well documented of the shortage of electricity in Palestine, especially in the Gaza Strip. The people suffer from power cuts on a daily basis for a period of not less than 8 hours, which leads to the used the small generators including the occurrence of noise and the risk of accidents, particularly in the small apartments, and houses. Thus, the situation leads to high demand for other devices to replace the generators such as power inverter. The current devices of inverter having high THD which causes problems in the loads. This study provides the best and creative solution to this problem by providing a new and safe product for the power inverter specifications to suit the home devices such as lighting, television and fans and does not cause any harm to these devices. This inverter is based on a new fuzzy logic controller design, which regulate the output voltage and reduce the harmonic distortion in the output signal.

### **1.5 Thesis Organization**

The remaining chapters of this thesis are organized as follows: Chapter 2 covers the review and background for some basic principles of inverter systems, type of inverter and harmonic distortion for the output signal. Chapter 3 gives a review and introduction to fuzzy logic and its application,



fuzzy sets operations, the main concepts in fuzzy sets such as membership functions, and linguistic variable. Chapter 4 presents the design of the system by applying comparative study between classical and fuzzy logic controller also the simulation results are presented to show the performance of the proposed control system.

Chapter 5 demonstrates the hardware implementation for the proposed system while Chapter 6 presents the conclusions, recommendation, future works, and final remarks.

## CHAPTER 2

---

# BACKGROUND & BASIC CONCEPTS

## 2.1 Introduction

In this chapter, the basic concept for designing power inverter is proposed to understand the behavior of the system. The design of the inverter system is based on voltage source inverter and the key of generating sine wave signal is obtained by using PWM technique. This technique is used for controlling the power inverter output by changing the modulation index for reference signal. The pulses are obtained by comparing the reference signal with triangular signal or sawtooth signal. The frequency of the reference signal is constant for the inverter where it is 50HZ or 60HZ depending on the loads. The voltage is regulated by controlling the modulation index, so the amplitude of the reference signal is changed from 0 to 1 depending on the load.

Historically, inverters have been made with every kind of switching apparatus, such as rotating or vibrating mechanical contacts, gas-filled electronic valves, and thyristors (SCRs). However, in contemporary use, the field is led by two special kinds of transistor. The first kind is the Metal-Oxide-Semiconductor Field-Effect Transistor (MOSFET). The second type of transistor Gate Bipolar Transistor (IGBT). For inverter system there is two circuits topologies half bridge and full bridge. The half bridge contains two switches and the full bridge inverter consists of four switches. This thesis, presents the circuit that utilizes full bridge inverter with four MOSFET transistor[1].

## 2.2 Type of Inverters Outputs:

Power inverters produce one of the three different types of wave output:

1. Square wave.
2. Modified square wave .
3. Pure sine wave.

The three different wave signals represent three different qualities of power output. Square wave inverters result in uneven power delivery that is not efficient for running most devices.

### 2.2.1 Square Wave

The earliest electronic inverters produced a square wave as shown in figure (2.1), which can be seen as a sine wave sampled twice per cycle. A square wave has a very high harmonic content and a Peak-to-RMS voltage ratio of one. Because electronic loads are usually sensitive to peak voltage while resistive loads such as incandescent lamps respond to the RMS value, the square wave is unsuitable for general use.

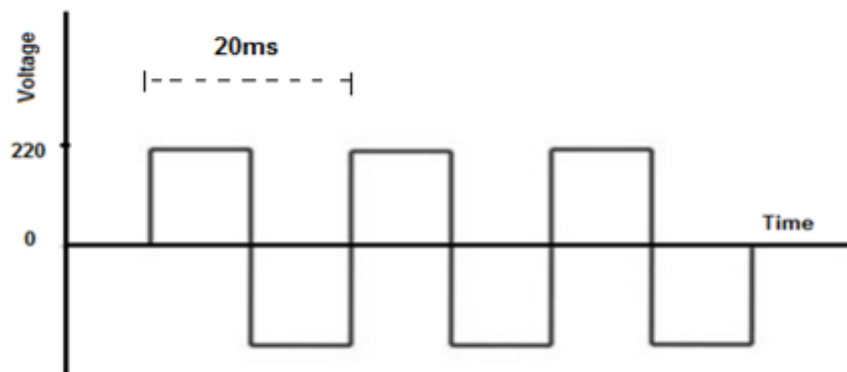


Figure 2.1: Square wave signal

### 2.2.2 Modified square Wave

A modified sine wave inverters approximate a sine wave as shown figure (2.2) has low enough harmonics that do not cause problem with household.

Modified sine wave inverters are designed to satisfy the efficiency requirements of the photovoltaic system while being less expensive than pure

sine waveform inverters; these inverters are capable of operating a wide variety of loads.

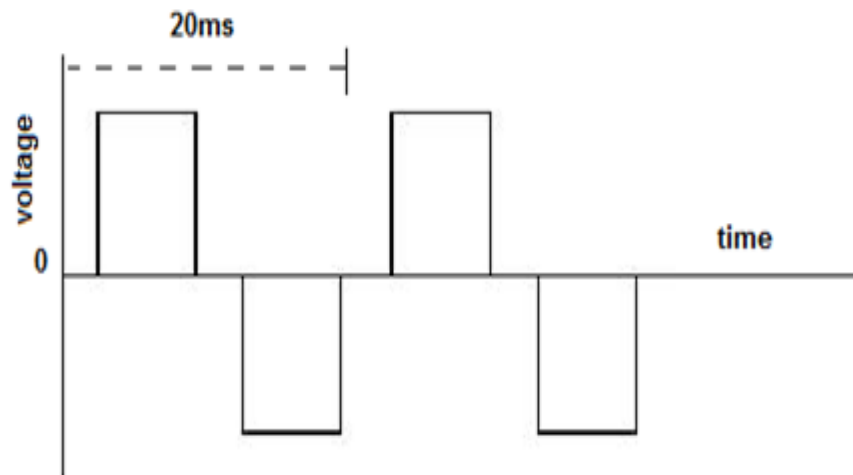


Figure 2.2: Modified sine wave

### 2.2.3 Pure Sine Wave Inverter

For any device that requires sensitive calibration, it is advisable to use a pure sine wave inverter. This type of inverter provides output voltage waveform, which is very similar to the voltage waveform that is received from the grid. The sine wave as shown in figure(2.3) has very little harmonic distortion resulting in a very clean supply and makes it ideal for running electronic systems such as computers, digital fax and other sensitive equipment without causing problems or noise.

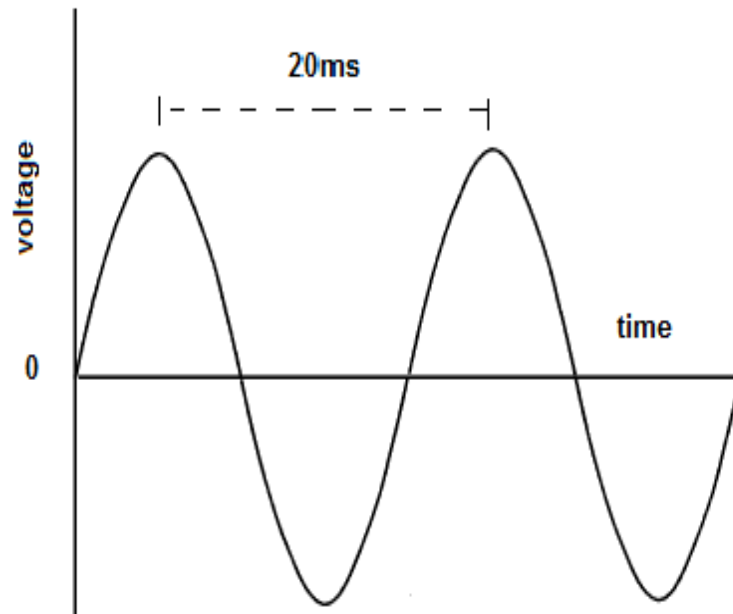


Figure 2.3: Pure sine wave

## **2.3 Voltage Source Inverter and Current Source Inverter**

### **2.3.1 Voltage Source Inverter:**

The type of inverter as independently controlled AC output is considered as the voltage waveform. The output voltage waveform is mostly remaining unaffected by the load. Due to this property, the VSI have many industrial applications such as adjustable speed drives (ASD) and also in power system for FACTS (Flexible AC Transmission).

### **2.3.2 Current Source Inverter:**

The type of inverter where the independently controlled AC output, is considered a current waveform. The output current waveform is mostly remaining unaffected by the load. These are widely used in medium voltage industrial applications, where high quality waveform is required.

## 2.4 Single Phase Half Bridge & Full Bridge VSI:

### 2.4.1 Single Phase Half Bridge Inverter:

It consists of two semiconductor switches T1 and T2 as shown in figure (2.4). These switches may be BJT, IGBT, MOSFET transistor etc. with a commutation circuit. D1 and D2 are called Freewheeling diode also known as the Feedback diodes as they feedback the load reactive power[8].

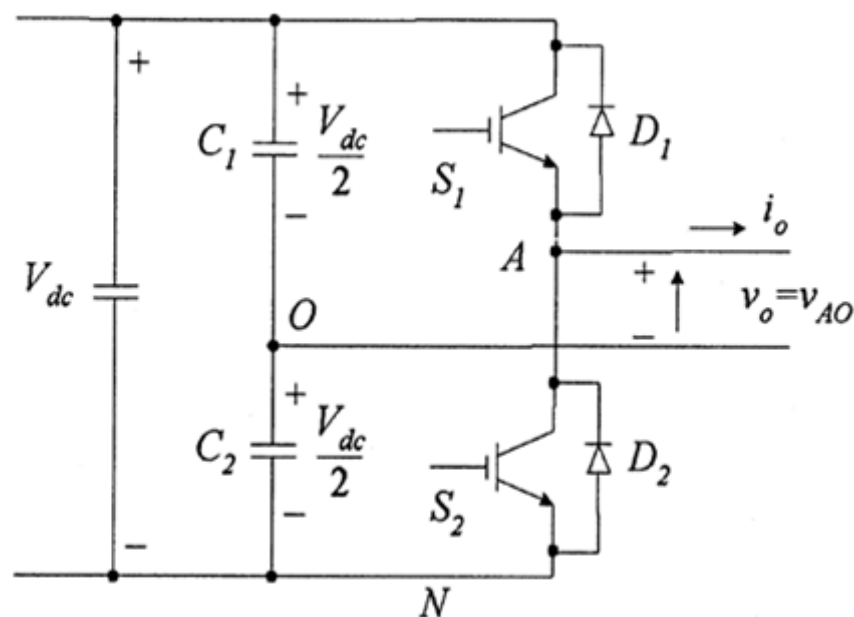


Figure 2.4: Single phase half bridge inverter

S1 is ON during the positive half cycle of the output voltage, which makes  $V_o = V_{dc}/2$  and S2 is ON during the negative half cycle which makes  $V_o = -V_{dc}/2$ . Both switches must operate alternatively otherwise, there may be a chance of short circuiting. In case of resistive load, the current waveform follows the voltage waveform but not in case of reactive load. The feedback diode operates for the reactive load when the voltage and current are of opposite polarities.

### 2.4.2. Single Phase Full Bridge Inverter:

It consists of two arms with a two semiconductor switches on both arms with antiparallel freewheeling diodes for discharging the reverse current as shown in figure (2.5). In case of resistive-inductive load, the reverse load current flow through these diodes. These diodes provide an alternate path to inductive current which continue so flow during the turn OFF condition [8].

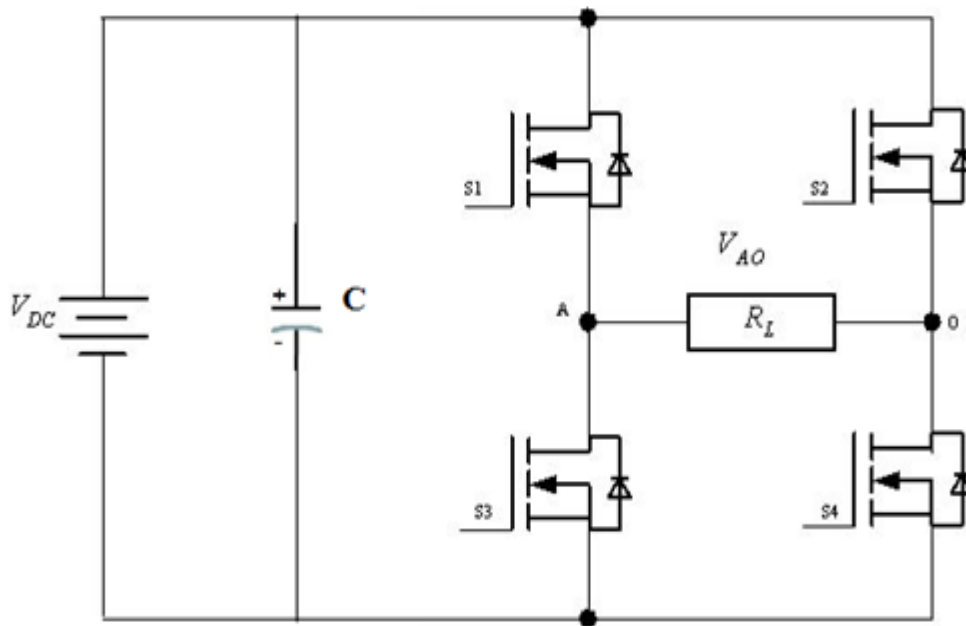


Figure 2.5: Single phase full bridge inverter

The switches are  $S_1$ ,  $S_2$ ,  $S_3$  and  $S_4$ . The switches in each branch operate alternatively so that the never in same mode (ON /OFF) simultaneously. In practice they are both OFF for short period of time called blanking time, to avoid short circuiting. The switches  $S_1$  and  $S_4$  or  $S_2$  and  $S_3$  should operate in pair to get the output. These bridges are switched such that the output voltage is shifted from one to another and hence the change in polarity occurs in voltage waveform. If the shift angle is zero, the output voltage is also zero and maximal when shift angle is  $\Theta$ .

## 2.5 Pulse Width Modulation (PWM)

The most common and popular technique of digital pure-sine wave generation is pulse-width-modulation (PWM). The PWM technique involves generation of a digital waveform, for which the duty-cycle is modulated such that the average voltage of the waveform corresponds to a pure sine wave. The simplest way of producing the PWM signal is through comparison of a low-power reference signal with carrier signal, the reference signal is the desired output signal maybe sinusoidal or square wave, while the carrier signal is either a sawtooth or a triangular wave at a frequency significantly greater than the reference. The advantage of this technique is to minimize the lower order harmonics, while the higher order harmonics can be eliminated using a filter. There are different PWM techniques that essentially differ in the harmonic content of their respective output voltages; thus, the choice of a particular PWM technique depends on the permissible harmonic content in the inverter output voltage[1],[8].

### 2.5.1 Single Pulse Width Modulation:

In single pulse-width modulation control, there is only one pulse per half-cycle and the width of the pulse is varying to control the output voltage. Figure (2.6) shows the generation of the input of single pulse width modulation. The input signals are generated by comparing the rectangular control signal of amplitude  $v_c$  with triangular carrier signal  $v_{car}$ . The frequency of the control signal determines the fundamental frequency of AC output voltage. The *amplitude modulation index* is defined as:

$$ma = \frac{v_c}{v_{car}} \quad 2.1$$



The RMS AC output voltage:

$$v_o = \left( \frac{2}{T} \int_{\left(\frac{T}{4} - \frac{t_{on}}{2}\right)}^{\left(\frac{T}{4} + \frac{t_{on}}{2}\right)} v_s^2 dt \right)^{\frac{1}{2}} = v_s \sqrt{\frac{2 t_{on}}{T}} \quad 2.2$$

or

$$v_o = v_s \sqrt{2\delta} \quad 2.3$$

Where the duty ratio is  $\delta = \frac{t_{on}}{T}$

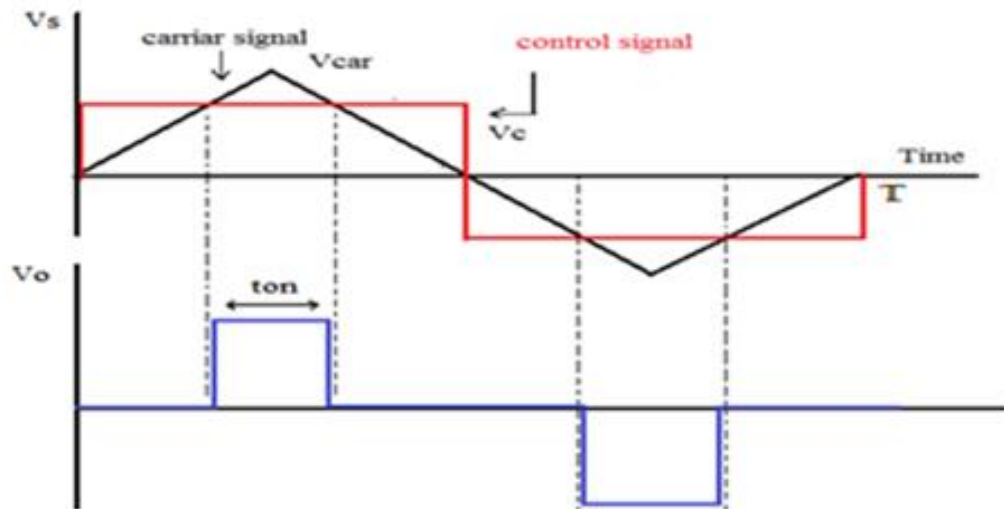


Figure 2.6: Output voltage of single phase width modulation

By varying the control signal amplitude  $v_c$  from 0 to  $v_{car}$ , the pulse width  $t_{on}$  can be modified from 0 sec to  $T/2$  sec and the RMS output voltage  $v_o$  from 0 to  $v_s$ .

## 2.5.2 Multiple Pulse Width Modulation:

The harmonic content can be reduced by using several pulses in each half-cycle of output voltage. The generation of gating signals for turning on and off of transistors is shown in figure (2.7) by comparing a reference signal with a triangular carrier wave[1].

The frequency of reference signal sets the output frequency ( $f_o$ ) and the carrier frequency ( $f_c$ ), determines the number of pulses per half cycle ( $p$ ), the modulation index controls the output voltage. This type of modulation is also known as uniform pulse width modulation UPWM. The number of pulses per half cycle is found from Eq. 2.4:

$$P = \frac{f_c}{2f_o} = \frac{mf}{2} \quad 2.4$$

where,  $mf = f_c/f_o$  is defined as the frequency modulation ratio.

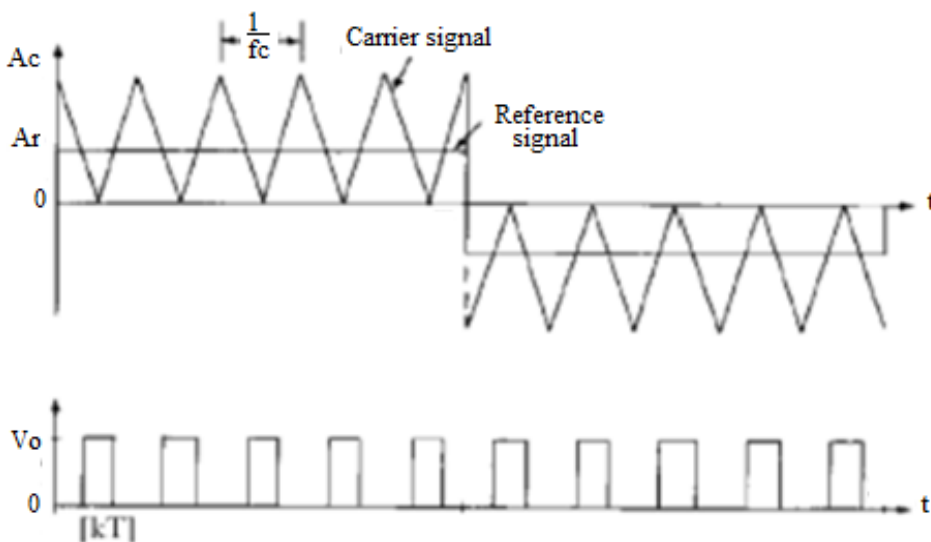


Figure 2.7: Multiple pulse width modulation

The variation of modulation index  $m$  from 0 to 1 varies the pulse width,  $Kt$ , from 0 to  $T/p$  and the output voltage from 0 to  $v_s$ , the RMS output voltage can be found from Eq. 2.5:

$$v_o = \sqrt{\frac{2p}{T} \int_{\frac{1}{2}(\frac{T}{2p}-\delta)}^{\frac{1}{2}(\frac{T}{2p}+\delta)} v_s^2 dt} = v_s \sqrt{\frac{2p\delta}{T}} \quad 2.5$$

### 2.5.3 Sinusoidal Pulse Width Modulation:

Instead of maintaining the width of all pulses the same as in the case of multiple-pulse modulation, the width of each pulse is varied in proportion to the amplitude of a sine wave evaluated at the center of the same pulse [10]. The distortion factor and lower-order harmonics are reduced significantly. The generation of gating signals for turning on and off of transistors is shown in figure(2.8) by comparing a sinusoidal reference signal with a triangular carrier wave of frequency( $f_c$ ).

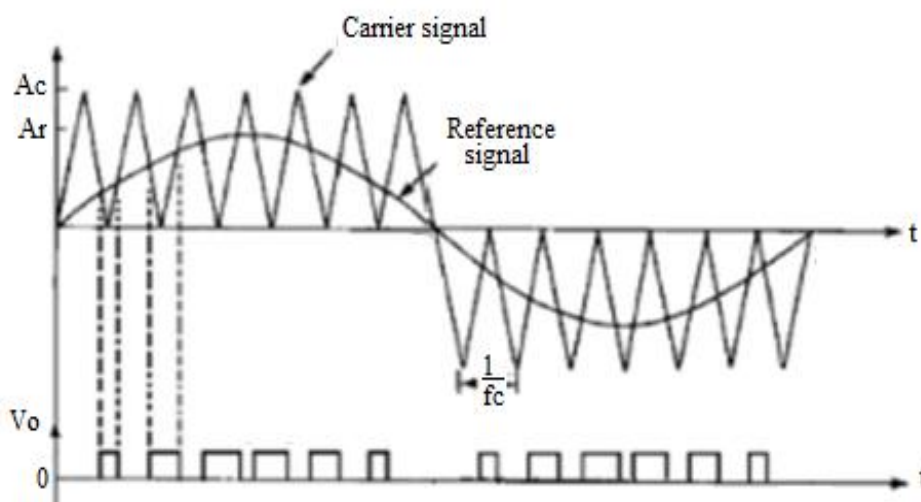


Figure 2.8: Sinusoidal pulse width modulation

The control signal is shown at the same figure this type of modulation is commonly used in industrial applications and abbreviated as SPWM. The frequency of reference signal ( $f_r$ ) determines the output frequency ( $f_o$ ) and its peak amplitude ( $A_r$ ) controls the modulation index  $m$  the number of pulses per half-cycle depends on the carrier frequency. The output voltage can be varied by varying the modulation index  $m$  the RMS output voltage can be found from Eq. 2.6:

$$v_o = v_s \sqrt{\sum_1^p \frac{2\delta_m}{T}}$$

#### **2.5.4 Fuzzy Sinusoidal Pulse Width Modulation:**

A lot of control strategies for regulation of PWM inverters in power supplies have been developed. Therefore a new approach for combining a fuzzy logic controller with sinusoidal pulse-width modulator is proposed to reduce the harmonic distortion and the output signal become pure sine wave, this type will be explain in chapter four.

## **2.6 Harmonic**

### **2.6.1 Harmonic History**

Before twentieth century, the predominant use of electricity for business and industry was power motors, lights and heating devices. These uses have little effect on the fundamental frequency. They called linear loads, because the current rises and falls in proportion to the voltage wave. In recent years, few industries use devices such as rectifiers or converters, power supplies and other device to improve product quality [11]. All of these make the current sinusoidal waveform distorted, because the current flow was not directly proportional to the voltage. These loads are called non-linear loads. which

cause waveforms that are multiples of the fundamental frequency of sine wave to be superimposed on the base waveform, these multiples are called harmonics, as the frequency of the second harmonic which it is two times the fundamental frequency, the third harmonic is three times the fundamental frequency. The combination of the sine wave with all the harmonics creates a new non sinusoidal wave of entirely different shape is called harmonic distortion.

### **2.6.2 Source of Harmonic**

The main source of the harmonics is any non-linear loads that produce the voltage harmonics and current harmonics. This occurs because the resistance of the device is not a constant. The resistance in fact, changes during each sine wave. So, nonlinear device is one in which the current is not proportional to the applied voltage.

### **2.6.3 Effects of Harmonic Distortion in Power Systems**

The effect of current distortion on power distribution systems can be serious, primarily because of the increased current flowing in the system. In other words, because the harmonic current doesn't deliver any power, its presence simply uses up system capacity and reduces the number of loads that can be powered. Harmonic current occur in a facility's electrical system can cause equipment malfunction, data distortion, transformer and motor insulation failure, tripping of circuit breakers, and solid-state component breakdown also, it is increase heat losses in transformers and wiring. Since the transformer impedance is depend on the harmonic order for the frequency, for example the impedance at the 5th harmonic is five times that of the fundamental frequency. So each ampere of 5th harmonic current causes five times as much heating as an ampere of fundamental current. More

specifically, the effects of the harmonics can be observed in many sections of electrical equipment and a lot machines and motors.

#### **2.6.4 Harmonic Distortion of Inverter:**

The switch in the simple inverter described above, when not coupled to an output transformer, produces a square voltage waveform due to its simple off and on nature as opposed to the sinusoidal waveform that is the usual waveform of an AC power supply. Using Fourier analysis, periodic waveforms are represented as the sum of an infinite series of sine waves. The sine wave that has the same frequency as the original waveform is called the fundamental component. The other sine waves, called *harmonics*, that are included in the series have frequencies that are integral multiples of the fundamental frequency. Fourier analysis can be used to calculate the total harmonic distortion (THD), which it is the square root of the sum of the squares of the harmonic voltages divided by the fundamental voltage.

$$\text{THD} = \frac{\sqrt{V_2^2 + V_3^2 + V_4^2 + \cdots + V_n^2}}{V_1} \quad 2.7$$

#### **2.6.5 Harmonic in Square Wave:**

square wave is a non-sinusoidal periodic waveform which can be represented as an infinite summation of sinusoidal waves as shown in figure (2.9), in which the amplitude alternates at a steady frequency between fixed minimum and maximum values, with the same duration at minimum and maximum the transition between minimum to maximum is instantaneous for an ideal square wave.

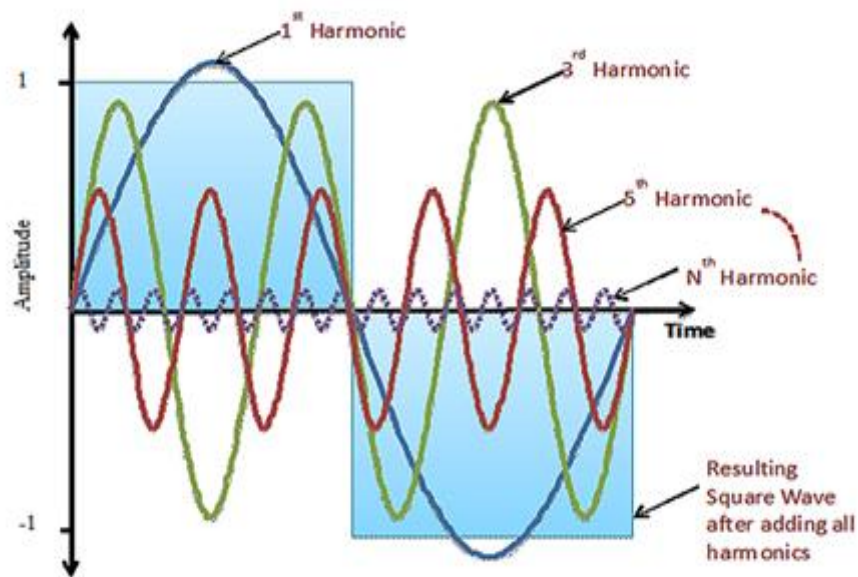


Figure 2.9: Harmonic waves for square wave

- **Examining the harmonic for square wave**

Using Fourier expansion with cycle frequency  $f$  over time  $t$ , we can represent an ideal square wave with a peak to peak amplitude of 2 as an infinite series of the form:

$$\begin{aligned}
 x_{\text{square}}(t) &= \frac{4}{\pi} \sum_{k=1}^{\infty} \frac{\sin(2\pi(2k-1)ft)}{(2k-1)} \\
 &= \frac{4}{\pi} \left( \sin(2\pi ft) + \frac{1}{3} \sin(6\pi ft) + \frac{1}{5} \sin(10\pi ft) + \dots \right)
 \end{aligned} \tag{2.8}$$

The FFT for square wave is shown in figure (2.10) implies that the lowest frequency is called the fundamental frequency and multiples of it are called

harmonics, also we can compute the THD by Eq.2.8 and we note that the THD is equal 43.8%. Actually, these types of signal ave large harmonic distortion.

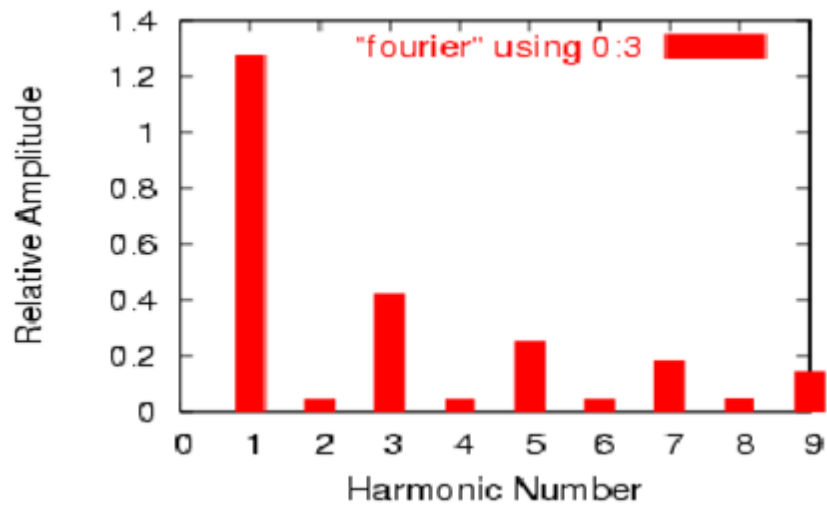


Figure 2.10: Square wave harmonic analysis



## CHAPTER 3

---

### FUZZY LOGIC CONTROL

#### 3.1 History Of Fuzzy Logic

In early 1960s, Lotfi A. Zadeh, a professor at University of California at Berkley well respected for his contributions to the development of system theories, began to feel that traditional systems analysis techniques were too precise for many complex real-world problems. The idea of grade of membership, which is the concept that became the backbone of fuzzy set theory, occurred to him in 1964 [12] , which lead to the publication of his seminal paper on fuzzy sets in 1965 and the birth of fuzzy logic technology [13]. In 1974, S. Assilian and E. H. Mamdani in United Kingdom developed the first fuzzy logic controller, which was for controlling a steam generator [14]. In the 1980's, several important industrial applications of fuzzy logic was launched successfully in Japan. After eight years of persistent research, development, and deployment efforts, Yasunobu and his colleagues at Hitachi put a fuzzy logic-based automatic train operation control system into operation in Sendai city's subway system in 1987 [15]. Another early successful industrial application of fuzzy logic is a water-treatment system developed by Fuji Electric. These and other applications motivated many Japanese engineers to investigate a wide range of novel fuzzy logic applications. This lead to the fuzzy boom. The fuzzy boom in Japan was a result of close collaboration and technology transfer between universities and industries.

## 3.2 Introduction

Fuzzy logic is a branch of artificial intelligence that deals with reasoning algorithms used to emulate human thinking and decision making in machines. These algorithms are used in applications where process data cannot be represented in binary form. For example, the statements “the air feels cool” and “he is young” are not discrete statements. They do not provide concrete data about the air temperature or the person’s age (i.e., the air is at 65°F or the boy is 12 years old). It is a superset of conventional (Boolean) logic that has been extended to handle the concept of partial truth. In the ( Boolean ) logic we see that the results for any operation can be true or false if we refer to true by one and the false by zero then the result may be one or zero [16]. For example binary logic, hot would be one discrete value (e.g., logic 1) and cold would be the other (e.g., logic 0), leaving no value to represent a cool temperature (see figure (3.1)).

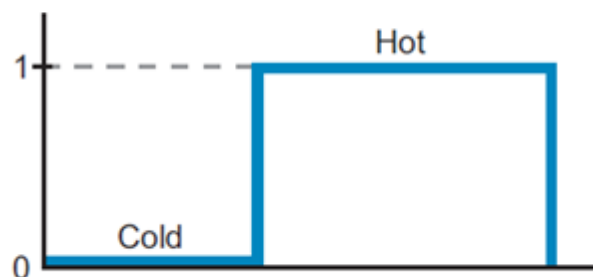


Figure 3.1: Binary logic representation of discrete temperature valve

In contrast to binary logic, fuzzy logic can be thought of as gray logic, which creates a way to express in-between data values. Fuzzy logic associates a grade, or level, with a data range, giving it a value of 1 at its maximum and 0 at its minimum. For example, figure (3.2) illustrates a representation of a cool air temperature range, where 70°F indicates perfectly cool air (i.e., a grade

value of 1). Any temperature over 80°F is considered hot, and any temperature below 60°F is considered cold.

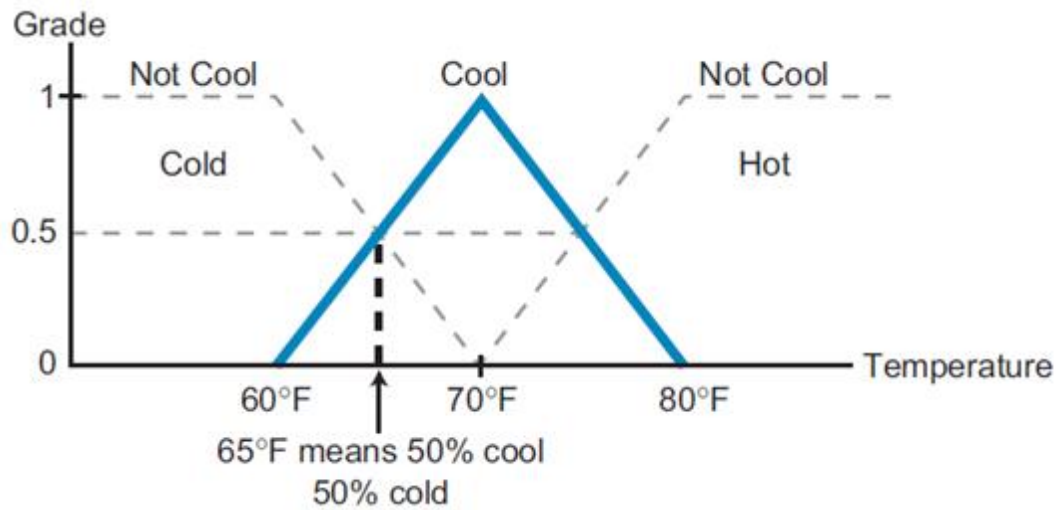


Figure 3.2: Cool air temperature range

### 3.3 Classical Sets versus Fuzzy Sets

The concept of a classical set is very fundamental to pure and applied mathematics. Intuitively, a set is defined as any collection of definite and distinct objects that is conceived as a whole, also objects that are included in a set are usually called its members.

Classical sets satisfy two basic requirements: first, members of each set are distinguishable from one another, and second, for any given object it is specified whether the object is, or is not, a member of the set the function of crisp set is

$$\mu_A(x) = \begin{cases} 0 & x \notin A \\ 1 & x \in A \end{cases} \quad \mu_A(x) \in \{0,1\} \quad 3.1$$

Fuzzy sets differ from classical sets by rejecting the second requirement. Contrary to classical sets, fuzzy sets do not require sharp boundaries that separate their members from other objects.

The membership of any object in a given fuzzy set is not a matter of affirmation or denial, as is required for classical sets, but a matter of degree which the membership between 0 and 1  $\mu_A(x) \in [0,1]$  .

### 3.4 Fuzzy Set Operations

Basic operations on sets in crisp set theory are the set complement, set intersection, and set union. Fuzzy set operations are very important because they can describe intersections between variables for a given element "x" of the universe, the following function theoretic operations for the set theoretic operations of complement, intersection, and union are defined[3][17]:

#### 1) Complement (NOT Operation):

Consider a fuzzy set "A" in universe "X". its complement "A" as shown in figure (3.3) which  $A' \rightarrow X_{A'}(x) = 1 - X_A(x)$ .

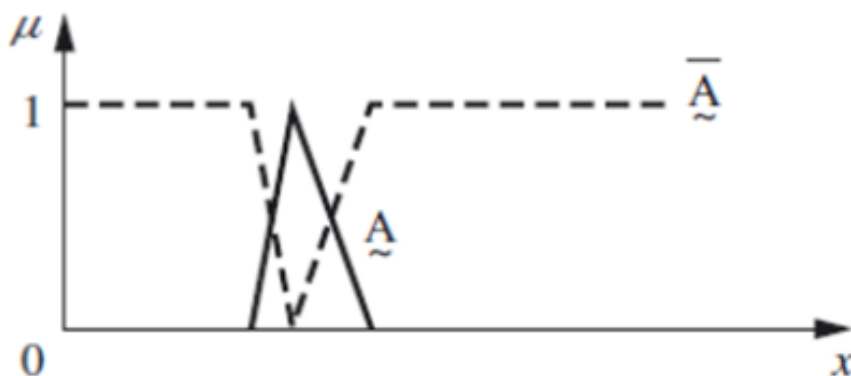


Figure 3.3: Complement of fuzzy sets A

## 2) Intersection (AND Operation):

Consider two fuzzy sets "A" and "B" in universe "X". as in figure (3.4) where  $A \cap B \rightarrow X_{A \cap B}(x) = \min(X_A(x), X_B(x))$ .

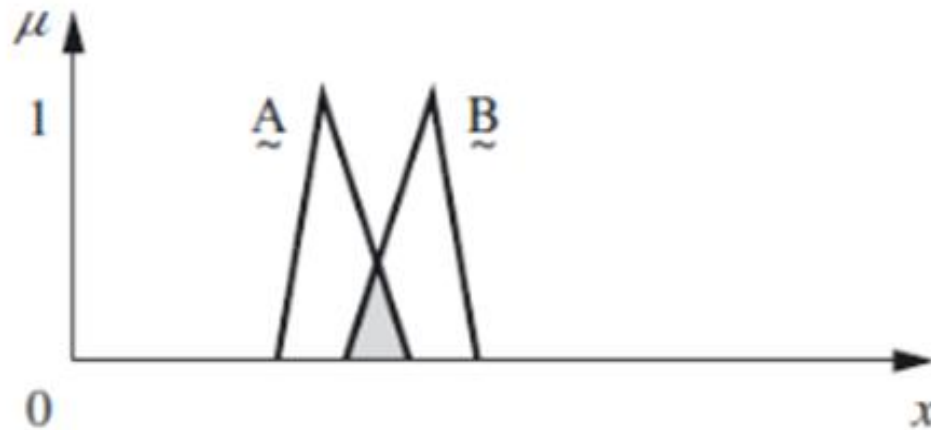


Figure 3.4: Intersection of fuzzy sets A and B

## 3) Union (OR Operation):

Consider two fuzzy sets "A" and "B" in universe "X".  $A \cup B$  is the whole area covered by the sets as shown in figure (3.5) where  $\mu_{A \cup B}(x) = \max(\mu_A(x), \mu_B(x))$ .

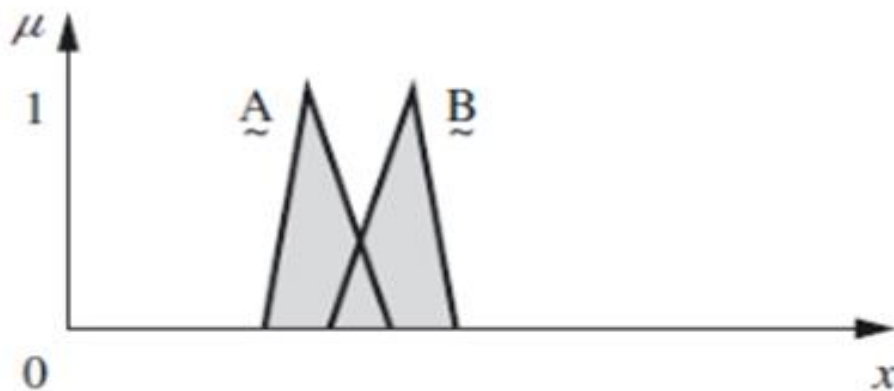


Figure 3.5: Union of fuzzy sets A and B

### 3.5 Fuzzy logic Control Component

In this part of this chapter, the main components of a fuzzy logic controller are discussed and a simple example is implemented. The three main actions performed by a fuzzy logic controller are:

- fuzzification
- fuzzy processing
- defuzzification

As shown in figure (3.6), when the fuzzy controller receives the input data, it translates it into a fuzzy form this process is called fuzzification.

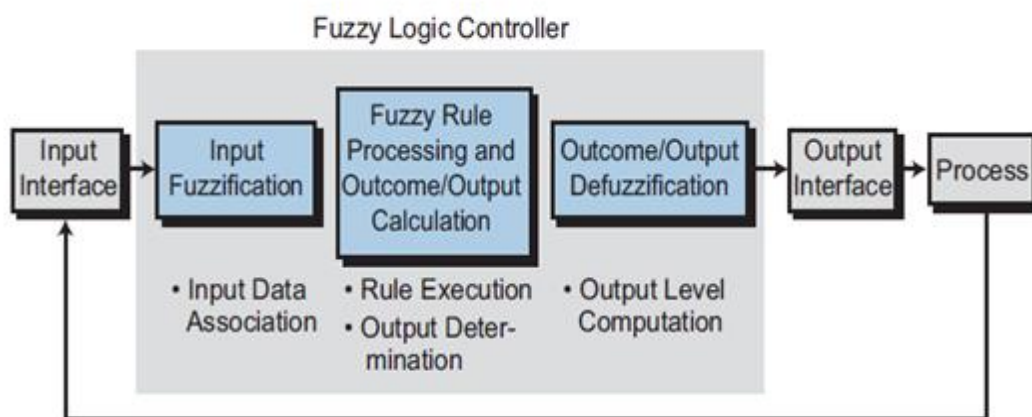


Figure 3.6: Fuzzy logic controller operation

The controller performs fuzzy processing, which involves the evaluation of the input information according to IF...THEN rules created by the user during the fuzzy control system's programming and design stages. Once the fuzzy controller finishes the rule-processing stage and arrives at an outcome conclusion, it begins the defuzzification process. In this final step, the fuzzy controller converts the output conclusions into "real" output data (e.g., analog counts) and sends this data to the process via an output module interface.

### 3.5.1 Fuzzification Component:

The fuzzification process is the interpretation of input data by the fuzzy controller. Fuzzification consists of two main components:

- (a) Membership functions
- (b) Labels

#### a . Membership Functions.

During fuzzification, a fuzzy logic controller receives input data, also known as the fuzzy variable, and analyzes it according to user-defined charts called membership functions (see figure 3.7). Membership functions group input data into sets, such as temperatures that are too cold, motor speeds that are acceptable, etc. The controller assigns the input data a grade from 0 to 1 based on how well it fits into each membership function (e.g., 0.45 too cold, 0.7 acceptable speed).

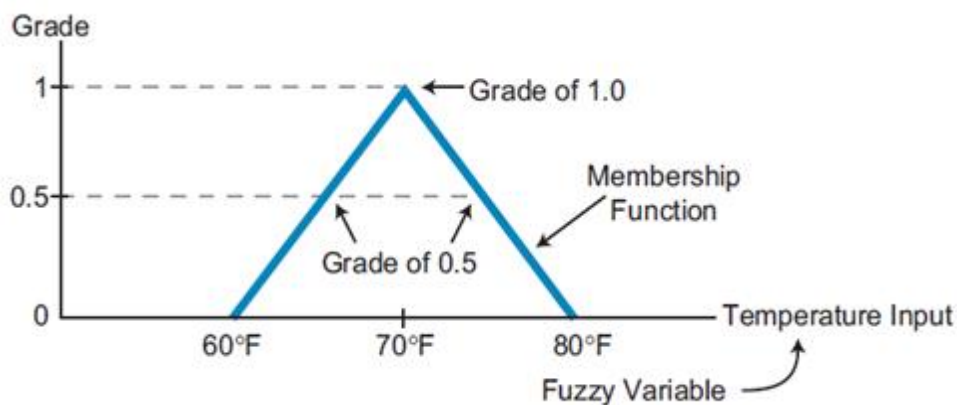


Figure 3.7: Membership function chart

Membership functions can have many shapes, depending on the data set, but the most common are the S,  $\Lambda$ , and  $\Pi$ , Z, shapes shown in figure (3.8). Note that these membership functions are made up of connecting line segments with a maximum of four end points.

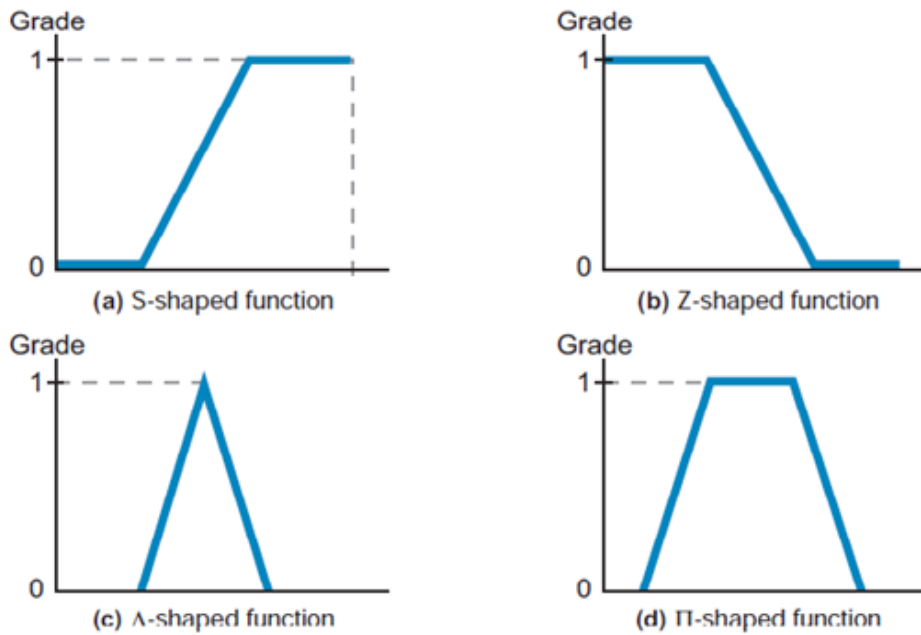


Figure 3.8 : Membership function shapes (a) S, (b) Z, (c) A, and (d)  $\Pi$ .

## b. Labels.

Each fuzzy controller input can have several membership functions, where the membership function is defined by a name called a label. For example, an input variable such as temperature might have five membership functions labeled as cold, cool, normal, warm, and hot. Generically, the seven membership functions have the following labels, which span from the data range's minimum point (negative large) to its maximum point (positive large):

- NL (negative large)
- NM (negative medium)
- NS (negative small)
- ZR (zero)
- PS (positive small)
- PM (positive medium)
- PL (positive large)



figure (3.9) illustrates an example of an input variable with seven shaped membership functions using all of the possible labels. A group of membership functions forms a fuzzy set.

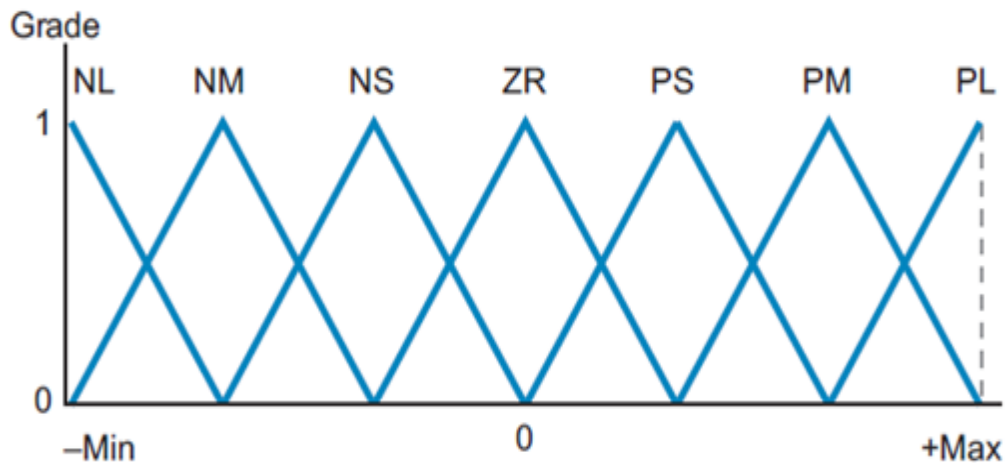


Figure 3.9: Fuzzy logic input seven membership function labels

### 3.5.2 Fuzzy Processing Components (Mamdani method)

A fuzzy controller or model uses fuzzy rules, which are linguistic if-then statements involving fuzzy sets, fuzzy logic, and fuzzy inference. Fuzzy rules play a key role in representing expert control/modeling knowledge and experience and in linking the input variables of fuzzy controllers/models to output variable (or variables). The major types of fuzzy rules exist, namely, Mamdani fuzzy rules, which is the most commonly used fuzzy inference technique. The Mamdani-style fuzzy inference process is performed in three steps [18]:

- 1) Fuzzification of the crisp input variables
- 2) Rule evaluation.
- 3) Fuzzy outcome calculation

To illustrate the fuzzy inference let's examine a simple two-input one-output problem that includes three rules:

Rule (1) .... IF X is A3 OR Y is B1 THEN z is C1

Rule (2).... IF X is A2 AND Y is B2 THEN z is C2

Rule (3).... IF X is A1 THEN z is C3

### Step 1: Fuzzification

The first step in the application of fuzzy reasoning is a fuzzification of inputs in the controller, which is to take the crisp inputs,  $x_1$  and  $y_1$ , and determine the degree to which these inputs belong to each of the appropriate fuzzy sets. It means that to every crisp value of input we attribute a set of degrees of membership ( $m_j, j=1,n$ ) to fuzzy sets defined in the universe of discourse for that input as shown in figure (3.10)[17].

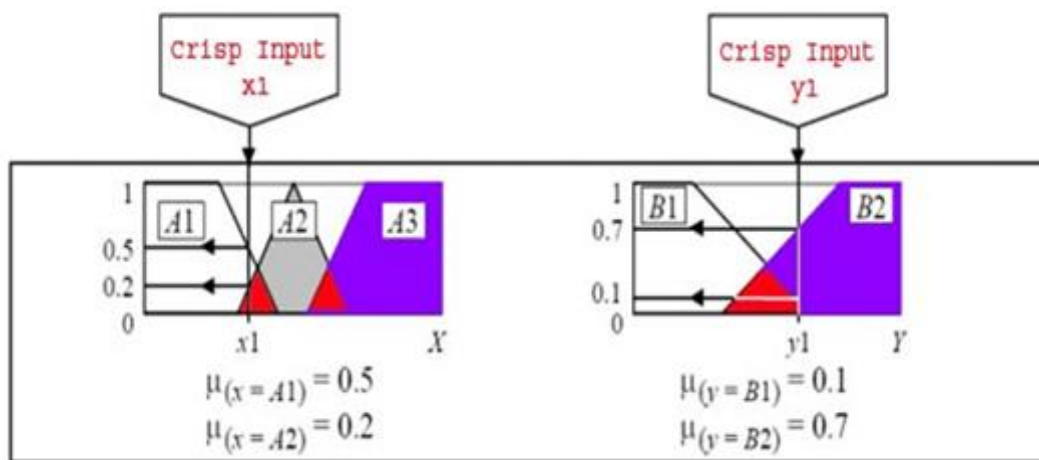


Figure 3.10: Fuzzification stage

### Step 2: Rule evaluation

The second step is to take the fuzzified inputs,  $\mu(x=A1) = 0.5$ ,  $\mu(x=A2) = 0.2$ ,  $\mu(y=B1) = 0.1$  and  $\mu(y=B2) = 0.7$ , and apply them to the antecedents of the fuzzy rules. If a given fuzzy rule has multiple antecedents, the fuzzy operator

(AND or OR) is used to obtain a single number that represents the result of the antecedent evaluation. This number (the truth value) applied to the consequent membership function. To evaluate the disjunction of the rule antecedents, the OR fuzzy operation is used. The most popular approaches used for the union to get the maximum value is  $\mu_{A \cup B}(x) = \max [\mu_A(x), \mu_B(x)]$ .

Similarly, in order to evaluate the conjunction of the rule antecedents, we apply the AND fuzzy operation intersection which used minimum approach:  $\mu_{A \cap B}(x) = \min [\mu_A(x), \mu_B(x)]$ . The rule evaluations are clearly appears in figure (3.11)[17].

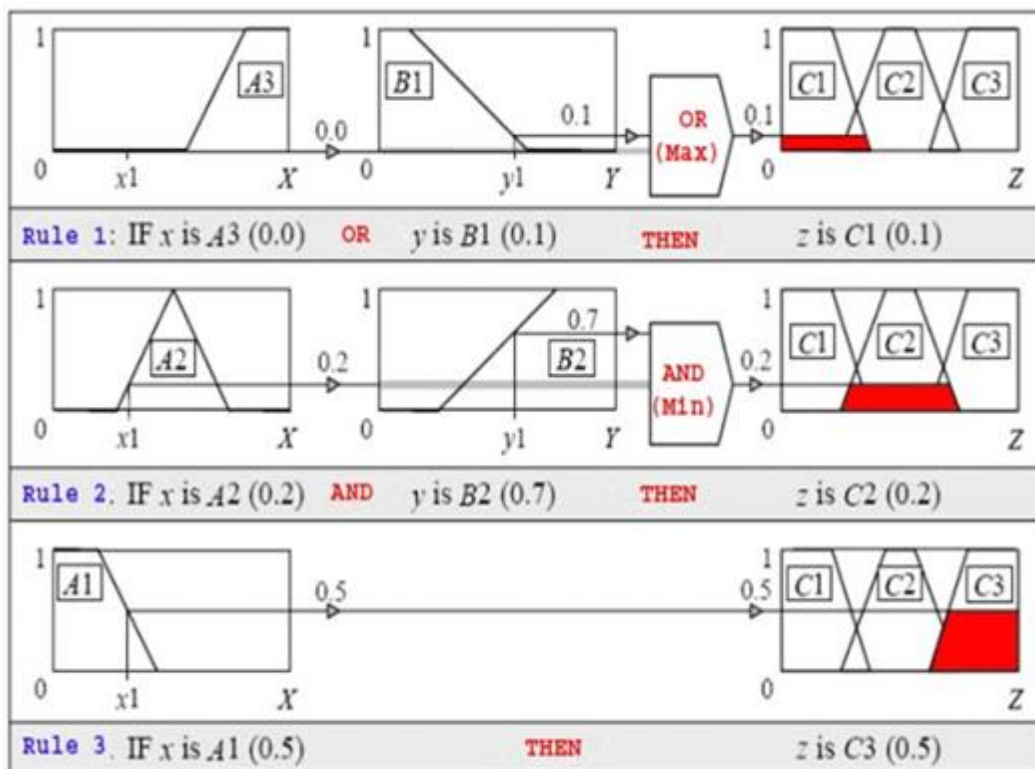


Figure 3.11: Rule evaluation in Mamdani method

### Step 3: Fuzzy outcome calculation

We take the membership functions of all rule consequents previously (Max-Min Composition) or (Max-Product Composition) and combine them into a single fuzzy set as figure (3.12).

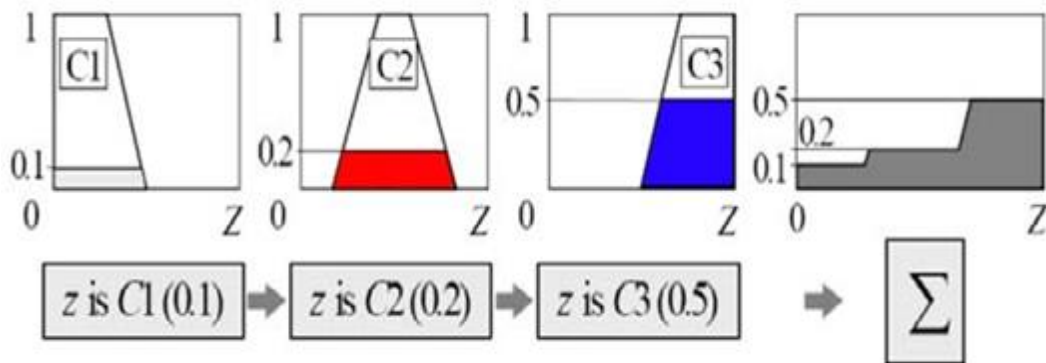


Figure 3.12 Fuzzy outcome evaluations

### 3.5.3 Defuzzification

The final output value from the fuzzy controller depends on the defuzzification method used to compute the outcome values corresponding to each label. The defuzzification process examines all of the rule outcomes after they have been logically added and then computes a value that will be the final output of the fuzzy controller. Thus, during defuzzification, the controller converts the fuzzy output into a real-life data value. There are many defuzzification methods, but all are based on mathematical algorithms. Some commonly used defuzzifying methods which are Center of gravity (COG), weighted average method, mean of maximum (MOM) and smallest of maximum (SOM) [17]. In this thesis the COG method and MOM will be used as describe below :

- **The mean of maximum method (MOM)**

The mean of maxima method generates a crisp control action by averaging the support values which their membership values reach the maximum. In the case of discrete universe:

$$Z = \frac{1}{\sum_{i=1}^l} \frac{Z_i}{l} \quad 3.2$$

Where l is the number of the quantized i values which reach their maximum memberships.

- **Center of gravity (COG)**

The center of gravity method, also referred to as “calculating the centroid,” mathematically obtains the center of mass of the triggered output membership functions. Figure (3.13) illustrates the centroid calculation for the example previously illustrated in figure (3.10). In mathematical terms, a centroid is the point in a geometrical figure whose coordinates equal the average of all the other points comprising the figure this point is the center of gravity of the figure. Mathematically the centre of gravity (COG) can be expressed as:

$$COG = \frac{\int_a^b A(x)X dx}{\int_a^b A(x)dx} \quad 3.3$$

$$COG = \frac{(0+10+20) \times 0.1 + (30+40+50+60) \times 0.2 + (70+80+90+100) \times 0.5}{0.1+0.1+0.1+0.2+0.2+0.2+0.2+0.5+0.5+0.5+0.5} = 67.4$$

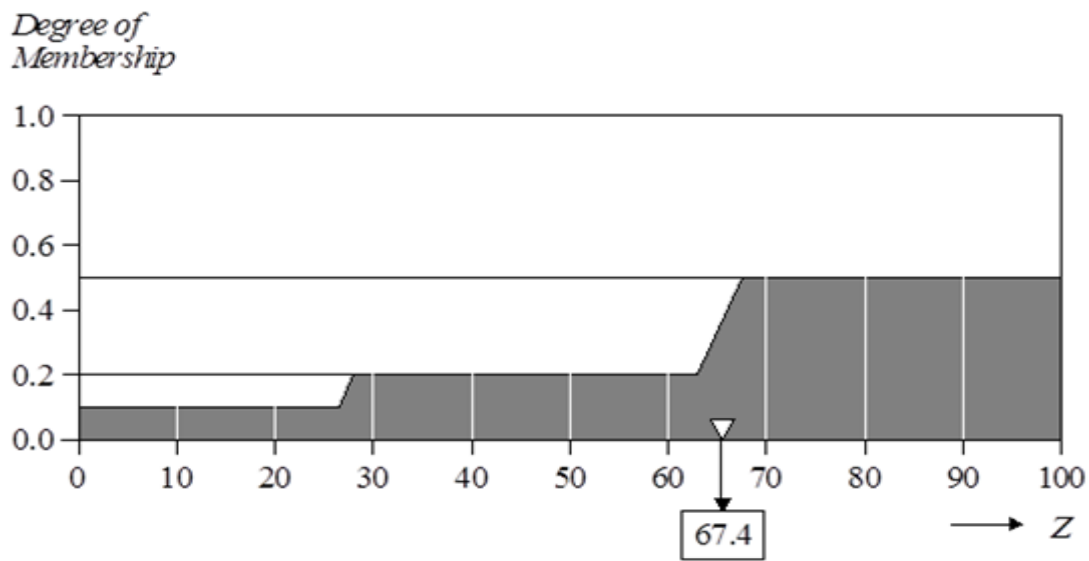


Figure 3.13: COG approach in defuzzification stage

### 3.6 Advantages and Disadvantages of Mamdani Method

#### 3.6.1 Advantages of The Mamdani Fuzzy Method:

- It is intuitive and simple to build.
- It is widely used for second order systems with both linear and nonlinear characteristics.
- It has widespread acceptance.
- It is well suited to human feeling.

#### 3.6.2 Disadvantages of The Mamdani Fuzzy Method:

- It is only suited to the long delay system, such as the temperature control system, since it is too simple to control the process quickly.
- It needs additional device to improve the efficiency, when it controls the high frequent input system.

### CONTROLLER DESIGN & SIMULATION RESULT

#### 4.1 Introduction

Power electronic inverters are widely used in various industrial drive applications such as uninterruptible power supplies (UPS), medical equipment and communication systems so there is increasing demand for high quality power inverter. Pulse-width modulated PWM inverter has been used as a key element for a high performance power conversion system. The output voltage is required to be sinusoidal with minimum total harmonic distortion (THD). This is usually achieved by employing a combination of pulse width modulation (PWM) scheme and a second order filter at the output of the inverter [1][8]. In industries, the THD value should not exceed 5% according to IEEE standard. Many control techniques have been proposed for obtaining pure sinusoidal output with good voltage regulation and fast dynamic response. Conventional closed loop control scheme employs PI controller is commonly used to achieve the desired output. Sometimes, there is problem using this kind of controller because it needs the mathematical model and tuning the parameter is very difficult in some application. To overcome this problem new controller based on fuzzy logic control is used to solve this problem. Dominance of FLC's over the conventional controllers has become tight as it can work with imprecise inputs, can handle nonlinearity and it is more robust than conventional nonlinear controllers. In this chapter, the comparative study has been carried out between FLC controller and PI controller where both controllers are designed for harmonic elimination in sinusoidal PWM inverters.

## 4.2 System Description for Single Phase DC-AC PWM Inverter

As shown in figure (4.1), the inverter consists of two sides (A, B) which supplies a single-phase AC output voltage  $V_{out}$  to the load. A certain switching algorithm is applied to each of the four switch modules T1, T2, T3, and T4 in order to control the inverter to generate the desired sinusoidal output with the desired frequency and magnitude[19].

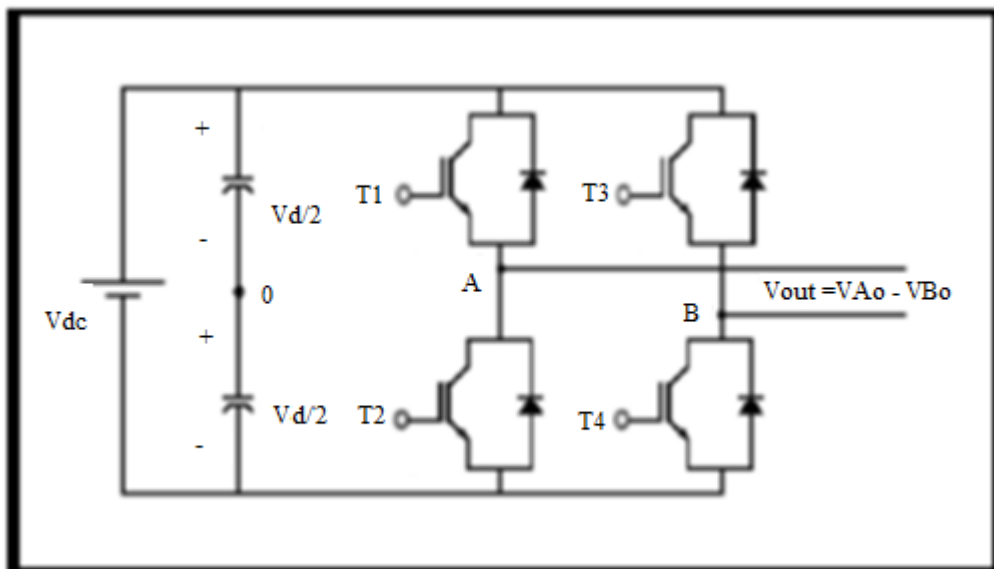


Figure 4.1 :Single phase full bridge inverter

In this study the unipolar SPWM technique is used to drive the inverter because it gives low THD and decreases the power switches losses. Comparing a control signal  $V_{control1}$  with the carrier signal results a logic signal to control the switches in side A, and comparing of  $V_{control2}$  with the carrier signal results in logic signal to control the switches in side B as shown in figure (4.2)[11].



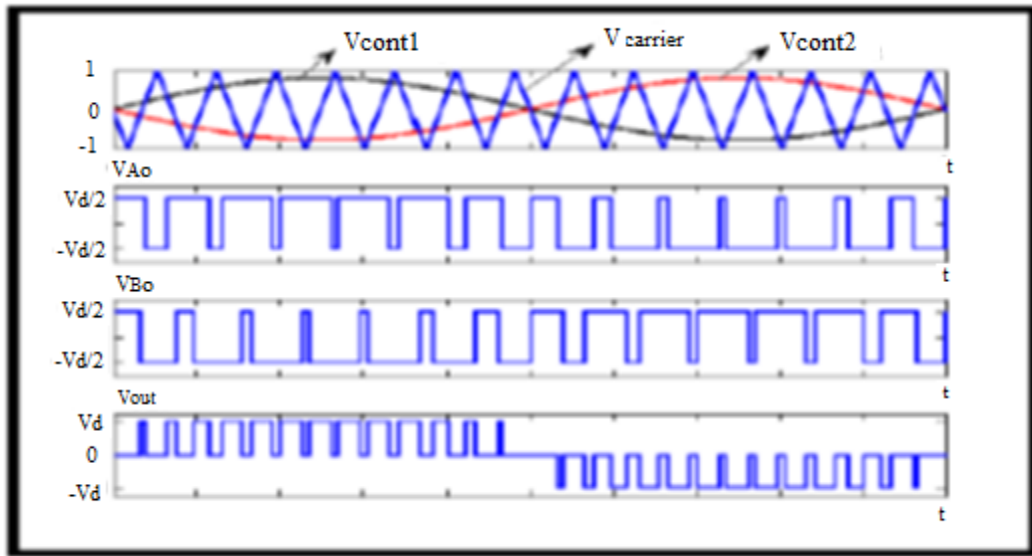


Figure 4.2: Unipolar PWM scheme

### 4.3 Component Selection

The magnitude of the ripple current and ripple voltage in the output of the inverter is determined by the size of the LC filters. The filter size has been chosen, and the design specification for the proposed inverter circuit is shown in Table 4.1.

Table 4.1 : Parameters of PWM inverter

Parameters	Value
PWM output Switching frequency	10 KHz
Input DC voltage	350 V
RMS load voltage	220 V
Full load resistance	44 $\Omega$
Output fundamental frequency	50 Hz
Rated output voltage	220V rms

## 4.4 Filter Design

A proper design of the LC filter results in a great reduction of the inverter output harmonics; hence, provides a very clean power to the load. The inductor ripple current depends on the size of the inductor and switching frequency. Figure (4.3) shows the ripple waveform of the inductor current value of the inductance of the output filter inductor is given by Eq.4.1[20].

$$L_f = \frac{v_d}{4f_s \Delta i} \quad 4.1$$

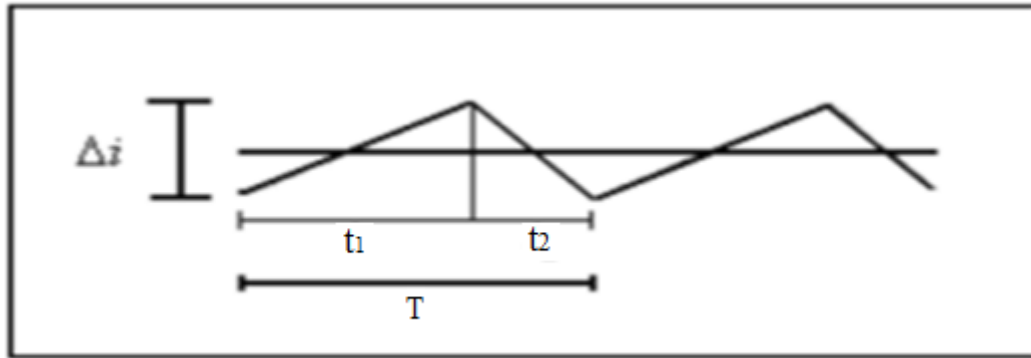


Figure4.3: Inductor ripple current

where  $v_d$  is the DC bus voltage,  $\Delta i$  is the inductor ripple current and ( $f_s$ ) is the inverter switching frequency. The output filter capacitor size is determined by the allowable output voltage ripple  $\Delta v_o$  and can be calculated from Eq.4.2 [20].

$$C_f = \frac{\Delta i}{8f_s \Delta v_o} \quad 4.2$$

If the DC input voltage is limited to 350 volt and the switching frequency is limited to 10 KHz, and if the maximum inductor ripple current is limited to 20% of the maximum peak to peak output current, then,  $L_f$  obtained such  $L_f = 1.768$  mH. The maximum ripple voltage is limited to 1% of the maximum peak to peak output voltage, then,  $C_f$  is obtained such  $C_f = 0.229$  uF.

## 4.5 The Mathematical Model for Single Phase Inverter

The mathematical model for the voltage controlled single-phase full bridge inverter based on bipolar voltage switching with Sinusoidal Pulse Width Modulation (SPWM) is considered here. It is assumed that all components are ideal. Figure (4.4) shows a schematic representation of the voltage controlled full-bridge inverter[19].

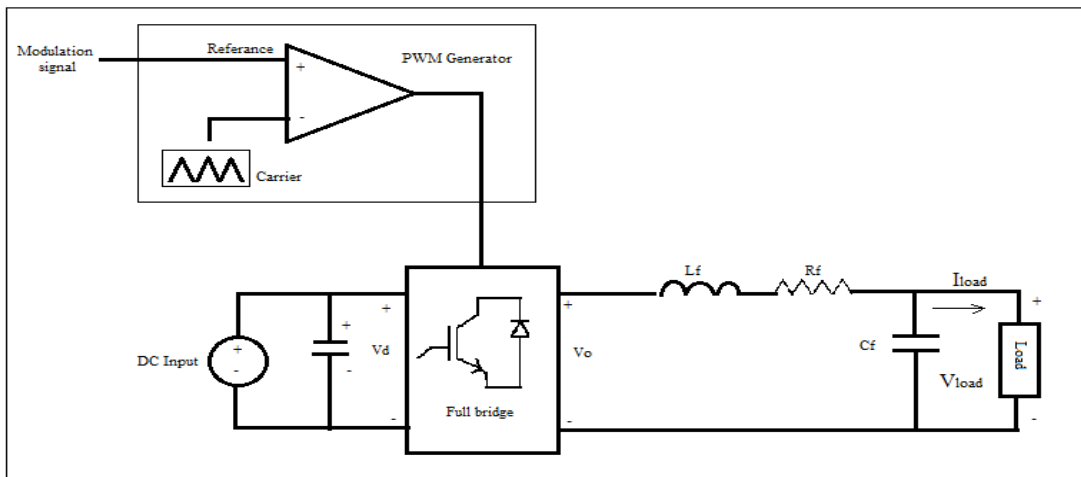


Figure 4.4: Schematic diagram for inverter with LC filter

From figure (4.4) the following differential equations have been derived which represents the linear model of L-C filter and  $z_l$  load of the inverter.

$$V_o(s) - V_{load}(s) - R_f i(s) = L_f i_l(s) \quad 4.3$$

$$i_l(s) = \frac{V_o(s) - V_{load}(s) - R_f i(s)}{L_f s} \quad 4.4$$

$$V_{load}(s) = \frac{i_c(s)}{C_f s} \quad 4.5$$

$$i_c(s) = i_l(s) - i_{load}(s) \quad 4.6$$

$$i_{load} = \frac{V_{load}}{Z_l} \quad 4.7$$

Figure (4.5) shows the linear model of the inverter system (PWM inverter plus the output filter and load), in which the proportional gain  $K$  represents the PWM inverter is equal to  $v_{DC} / v_c$  ( $v_{DC}$  is the voltage of DC power supply and  $v_c$  is the peak voltage of triangular carrier wave).

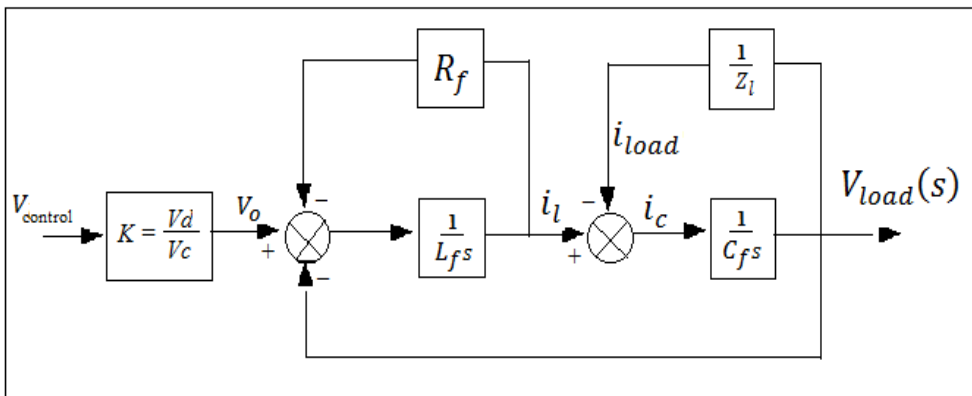


Figure 4.5: Block diagram of the linear model for PWM inverter

Based on the analysis of figure (4.5), the system transfer function can be obtained as shown in Eq. (4.8).

$$G(s) = \frac{1}{C_f L_f s^2 + \left(\frac{L_f}{z_L} + C_f R_f\right) s + \frac{R_f}{z_L} + 1} \quad 4.8$$

since  $R_f$  is very small so we can neglect it and the transfer function in Eq.(4.8) can be rewritten as :

$$G(s) = \frac{1}{C_f L_f s^2 + \frac{L_f}{z_L} s + 1} \quad 4.9$$

## 4.6 Designing Controller

In figure (4.6), single phase load is connected to the SPWM voltage source inverter, the load voltage,  $v_a$ , is compared with the reference signal and the error signals are passed through controller to generate the pulses which are operated to produce sinusoidal signal output with small harmonic distortion[19] [21].

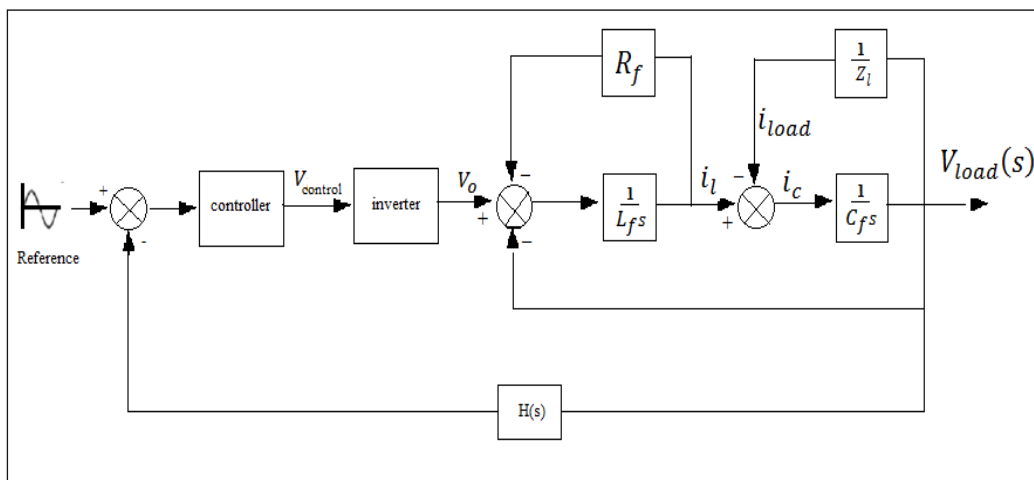


Figure 4.6: Block diagram for the system with controller

### 4.6.1 Designing PI Controller

In control engineering, PI Controller (proportional-integral controller) is a feedback controller which drives the plant to be controlled by a weighted sum of the error (difference between the output and desired set-point) and the integral of that value[22]. It is a special case of the PID controller in which the derivative (D) part of the error is not used. The PI controller is mathematically denoted as:

$$u(t) = ke(t) + k_i \int_0^t e(\tau) d\tau \quad 4.10$$

where  $u$  is the control signal and  $e$  is the control error ( $e = r - y$ ), the reference value is also called the set point. The controller parameters are proportional gain  $k$ , integral gain  $k_i$  parameterized as:

$$u(t) = k \left( e(t) + \frac{1}{T_i} \int_0^t e(\tau) d\tau \right) \quad 4.11$$

Where  $k$  is gain of the controller and  $T_i$  is the integral time constant. Integral control action added to the proportional controller converts the original system into high order. Hence, the control system may become unstable for a large value of  $K$ . Since roots of the characteristic equation may have positive real part, so the proportional control action tends to stabilize the system, while the integral control action tends to eliminate or reduce steady-state error in response to various inputs. As the value of  $T_i$  is increased:

- Overshoot tends to be smaller
- Speed of the response tends to be slower

### 4.6.2 Selection of PI Controller Parameter

The parameters of the proportional and integral controller in the voltage loop is selected by using the MATLAB/ SISO tools for the approximate linearized control model of the inverter by ignoring the resistance  $R_f$  as shown in figure (4.7).

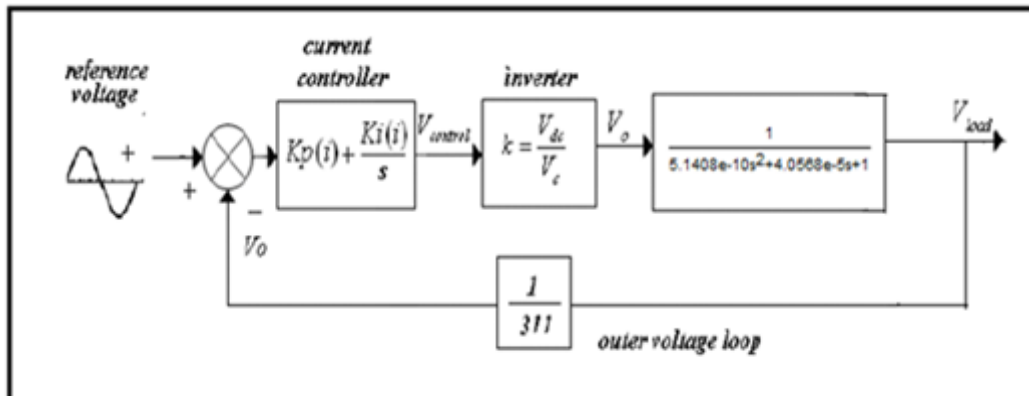


Figure 4.7: An approximate linearized control model

The feedback signal of the load voltage obviously have to be scaled down to low voltage control signals which the feedback signals are converted to per unit (pu) values of full load for example (1/unit) voltage represent 311 V ( $\sqrt{2} \cdot 220$ ) and the triangular carrier waveform  $v_c$  also has amplitude of 1 pu.

### 4.6.3 Closed Loop Control Design

By applying the MATLAB SISO tool as figure (4.8) the PI controller for the close loop system is implemented and the parameter  $k_p=1.6344$  and  $k_i=28181$  which grantee all the poles lie in the left half plane. The stability of the closed-loop system must be ensured by root locus plot, and step response where the most important aspect in this design is the steady state error, peak overshoot and settling time.

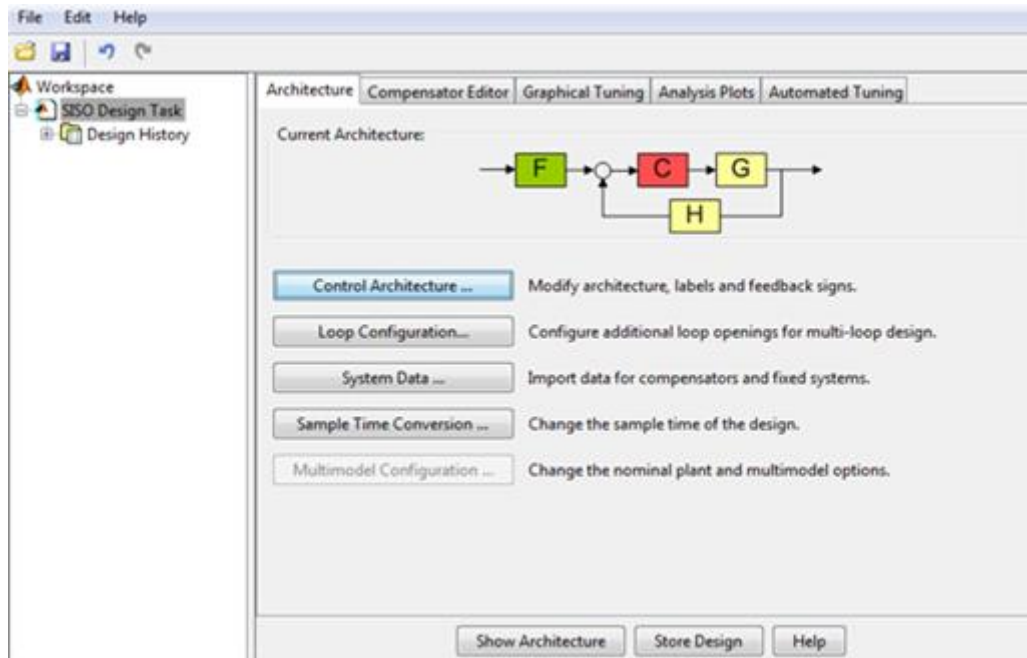


Figure 4.8: Closed loop design by MATLAB SISO TOOLS

From the root locus plot as shown in figure (4.9) it is noted that the over all closed loop system is stable due to the location of the root locus which are located on the left of the imaginary axis. The step response is shown in figure (4.10), where the settling time is approximately equal to the required value which is 0.182 ms. The peak over shoot is 3.62% and the steady state error of the output voltage is equal to zero.

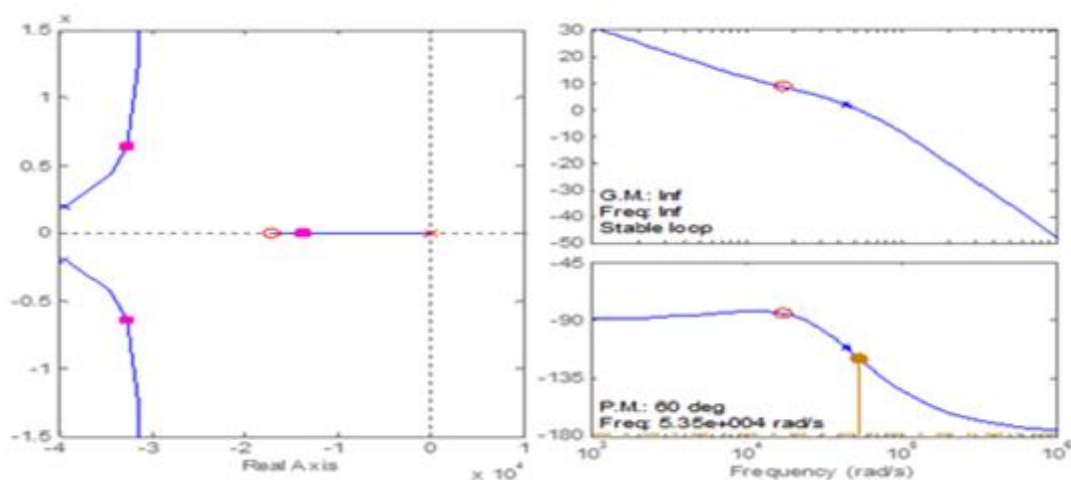


Figure 4.9: Root locus design for closed loop system



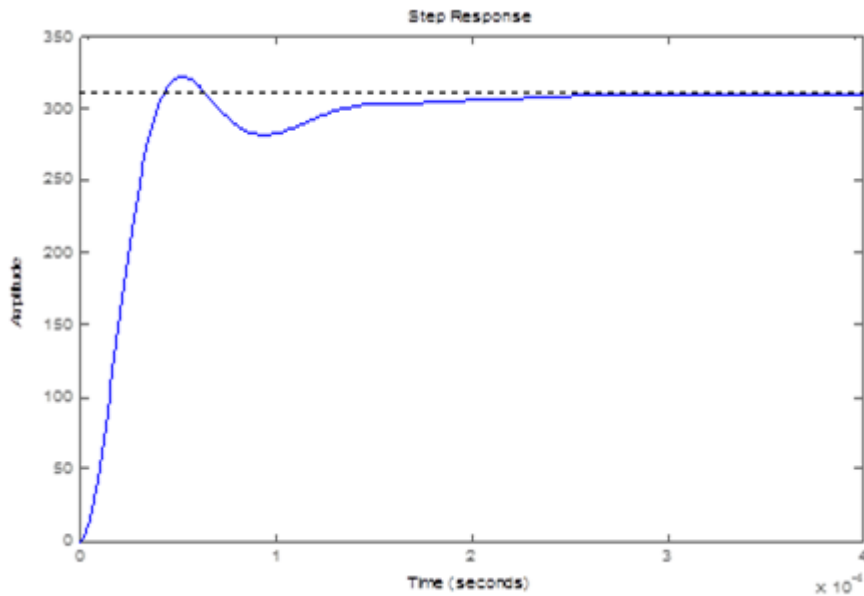


Figure 4.10: Step response for the system

## 4.7 Design of Fuzzy Logic Controller

FL is a direct method for controlling a system without the need of a mathematical model. FL gets crisp data from various sensors these data are changed to linguistic or fuzzy membership functions via the fuzzification process after that, they go through a set of fuzzy “IF-THEN” rules in an inference engine and result in fuzzy outputs these fuzzy outputs changed back to crisp values by the defuzzification.

The fuzzy controller for the inverter system is implemented in MATLAB using the fuzzy logic toolbox. This toolbox allows for the creation of input membership functions, fuzzy control rules, and output membership functions [23]. To implement the fuzzy controller for the system as shown in figure (4.11), it should have two input and one output and the membership function is chosen to be triangular shape as it is demonstrated in figure (4.12).

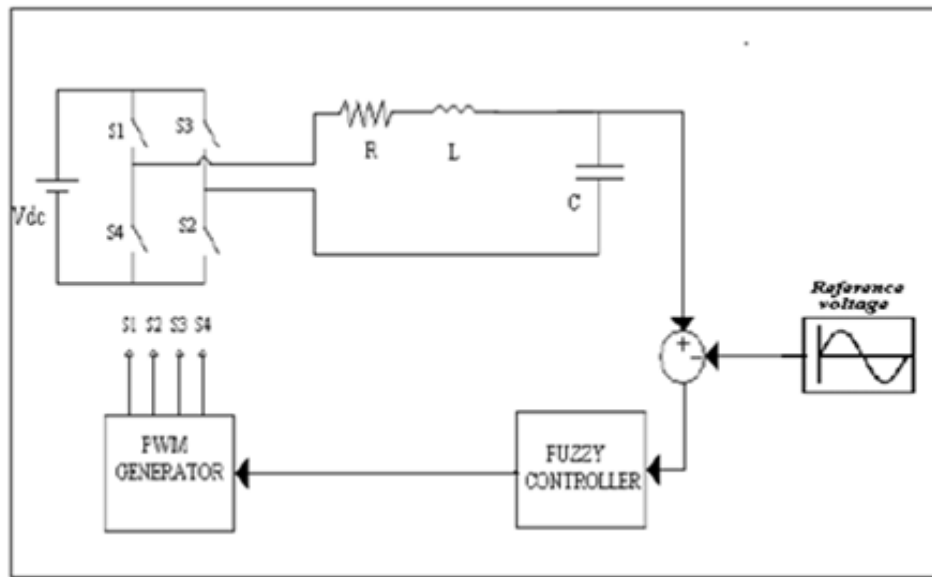


Figure 4.11: Schematic diagram for the system with fuzzy controller

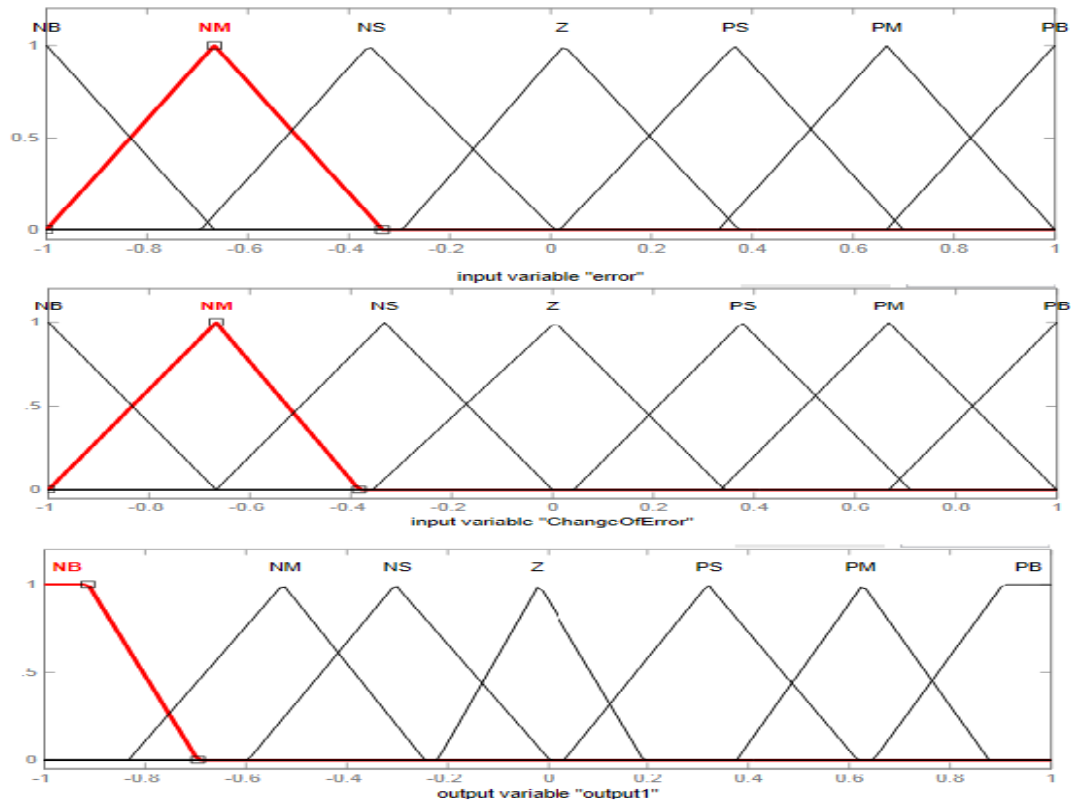


Figure 4.12: Fuzzy membership for input and output

which have PB(positive big), PM(positive mediam), PS(positeve small), Z(zero), NS(negative small), NM(negative mediam) and NB(negative big) the input is taken as error (e) and the change in error ( $\Delta e$ ).

A 7\*7-membership function having 49 rules are taken into account, where it is describe in Table 4.2.

Table 4.2: Fuzzy rules

$E$ $CE$	NB	NM	NS	Z	PS	PM	PB
NB	NB	NB	NB	NB	NM	NS	Z
NM	NB	NB	NB	NM	NS	Z	PS
NS	NB	NB	NM	NS	Z	PS	PM
Z	NB	NM	NS	Z	PS	PM	PB
PS	NM	NS	Z	PS	PM	PB	PB
PM	NS	Z	PS	PM	PB	PB	PB
PB	Z	PS	PM	PB	PB	PB	PB

The rule base contains linguistic variables is provided based on experience and it should have smooth surface as show in figure (4.13).

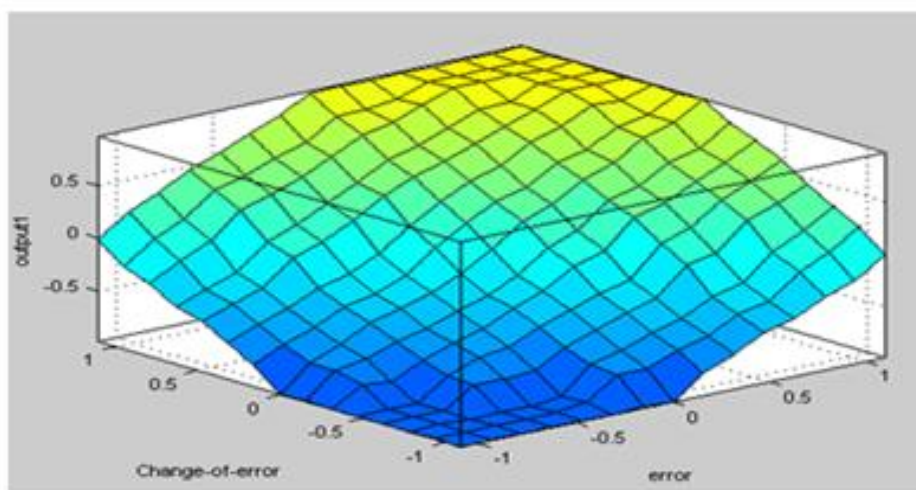


Figure 4.13: Input output relationship surface

## 4.8 Simulation Result

In this section, Matlab simulation for the proposed system is implemented with controllers and the comparative study between classical PI controller and fuzzy logic controller is discussed with emphasis on the influence of the harmonic distortion in the output voltage and current for the load.

### 4.8.1 PI Controller Simulink

The block diagram is shown in figure (4.14) and it contains the universal H-bridge, LC filter, pulse width generator and the PI controller with the parameter of  $K_P=1.6344$  and  $K_i=28181$  as designed in previous section. The feedback gain is  $1/310$ . The aim of this design is tracking sinusoidal signal with small harmonic distortion. The carrier frequency was selected as a triangular wave with 10kHz base frequency and the simulation was activated for the system by applying the FFT analysis from the GUI tools.

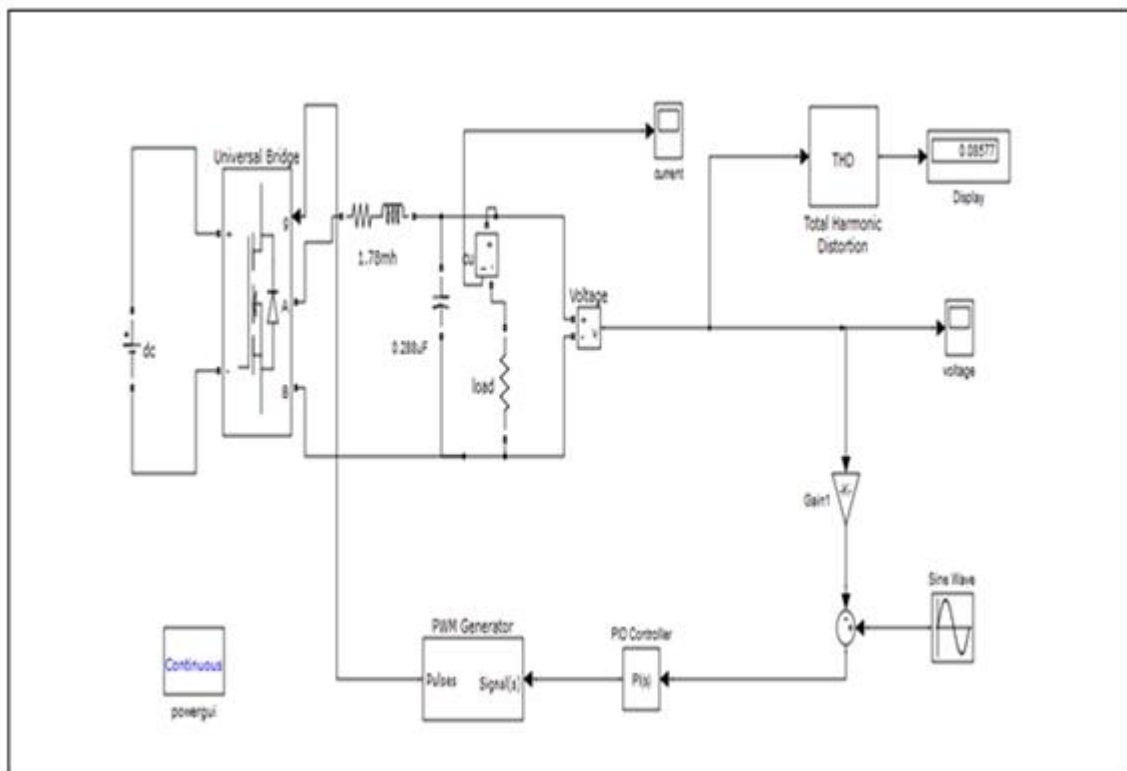


Figure 4.14: Matlab Simulink for PWM inverter under PI controller

The output voltage for the load as figure (4.15) is sinusoidal wave with peak output voltage equal 310.4 volt (RMS value equal 219.48 volt and the frequency at 50 Hz), and the THD is about 8.04%. This distortion is grater than IEEE which recommends 5%. Figure (4.16) describe the output current for the load which has peak value equal 7.05A (RMS equal 4.98A) and THD is the same as voltage output distortion.

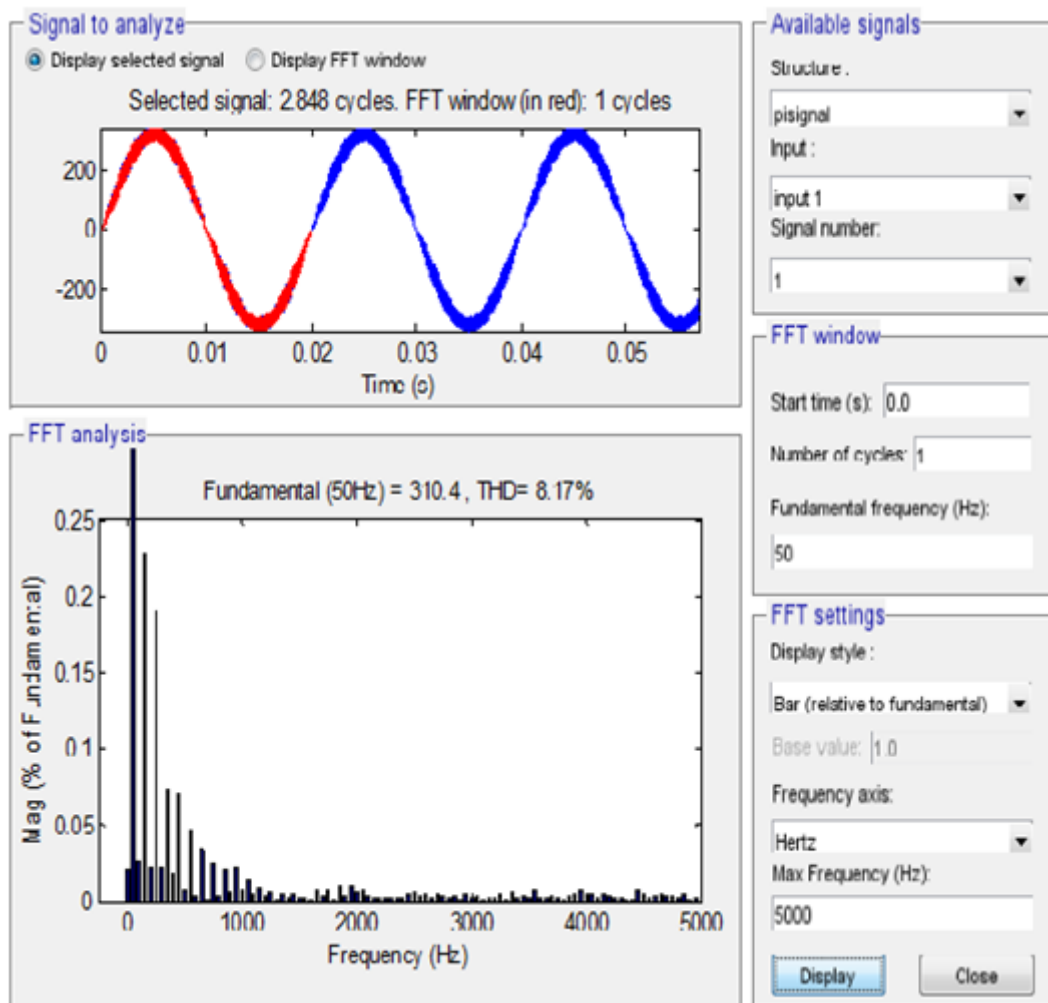


Figure 4.15: Load voltage and spectrum analyzer for full load PWM inverter under PI controller

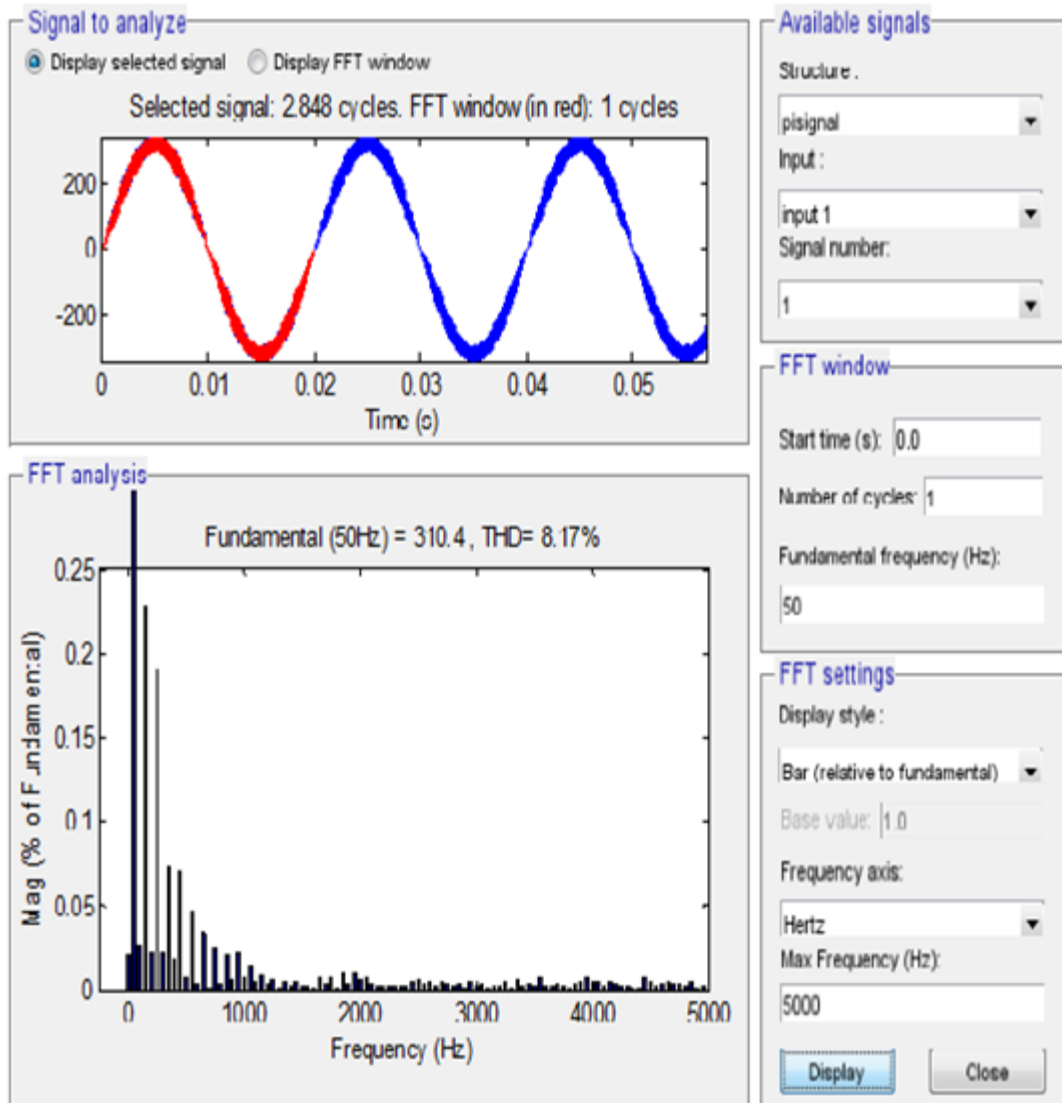


Figure 4.16: Load current and spectrum analyzer for full load PWM inverter

#### 4.8.2 Fuzzy Controller Simulink

By applying the fuzzy tools in Matlab, the model of the system is implemented with fuzzy logic controller as figure (4.17). This controller is based on Mamdani method as uses 49 rules as shown in Table 2.

The membership for the input and output is described as figure (4.12) and the fuzzy output is defuzzified by the centroid method to convert the signal to crisp signal.

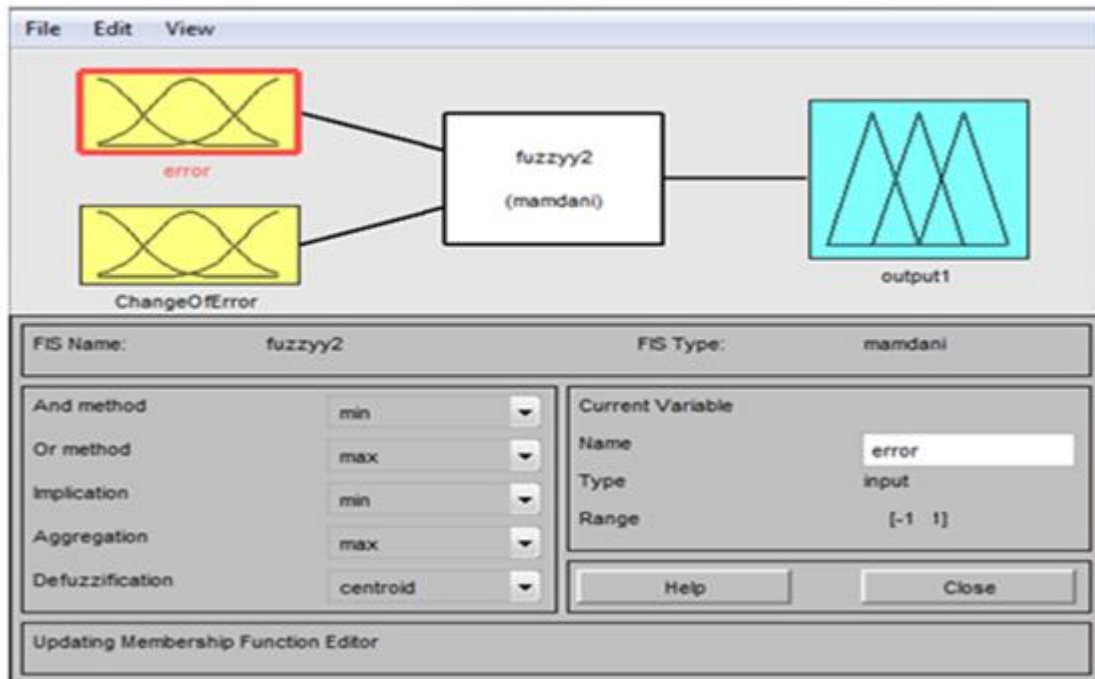


Figure 4.17: Input and output membership by Matlab fuzzy logic control tool

Before simulating the system, it should be sent the file of the fuzzy controller to workspace to start simulation. The block diagram in simulink is described by figure (4.18) and the output voltage result for the load is shown in figure (4.19).

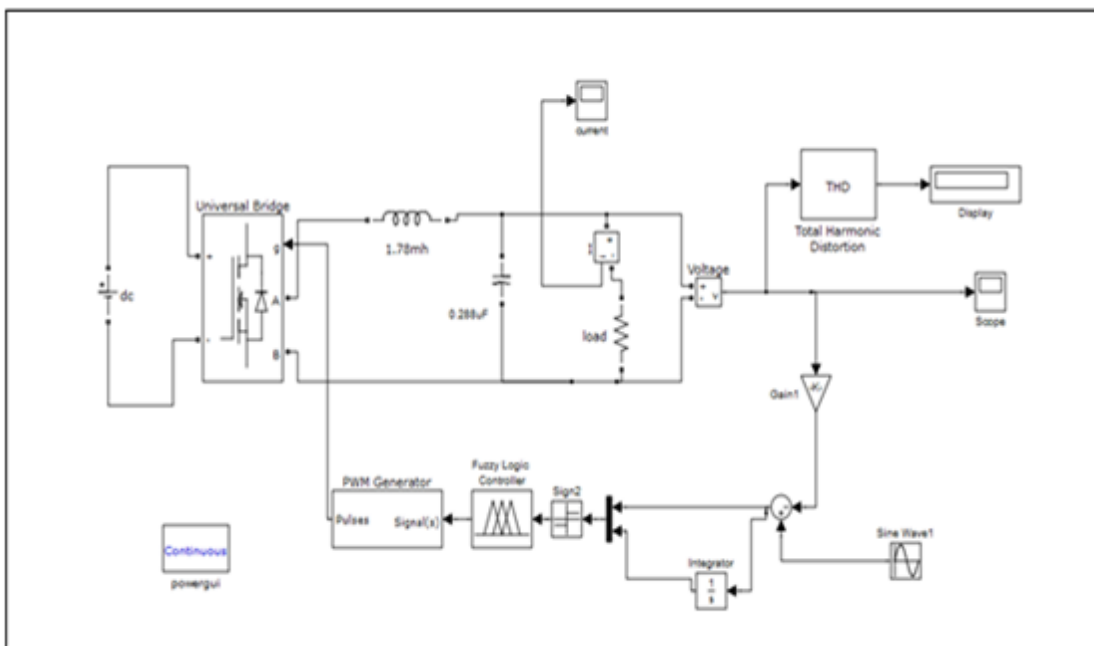


Figure 4.18: Matlab simulation for PWM inverter under fuzzy controller

The output is a sinusoidal wave with peak output voltage equal 309.5 volt where the RMS value equal 219 volt and the output frequency 50 Hz also it can be seen that the THD is equal 3.69%, which is well below the IEEE recommendation. So, it can be observed that the fuzzy logic controller has resulted in better than PI controller also the output current result for the load as figure(4.20) has peak value equal 7.03A (RMS equal 4.97A) and THD is the same as voltage output distortion .

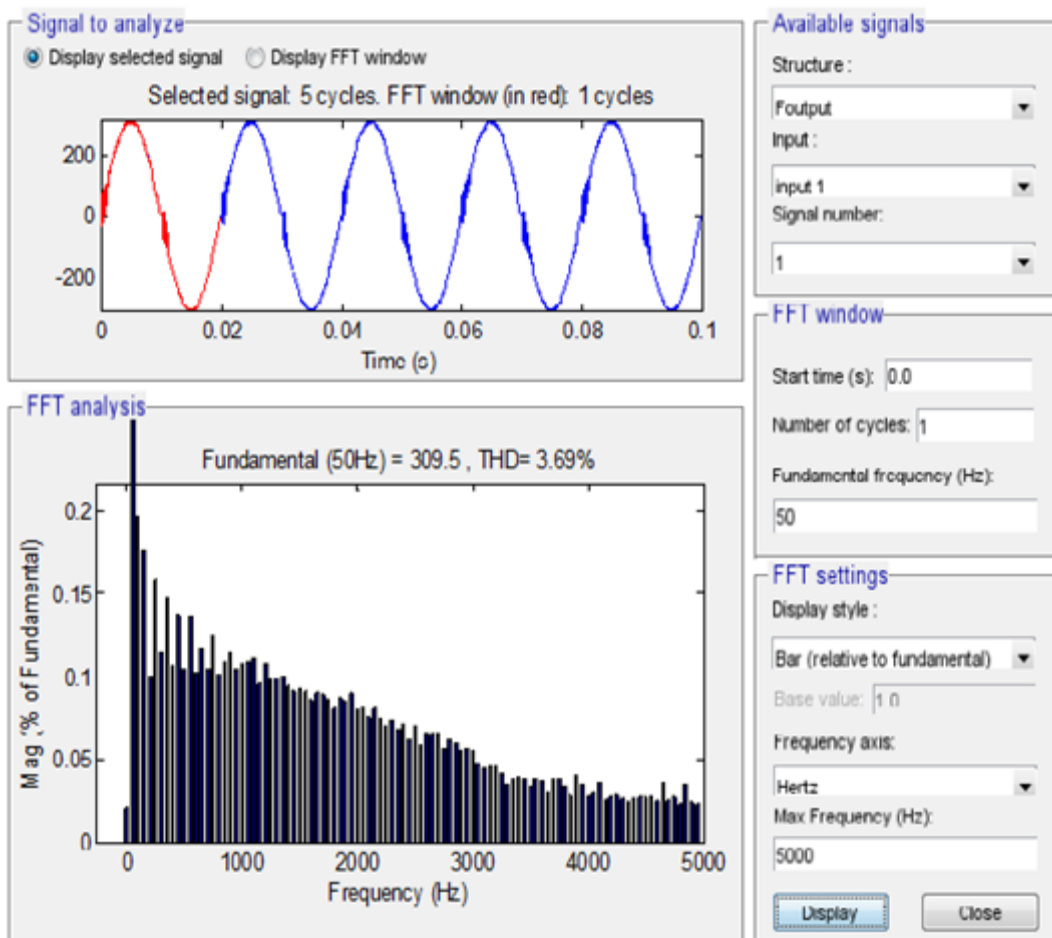


Figure 4.19: Load voltage and spectrum analyzer for full load PWM inverter under fuzzy logic controller



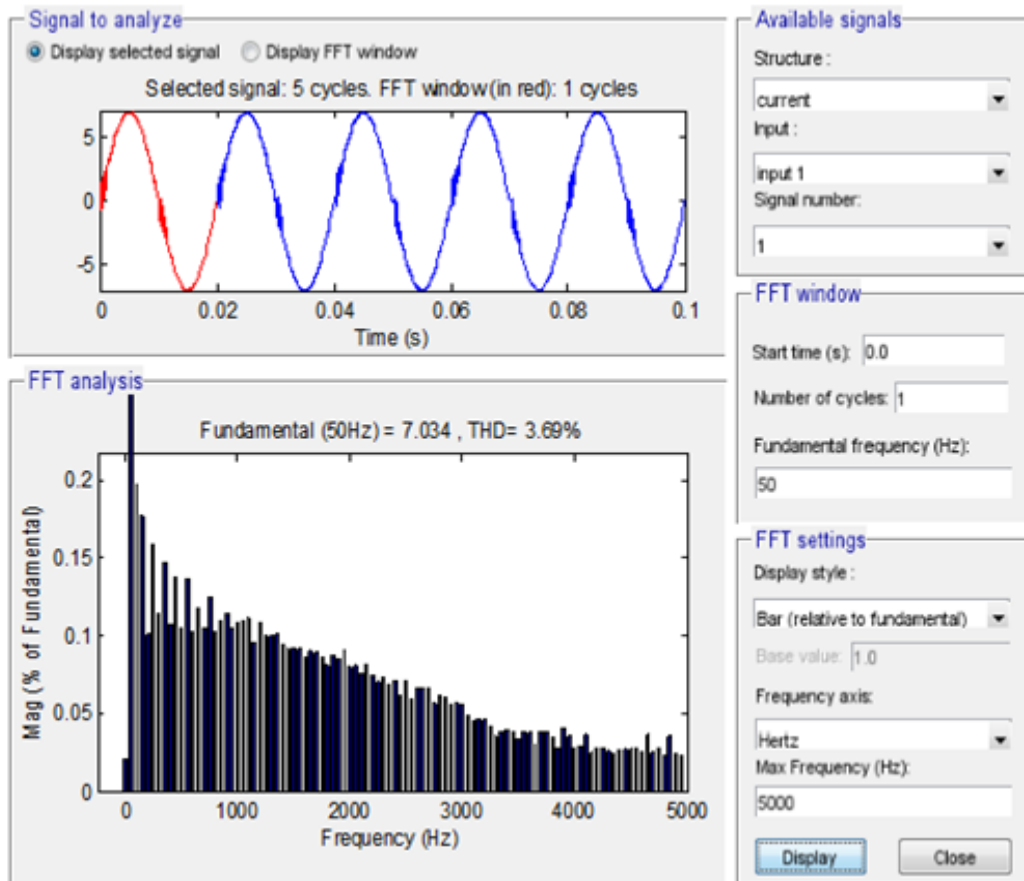


Figure 4.20: Load current and spectrum analyzer for full load PWM inverter under fuzzy logic controller

## CHAPTER 5

---

### HARDWARE IMPLEMENTATION FOR PROPOSED SYSTEM

#### 5.1 Introduction

In this chapter, the hardware implemented for the SPWM single phase inverter design is based on four schematic circuit which are: The push pull converter, PWM generator, MOSFET H-bridge and the fuzzy controller. The push pull converter is used to convert the low voltage coming from battery to high voltage where the standard voltage for the liquid battery is 12.6 v. The PWM generator is the main object in this design and it is done by comparing the reference signal with carrier signal. This signal is generated by using operational amplifier such as IC LM324 to generate the pulses that fed the gate. Actually the gate needs specific voltage to drive the MOSFET transistor in safe mode which guarantee that the transistor is fully turn on. The IR2110 integrated circuit is used to drive this transistor. Then a microcontroller with fuzzy rules is used to control PWM generator. The following design was implemented by the Proteus design suite simulator program and the Micro C language used to program the microcontroller[1].

#### 5.2 Push Pull Converter

Push-pull converter uses the transformer in a more traditional manner to transfer the energy directly between input and output. The schematic circuit for push pull converter proposed as figure (5.1) where the input for the converter is 12 VDC coming from battery. The output will be 350 VDC this mean that the transformer to be used is step up type . The output signal for transformer will be AC squared wave. The bridge rectifier BR1 rectifies this wave again and the capacitor is used to filter the output DC signal by removing the ripples.

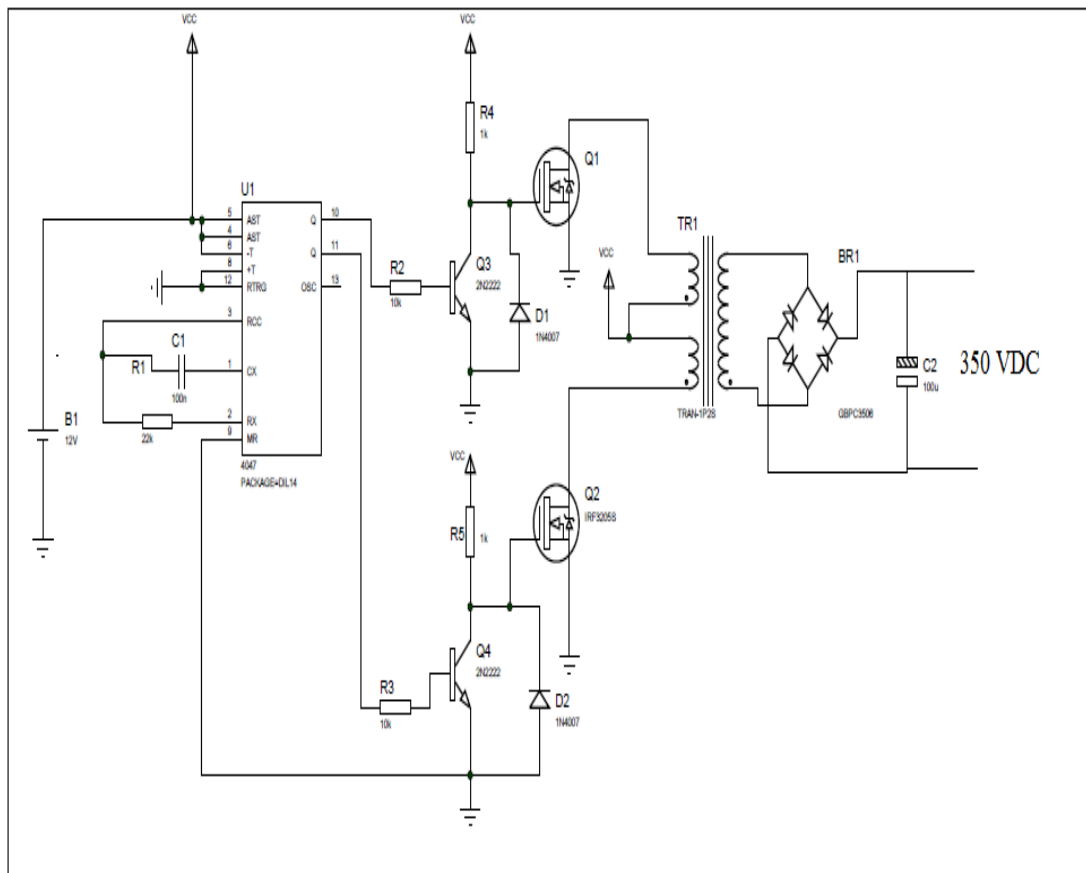


Figure 5.1: Schematic circuit for push pull converter

As illustrated figure (5.1), the pulses are generated by CD 4047 which is capable of operating in either the monostable or a stable mode. It requires an external capacitor (between pins 1 and 3) and an external resistor (between pins 2 and 3) to determine the output pulse width, the monostable mode, and the output frequency in the a stable mode.

A stable operation is enabled by a high level on the a stable input. The output frequency (at 50% duty cycle) at Q and Q' outputs is determined by the timing components where it is be  $(1/4.4 \cdot RC)$  see Appendix( B).

The other component circuit is used to amplify the signal and used to protect the integrated circuit.

### 5.3 SPWM Generators

PWM generator will be implemented by comparing reference signal with carrier signal, the reference signal will be sine wave signal with 1 volt /50HZ and the carrier signal is triangular wave with amplitude 1 volt /10KHZ the result for comparing tow signal is SPWM pulses.

The implemented circuit for SPWM pulses is based on three schematic circuits where it is bubba oscillator, carrier wave generator and the comparator circuit.

#### 5.3.1 Bubba Oscillator

The ability to generate a periodic signal without any crystals or resonators and using only a DC input source is useful for a large number of applications. This is exactly what the Bubba oscillator is capable of. Using only a single power supply in the unipolar version, the Bubba oscillator can create low distortion sine waves using op amps [24].

The implemented schematic circuit is shown in figure (5.2). It uses four stages to yield a remarkably stable output frequency. The availability of

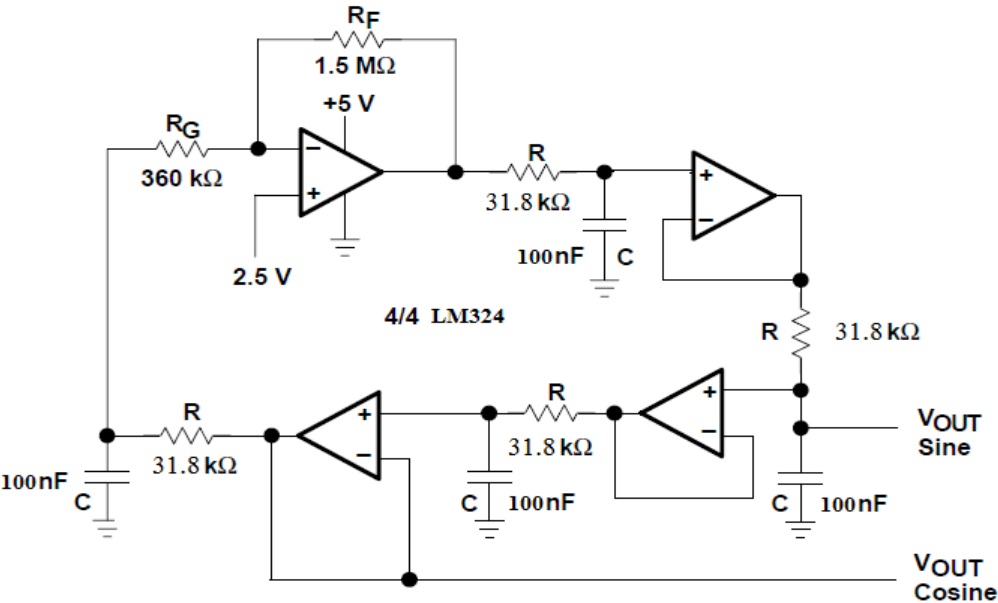


Figure 5.2: Schematic circuit for bubba oscillator

quad op amp integrated circuits makes implementation especially easy. Each one of the four op amps has a corresponding RC network external to the chip. Each of these networks contributes a phase shift of 45° for a total phase shift of 180° which is necessary to put the solution of the transfer function in oscillation. The most important equation when working with this circuit is the one that relates how the oscillation frequency depends on the values for R and C. This equation is found as :

$$f_0 = \frac{1}{2\pi RC} \quad 5.1$$

The above circuit has R=31.8 Kohm and C=100 nF so it is easily to find the frequency for reference signal where it is 50Hz , also the choice for selecting the signal output from bubba oscillator depends on THD. For more accuracy and small harmonic distortion the best signal output for above circuit is cosine wave .

### 5.3.2 Carrier Wave Generator

Carrier waves can be either sawtooth or triangular signals; in this study a triangular wave will be used. This wave will be at 10KHz and the generation of the triangular carrier wave will be done by using LM324. The circuit for the construction of the triangle wave generator consists of a square wave generator and integrator, as shown in figure (5.3). The circuit will oscillate at a frequency of  $1/4RtC$ , and the amplitude can be controlled by the amplitude of R1 and R2.

For this design R1= 100k R2=300K, R3=75k , Rf=2.5K, and C=0.01uF, the generated square and triangle waves oscillating at 10Khz.

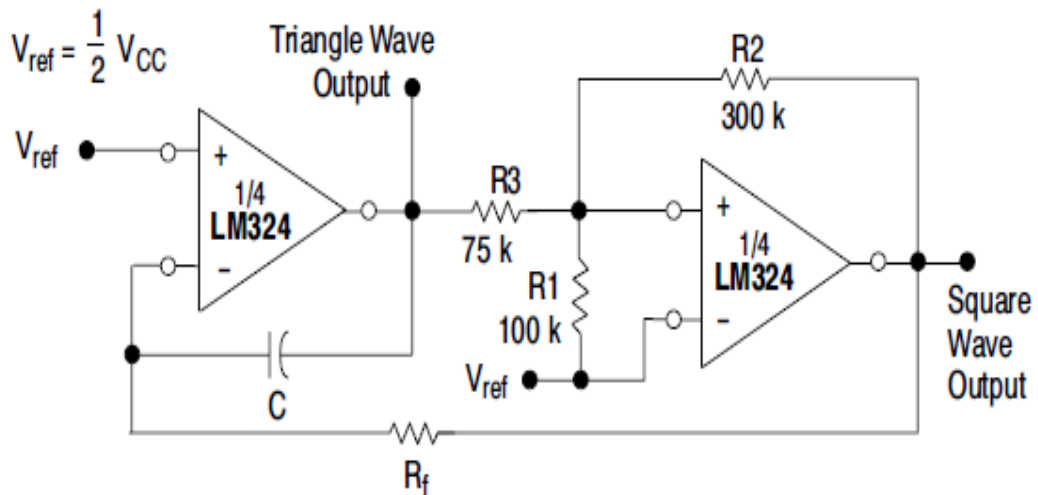


Figure 5.3: Schematic circuit for triangular generator

### 5.3.3 The Comparator Circuit

The final step for getting PWM pulses is to make comparison for the signals above this comparing is based on three procedure:

#### Step 1

Shift the carrier wave by one to be in positive y- axes side. This step is done by using adder circuit .

#### Step 2

Select the half cycle for reference signal and compare it with shifted carrier wave to get V<sub>gate1</sub>.

#### Step 3

Use the same procedure above to get V<sub>gate2</sub> but it should use the inverse of reference signal.

Figure (5.4) show the schematic circuit for all procedures by using Protuse simulator, the PWM generator is tested for 1KHz carrier frequency and the result signals is obtained by digital oscilloscope simulation as figure (5.5).

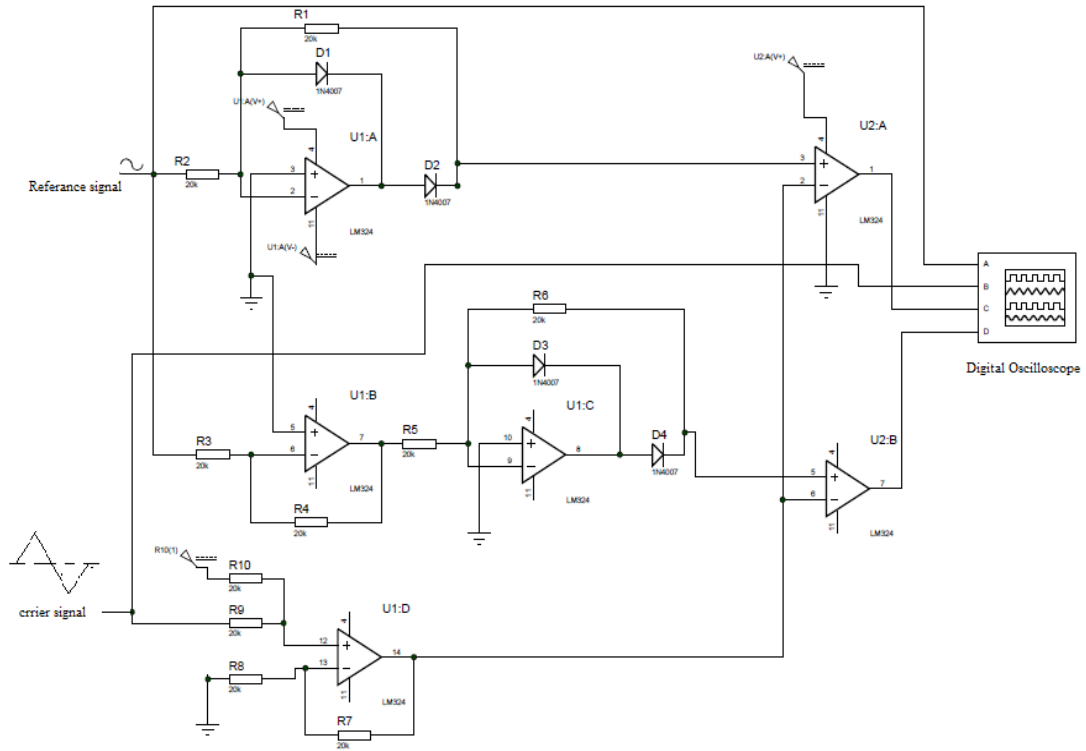


Figure 5.4: Schematic circuits for comparator circuit

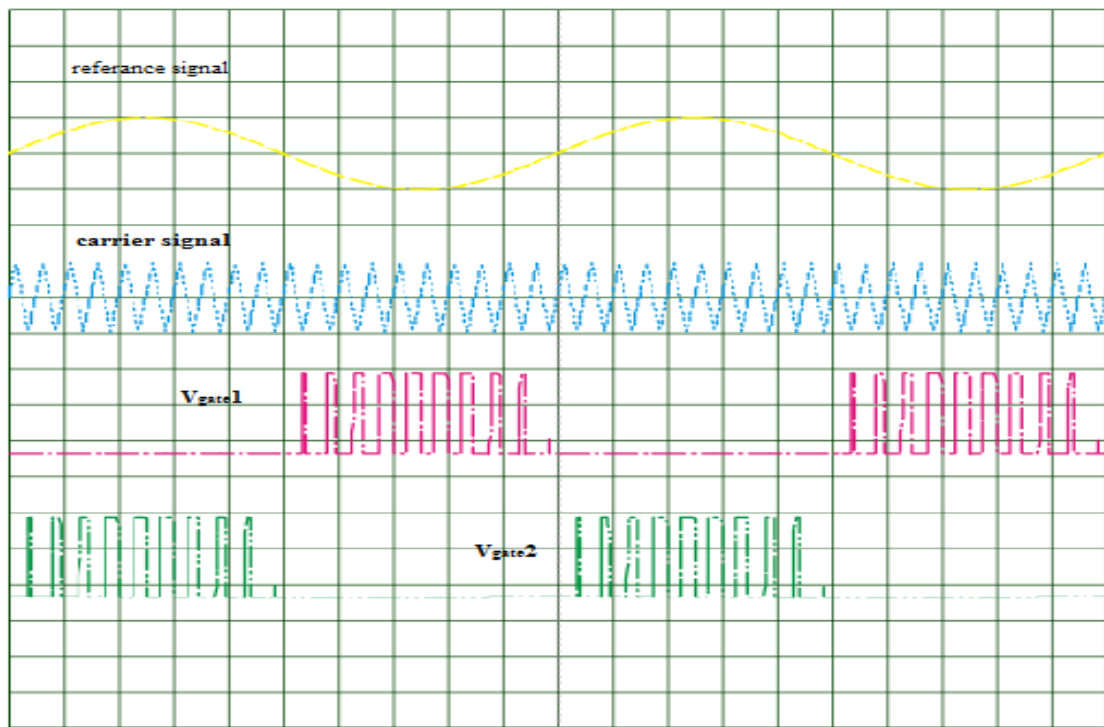


Figure 5.5: The output waves for PWM generator

## 5.4 H-Bridge and Driver Circuit

Generating a sine wave centered on zero volts requires both a positive and negative voltage across the load, for the positive and negative parts of the wave, respectively. This can be achieved from a single source through the use of four MOSFET IRF740 switches arranged in an H-Bridge configuration. Level translation between PWM signals and voltages is required to forward bias high side N-Channel MOSFETS, the IR2110 MOSFET driver integrated circuit was chosen where the high and low side drive device exceeds all requirements for driving the MOSFETs in the bridge. It is capable of handling up to 500V at a current rating of 2A at fast switching speeds. This device is required to drive the high side MOSFETS in the circuit designated HO, due to the fact that the gate to source voltage must be higher than the drain to source voltage, which is the highest voltage in the system. A typical connection of a single IR2110 device is shown in figure (5.6).

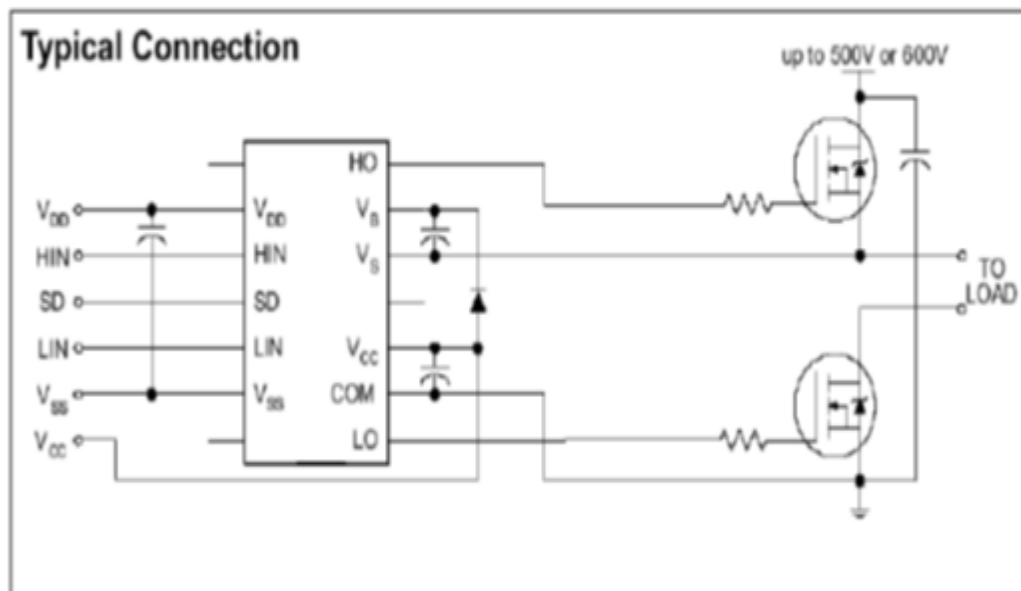


Figure 5.6: Typical connections for IR2110 driver



Operation of the IR2110 device will be controlled through generated PWM signals. The PWM signal will be fed to the HIN and LIN pins simultaneously. If the internal logic detects a logic high, the HO pin will be driven; if a logic low is detected, the LO pin will be driven. The SD pin controls shut down of the device and will be unused and tied to ground. A diagram of the H-Bridge circuit with MOSFETS and drivers is shown in figure (5.7).

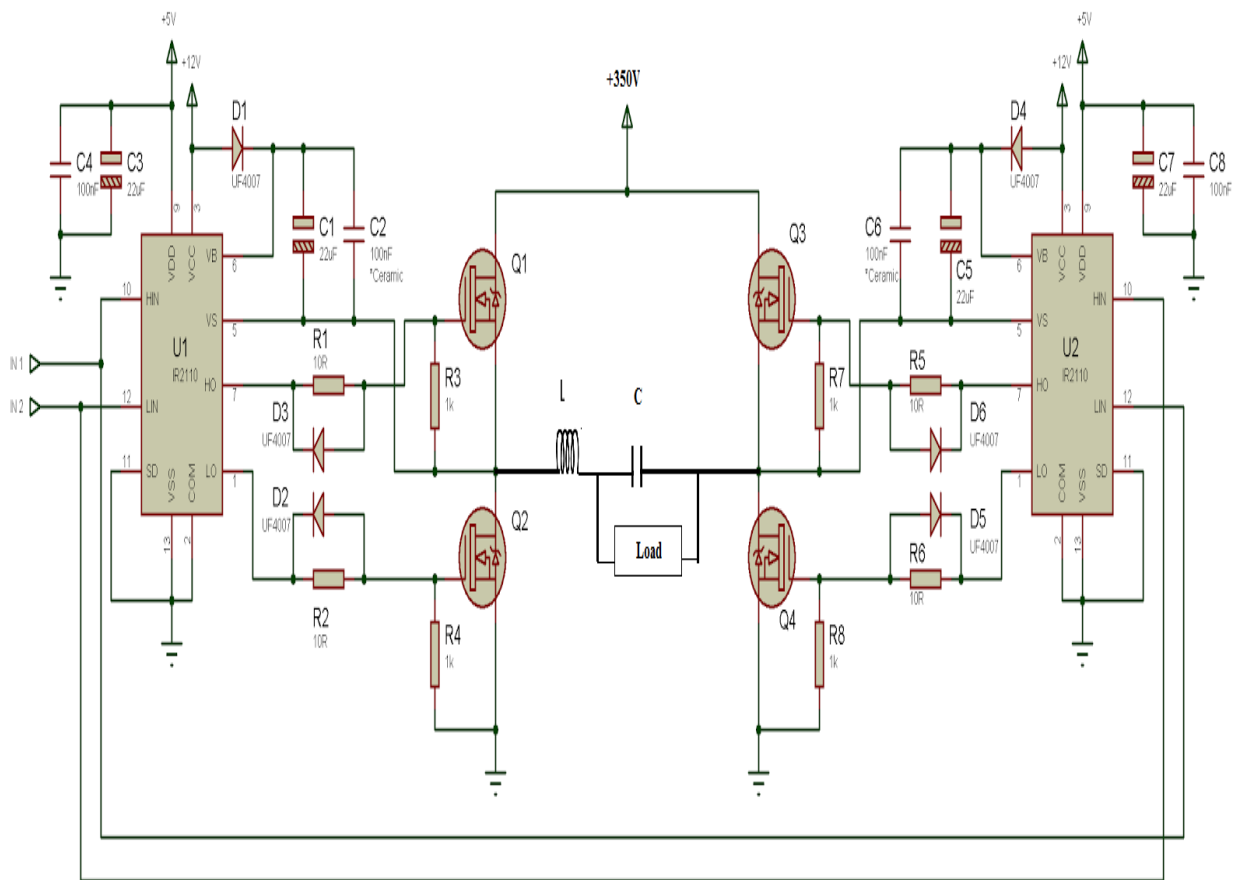


Figure 5.7: Schematic circuit for full bridge inverter with driver

## 5.5 Design Fuzzy Controller

In many application the controller is the main part of the system and changing it depend on the task of application. In this project, the PIC 16F877A microcontroller is used to implement the fuzzy controller. The PIC16F877A

provides several advantages over other microcontrollers. Different series of PIC microcontroller are popular because of high performance, low cost, low power consumption and small in size. The PIC 16F877A uses 35 single word instructions, and has 20MHZ operating frequency. The key features of PIC 16F877A are shown in table 5.1.

Table 5.1: Key features of PIC16F877A

Serial No	Key Features	PIC 16F877A
1	Operating Frequency	DC -20 MHZ
2	FLASH Program Memory	8K
3	Data memory (bytes)	368 Bytes
4	EEPROM Data Memory	15
5	Interrupts	14
6	I/O Ports	PORTS(A,B,C,D,E)
7	Timers	3
8	PWM modules	2
9	Serial Communications	MSSP,USART
10	Parallel Communications	PSP
11	10-bit A/D Module	8 INPUT CHANNELS
12	Instruction Set	35

### 5.5.1 How to Build Program in Microcontroller

Microcontrollers were originally programmed only in assembly language, but various high-level programming languages are now also in common use to target microcontrollers. These languages are either designed specially for the purpose, or versions of general purpose languages such as the C programming language. The most common program for this application is MikroC, a powerful, feature rich development tool for PICmicros. It is designed to provide the possible solution for developing applications for embedded systems, without compromising performance or control.

### 5.5.2 The Operation of Fuzzy Controller

Output voltage for the system is sensed and scaled to per unit for the based voltage 220 volt RMS, then it evaluates the error between the actual and set value. This result determines the main fuzzy rules of the system. the following criteria for fuzzy controller operation are as follow :

- i. If the output of the inverter deviates far from the reference, the change of modulation index must be large to bring the output to the reference quickly.
- ii. If the output of the inverter is approaching the reference, small change of modulation index is necessary.
- iii. If the output of the inverter is near the reference and is approaching it rapidly the modulation index must be kept constant so as to prevent further deviation.
- iv. If the reference is reached and the output is still changing the modulation index must be changed a little bit to prevent the output from moving away.
- v. If the reference is reached and the output is steady the modulation index remain unchanged.
- vi. If the output is larger than the reference, the sign of the change of modulation index must be negative and vice versa.

Fuzzy logic processing runs under these rules and the rules related to the rate of change of the set/actual offset, which allows a very smooth adjustment of voltage rate. Input data of the offset is calculated by means of taking relative voltage difference of actual voltage to the set value as shown below:-

$$\text{Error } (E) = (\text{Actual voltage of the System}) - (\text{Set Value})$$

Input data for integral error (IE) is the summation between the current value of error ( $E_n$ ) and the previous value of ( $E_{n-1}$ ):-

$$\text{Rate of integral error } (IE) = ((E_n) + (E_{n-1}))$$

The analog inputs is stored in 10-bit A/D converter in microcontroller and the output of modulation index takes values from 0 to 255 this value is converted to analog by using external D/A to keep the modulation index from 0 to 1.

### **5.6 Actual Hardware Implementation**

The following implementation hardware circuits are designed based on the results of the circuit that was designed by the simulation for example; figure (5.8) shows the actual hardware implementation for the push pull converter where the input is 12.6 VDC from battery and the output is 350V.

The output signal for the implemented circuit tested by oscilloscope before rectifying where it should to be square wave signal as shown in figure (5.9).

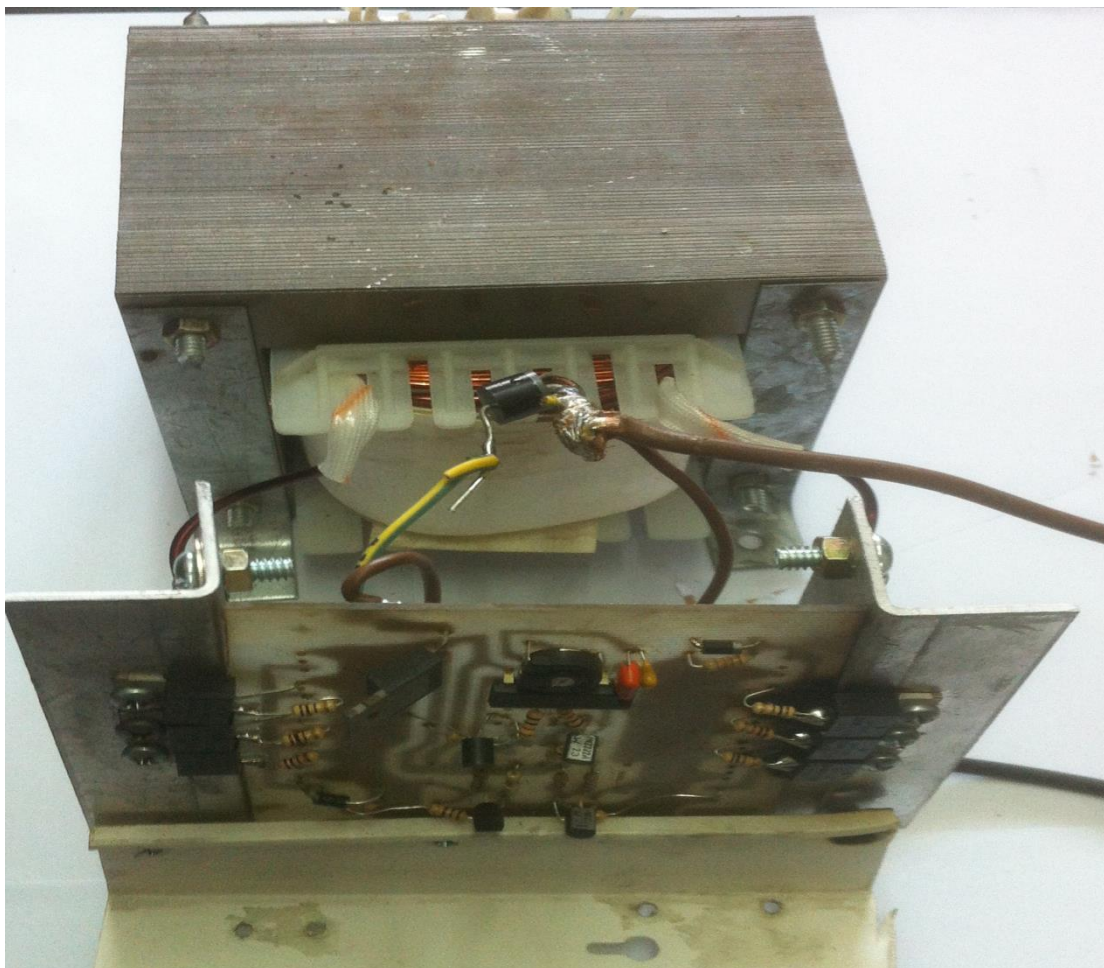


Figure 5.8: The actual hardware for push pull converter

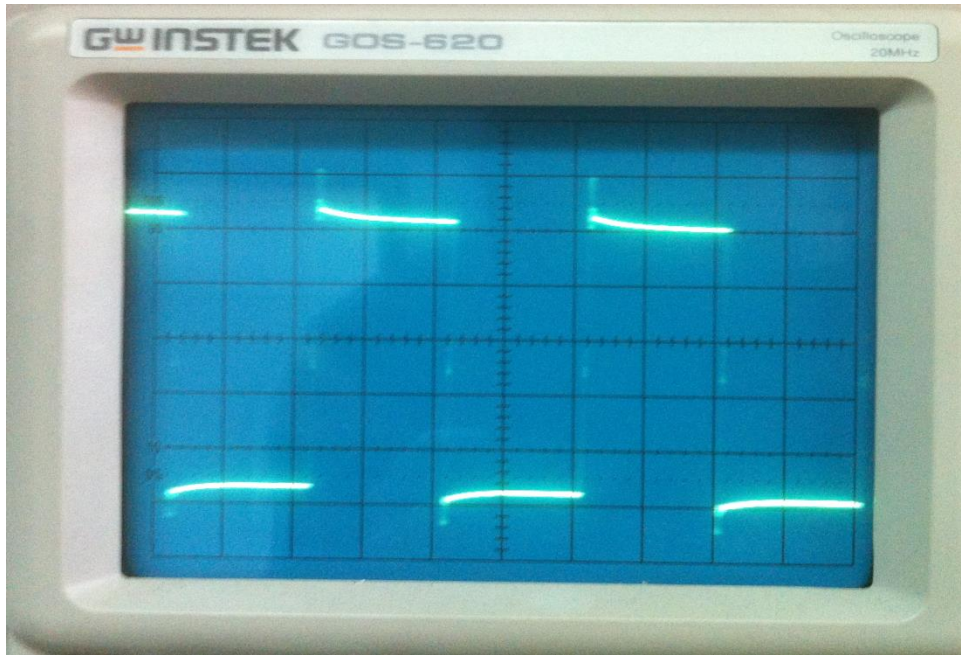


Figure 5.9: The AC output signal for the push pull converter

In addition, figure (5.10) shows the actual hardware implementation for the SPWM generator with fuzzy logic controller, which contains the bubble oscillator, triangular wave generator and the comparator circuits. The results outputs of this circuit is obtained by oscilloscope where figure (5.11) shows the reference cosine wave at 50Hz, figure(5.12) shows the carrier triangular wave at 10kHz and figure(5.13) shows the results output of comparing reference and carrier waves .

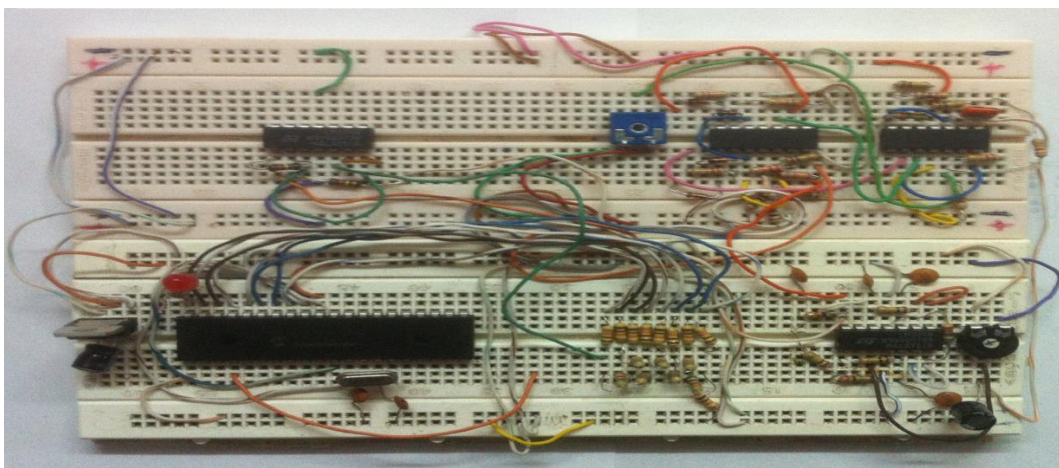


Figure 5.10: The actual hardware for SPWM generator with FLC.



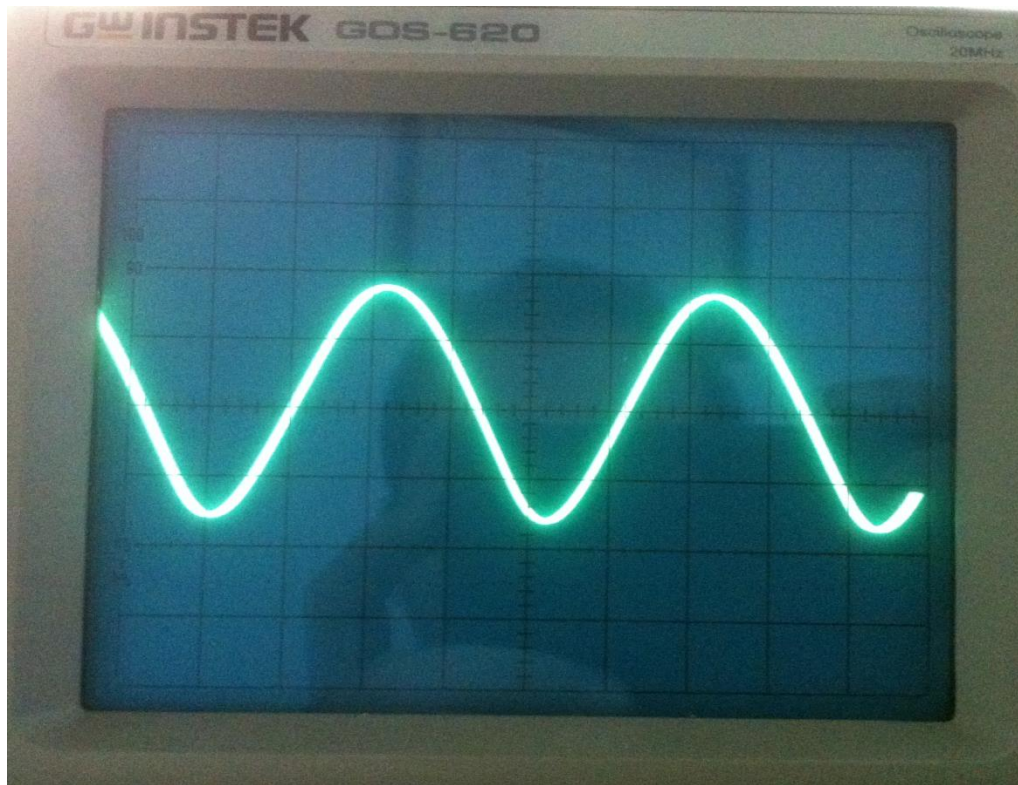


Figure 5.11: The result output from Bubba oscillator

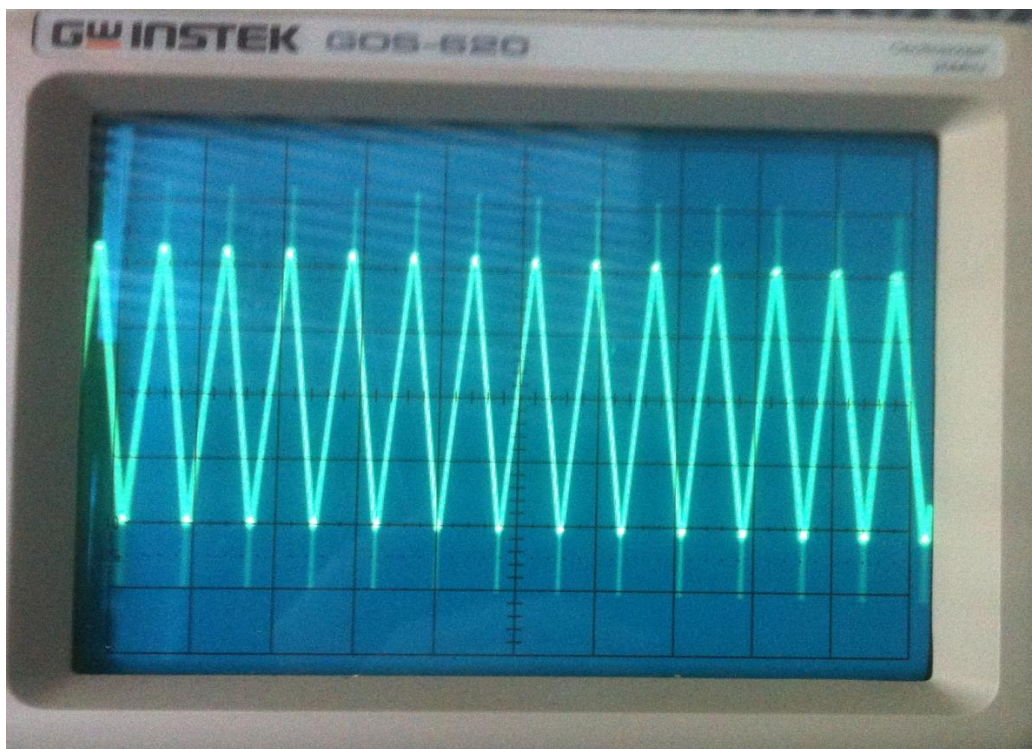


Figure 5.12: The result output from triangular generator

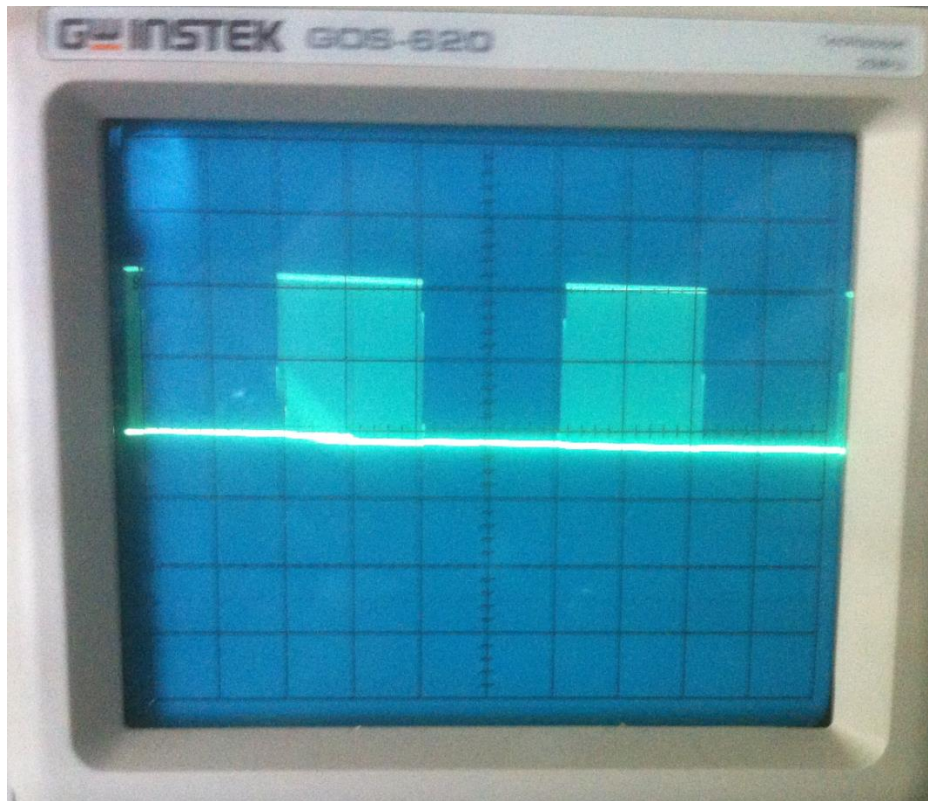


Figure 5.13: The generated pulses for SPWM generator

Also, figure (5.14) demonstrate the hardware implementation for H-Bridge with MOSFETS transistor and drivers circuit.

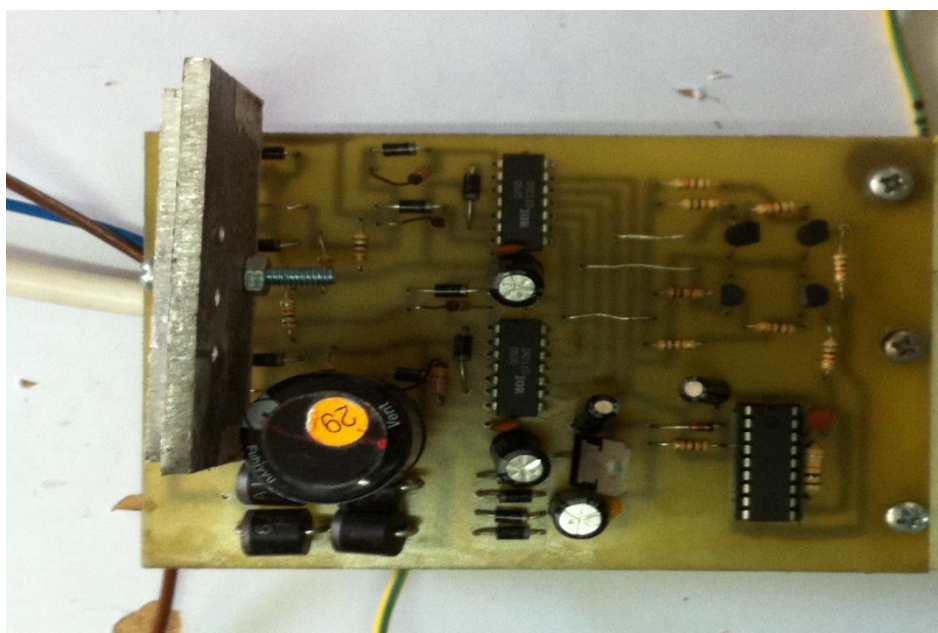


Figure 5.14: H-Bridge and driver circuit



## 5.7 Hardware Results

After collecting all parts of inverter, the new circuit is reconstructed as shown in figure (5.15) which it is tested under approximated load at 1KVA. The result output signal is shown in figure (5.16) which it is almost sine wave signal and having lower harmonic distortion. The result of RMS output voltage is (216 V), while the error of the output voltage is (1.8%) for fully loaded inverter. For more detail about the hardware implementation, refer to appendix C.

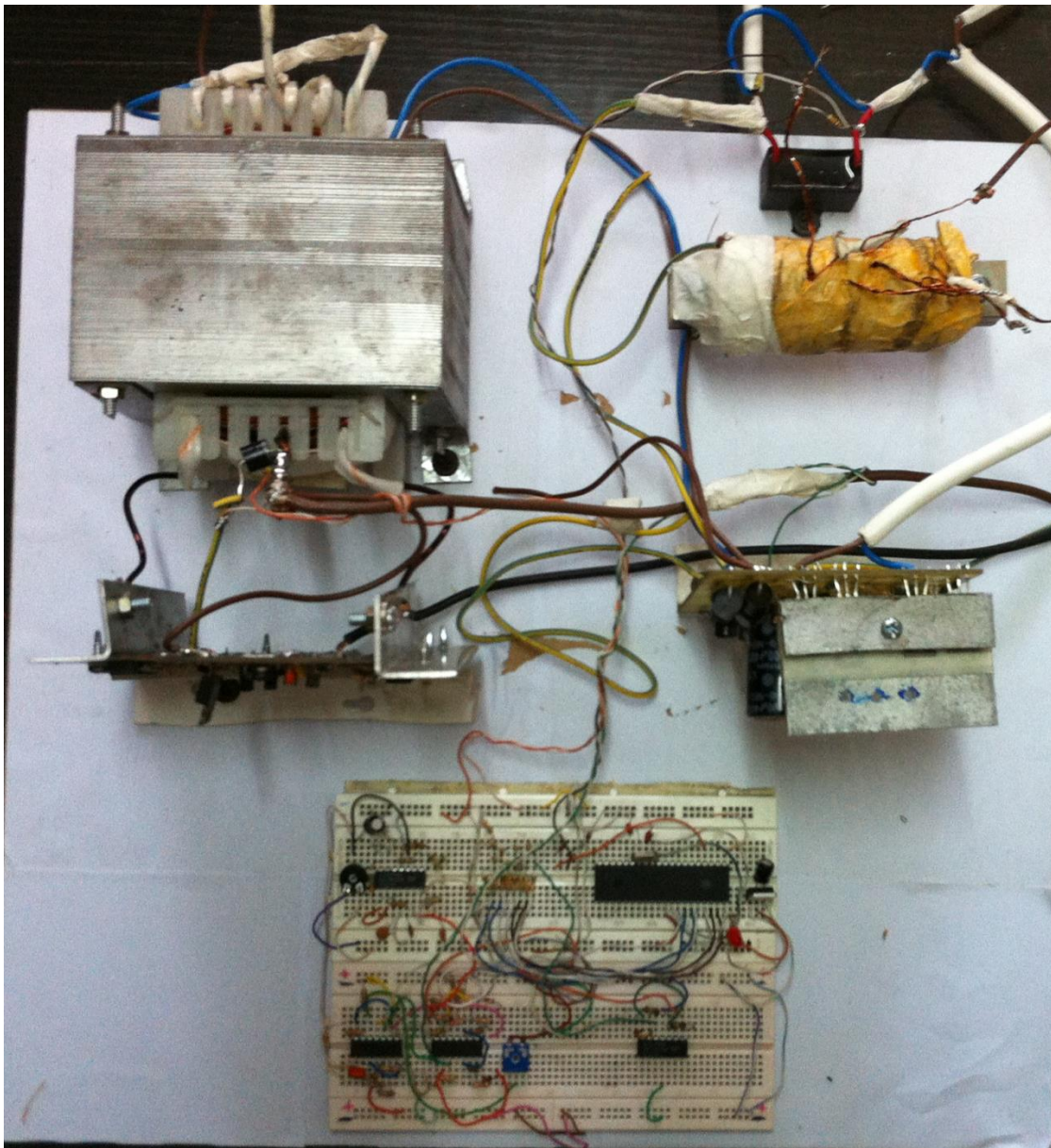


Figure 5.15: SPWM full bridge inverter



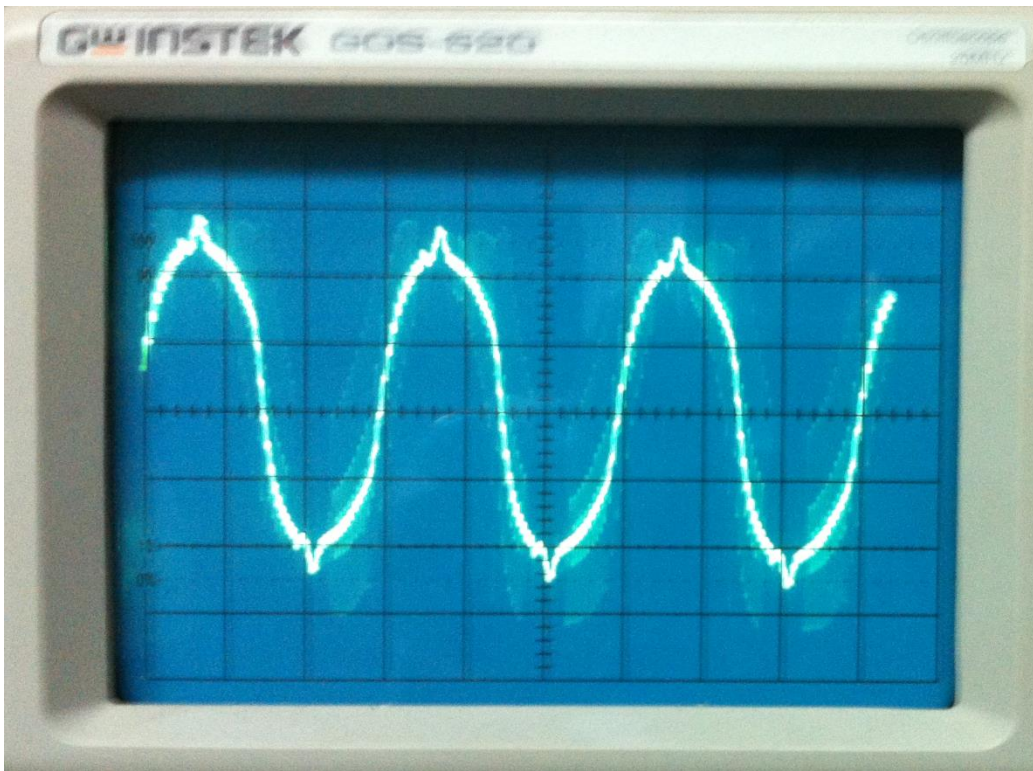


Figure 5.16: The result output signal for full load inverter

### CONCLUSIONS AND FUTURE WORKS

#### 6.1 Conclusions

Recently, inverters play an important role in various renewable energy applications where they are used for grid connection of wind energy system or photovoltaic system. Much progress has been made in successfully applying FLC in industrial control systems. Dominance of FLC's over the conventional controllers has become tight as it can work with imprecise inputs, can handle nonlinearity and it is more robust than conventional controllers. FLC techniques represent means of both collecting human knowledge and expertise and dealing with uncertainties in the process of control. The following points are accomplished:

1. In this research, the fuzzy logic and classical PI controllers are used for controlling inverter system as the output voltage is regulated and the total harmonic distortion (THD) is reduced controlling the modulation index also. The PWM technique was proposed to generate pure sine wave with small harmonic distortion .
2. The controllers fuzzy logic and PI were tested by using MATLAB simulink program and the comparison result shows that the fuzzy logic controller is the best choice for such application.
3. In this thesis, the controller for proposed system was implemented using microcontroller PIC16F877A and MICRO C program was used for programming this microcontroller. The hardware schematic circuits for all parts of the system was implemented and tested using Proteus program, which contain push-pull converter, PWM generator, H-bridge with MOSFET transistors and driver circuit.

4. The result of the hardware design implementation of the experiment almost matched the results that is obtained through simulations.

## **6.2 Future Works**

In this thesis, the fuzzy controller was implemented based on Mamdani approach for a single phase inverter system, it can be used in other application such as inductance heating and wilding machine also a good area for researching are multilevel and three phase inverters .

As future works, this study can be use Sugeno approaches along with optimization methods in order to reduce the rules of fuzzy controller.

## References

- [1] Sanjay Dixit, Ambreesh Tripathi, Vikas Chola, " 800VA pure sine wave inverter's reference design" *Texas instruments*, Application report SLAA602, June 2013.
- [2] Ang, Simon S T; Balda, Juan Carlos; Chiacchiarini, Héctor G. "Harmonic distortion reduction in power inverters" Power Electronics Specialists Conference, *IEEE 35th Annual*, Page(s): 1226 - 1231 Vol.2 , June 2004.
- [3] Timothy J. Ross, *Fuzzy Logic with Engineering Applications*, Third Edition, John Wiley & Sons, Ltd, 2010.
- [4] Aleksey Trubitsyn "high efficiency DC/AC power converter for photovoltaic application" Master Thesis, Boston University, 2010.
- [5] Rickard Ekström " Inverter System Design and Control for a Wave Power Substation" Master Thesis, Uppsala University, 2009.
- [6] Keith Jeremy McKenzie "Eliminating Harmonics in a Cascaded H-Bridges Multilevel Inverter Using Resultant Theory" Master thesis, University of Tennessee, Knoxville, 2004.
- [7] Robert A. Gannett "Control strategies for high power four-leg voltages source inverter" Master Thesis, Blacksburg Virginia, 2001.
- [8] Obasohan I. Omozusi " Dynamics and Control of A Batery Inverter Single-Phase Induction Generator System" Master thesis, Tennessee Technological University, Cookeville, 1998.
- [9] Yuqing Tang " High Power Inverter EMI characterization and Improvement Using Auxiliary Resonant Snubber Inverter" Master thesis, Virginia Polytechnic Institute and State University, Virginia, 1998.
- [10] L. Hassaine E. Olías1, M. Haddadi and A. Malek, "Asymmetric SPWM used in inverter grid connected" *Revue des Energies Renouvelables* Vol. 10 N°3, 421 – 429, 2007.
- [11] Surladi "Analysis Of Harmonic Current Minimization on Power Distribution System Using Voltage Phase Shifting Concepts " Master thesis, University of sains Malaysia, 2006
- [12] T. S. Perry. Lotfi A. Zadeh , "Fuzzy Logic Inventor Biography " *IEEE Spectrum*, pp. 32- 35, June 1995.
- [13] L. A. Zadeh. "Fuzzy sets", *Information and Control*, vol. 8, pp. 338-353, Berkeley California, 1965.

- [14] E. H. Mamdani and S. Assilian. "An experiment in linguistic synthesis with a fuzzy logic controller" *International Journal of Machine Studies*, 1975.
- [15] S. Yasunobu and S. Miyamoto. "Automatic train operation by fuzzy predictive control" In M. Sugeno, editor, *Industrial Applications of Fuzzy Control*. North Holland, 1985.
- [16] L.X. Wang , *A Course in Fuzzy Systems and Controls* , Englewood Cliffs, Prentice-Hall, 1997.
- [17] Basil Hamed, Lecture note for fuzzy logic control course, which was taught at Islamic university of Gaza strip, 2nd semester 2012.
- [18] John Yen & Langari Reza, *Fuzzy Logic Intelligence Control and Information*, Englewood Cliffs, Prentice-Hall, 1999.
- [19] Abdul Kareem Z. Mansoor and Ahmed G. Abdullah, "Analysis and Simulation of Single Phase Inverter Controlled By Neural Network" *Technical College, Al-Rafidain Engineering*, Vol.20 No. 6, Mosul, 2012.
- [20] M. E. Fraser , C. D. Manning "Performance of Average Current Mode Controlled PWM UPS Inverter with High Crest Factor Load," *IEEE Power Electronics and Variable-Speed Drives*, Conference Publication No 399, pp 661-667, 26 - 28 October 1994.
- [21] V. Tipsuwanporn A. Charoen , A. Numsomran and K. Phipek4, "A Single-Phase PWM Inverter Controlling Base on PLL Technique" *SICE Annual Conference*, Waseda University, Tokyo, Japan 2011.
- [22] S. M. Cherati N. A. Azli S. M. Ayob and A. Mortezaei," Design of a Current Mode PI Controller for a Single-phase PWM Inverter" *Power Electronics and Drive Research Group IEEE*, 2011.
- [23] N.Karthik, "Sib Converter with Reduced Harmonic Distortion Using Fuzzy Logic Controller" *IOSR Journal of Electrical and Electronics Engineering (IOSRJEET)* ISSN: 2278-1676 Volume 2, Issue 1, PP 46-50, July-Aug. 2012.
- [24] Ron Mancini and Richard Palmer "Sine-Wave Oscillator" *Texas instruments*, Application Report SLOA060 - March 2001.

## VITA



Farok Y. Sharaf has earned his B.Sc. degree in Electrical Engineering from Islamic University of Gaza on July 2006 and is currently pursuing M.S. degree in the Electrical Engineering with emphasis in Control Systems. His research thesis is focusing on re-designing and treating an Electrical Inverter Systems with Fuzzy Logic Controller for enhancing the performance and reducing the total harmonic distortion.

Also Mr. Sharaf is currently working as a Director of ElectroSharaf Company for Electronic Industries since 2006. His future plan is to pursue his Ph.D. study in Europe in the area of Solar Renewable Energy. Mr. Sharaf is married with two lovely kids, Yousef and Leen, also he is enjoying playing sports and reading.

# APPENDICES

## Appendix (A) Datasheet for Electronics Components



# PIC16F87XA

## 28/40/44-Pin Enhanced Flash Microcontrollers

### Devices Included in this Data Sheet:

- PIC16F873A
- PIC16F874A
- PIC16F876A
- PIC16F877A

### High-Performance RISC CPU:

- Only 35 single-word instructions to learn
- All single-cycle instructions except for program branches, which are two-cycle
- Operating speed: DC – 20 MHz clock input  
DC – 200 ns instruction cycle
- Up to 8K x 14 words of Flash Program Memory,  
Up to 368 x 8 bytes of Data Memory (RAM),  
Up to 256 x 8 bytes of EEPROM Data Memory
- Pinout compatible to other 28-pin or 40/44-pin  
PIC16CXXX and PIC16FXXX microcontrollers

### Peripheral Features:

- Timer0: 8-bit timer/counter with 8-bit prescaler
- Timer1: 16-bit timer/counter with prescaler,  
can be incremented during Sleep via external  
crystal/clock
- Timer2: 8-bit timer/counter with 8-bit period  
register, prescaler and postscaler
- Two Capture, Compare, PWM modules
  - Capture is 16-bit, max. resolution is 12.5 ns
  - Compare is 16-bit, max. resolution is 200 ns
  - PWM max. resolution is 10-bit
- Synchronous Serial Port (SSP) with SPI™  
(Master mode) and I<sup>2</sup>C™ (Master/Slave)
- Universal Synchronous Asynchronous Receiver  
Transmitter (USART/SCI) with 9-bit address  
detection
- Parallel Slave Port (PSP) – 8 bits wide with  
external RD, WR and CS controls (40/44-pin only)
- Brown-out detection circuitry for  
Brown-out Reset (BOR)

### Analog Features:

- 10-bit, up to 8-channel Analog-to-Digital  
Converter (A/D)
- Brown-out Reset (BOR)
- Analog Comparator module with:
  - Two analog comparators
  - Programmable on-chip voltage reference  
(VREF) module
  - Programmable input multiplexing from device  
inputs and internal voltage reference
  - Comparator outputs are externally accessible

### Special Microcontroller Features:

- 100,000 erase/write cycle Enhanced Flash  
program memory typical
- 1,000,000 erase/write cycle Data EEPROM  
memory typical
- Data EEPROM Retention > 40 years
- Self-reprogrammable under software control
- In-Circuit Serial Programming™ (ICSP™)  
via two pins
- Single-supply 5V In-Circuit Serial Programming
- Watchdog Timer (WDT) with its own on-chip RC  
oscillator for reliable operation
- Programmable code protection
- Power saving Sleep mode
- Selectable oscillator options
- In-Circuit Debug (ICD) via two pins

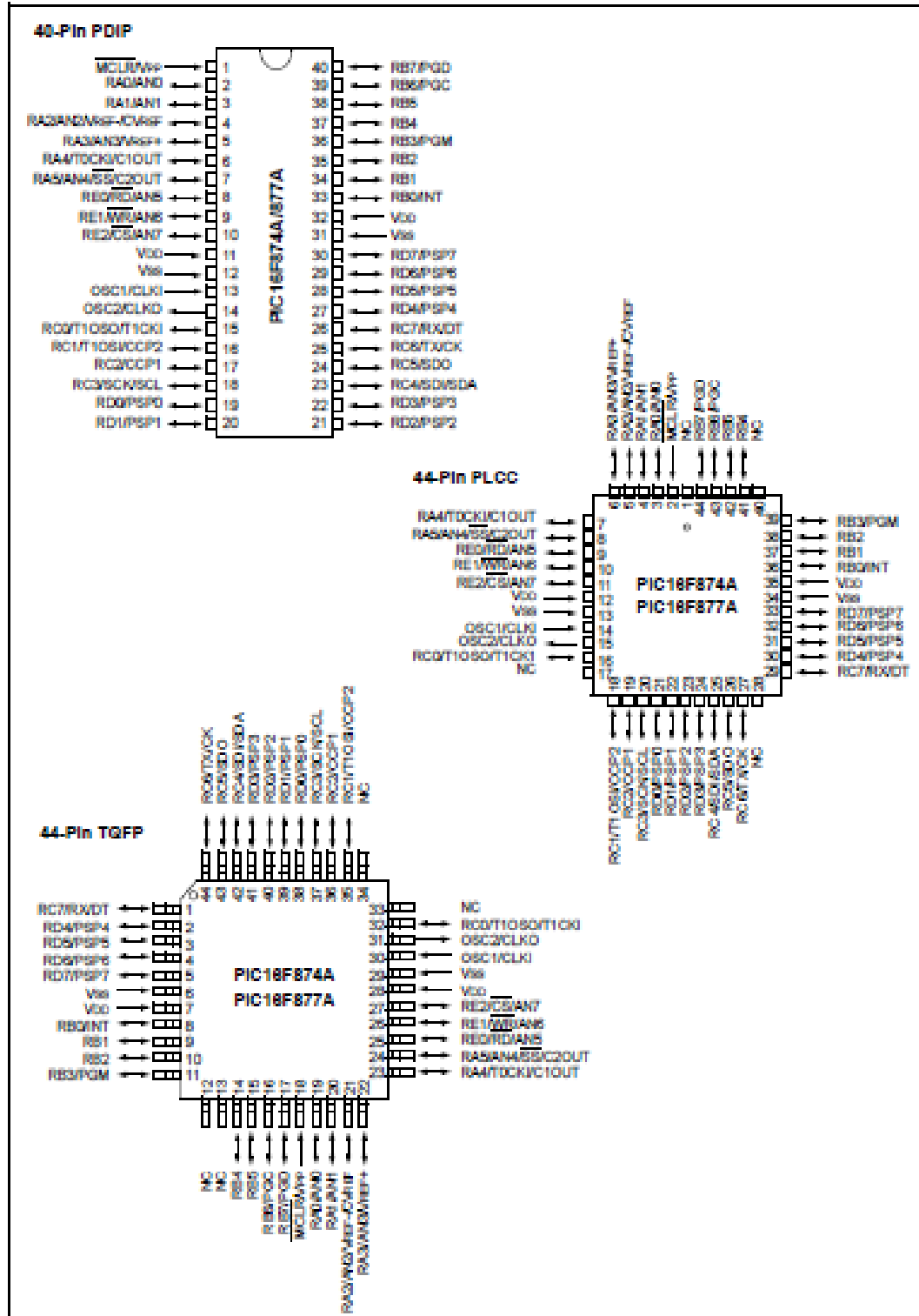
### CMOS Technology:

- Low-power, high-speed Flash/EEPROM  
technology
- Fully static design
- Wide operating voltage range (2.0V to 5.5V)
- Commercial and Industrial temperature ranges
- Low-power consumption

Device	Program Memory		Data SRAM (Bytes)	EEPROM (Bytes)	I/O	10-bit A/D (ch)	CCP (PWM)	MSSP		USART	Timers 8/16-bit	Comparators
	Bytes	# Single Word Instructions						SPI	Master I <sup>2</sup> C			
PIC16F873A	7.2K	4096	192	128	22	5	2	Yes	Yes	Yes	2/1	2
PIC16F874A	7.2K	4096	192	128	33	8	2	Yes	Yes	Yes	2/1	2
PIC16F876A	14.3K	8192	368	256	22	5	2	Yes	Yes	Yes	2/1	2
PIC16F877A	14.3K	8192	368	256	33	8	2	Yes	Yes	Yes	2/1	2

# PIC16F87XA

## Pin Diagrams (Continued)





## CD4047BC

### Low Power Monostable/Astable Multivibrator

#### General Description

The CD4047B is capable of operating in either the monostable or astable mode. It requires an external capacitor (between pins 1 and 3) and an external resistor (between pins 2 and 3) to determine the output pulse width in the monostable mode, and the output frequency in the astable mode.

Astable operation is enabled by a high level on the astable input or low level on the  $\overline{\text{astable}}$  input. The output frequency (at 50% duty cycle) at Q and  $\overline{Q}$  outputs is determined by the timing components. A frequency twice that of Q is available at the Oscillator Output; a 50% duty cycle is not guaranteed.

Monostable operation is obtained when the device is triggered by LOW-to-HIGH transition at + trigger input or HIGH-to-LOW transition at - trigger input. The device can be retriggered by applying a simultaneous LOW-to-HIGH transition to both the + trigger and retrigger inputs.

A high level on Reset input resets the outputs Q to LOW,  $\overline{Q}$  to HIGH.

#### Features

- Wide supply voltage range: 3.0V to 15V
- High noise immunity:  $0.45 V_{DD}$  (typ.)
- Low power TTL compatibility: Fan out of 2 driving 74L or 1 driving 74LS

#### SPECIAL FEATURES

- Low power consumption: special CMOS oscillator configuration
- Monostable (one-shot) or astable (free-running) operation

- True and complemented buffered outputs
- Only one external R and C required

#### MONOSTABLE MULTIVIBRATOR FEATURES

- Positive- or negative-edge trigger
- Output pulse width independent of trigger pulse duration
- Retriggerable option for pulse width expansion
- Long pulse widths possible using small RC components by means of external counter provision
- Fast recovery time essentially independent of pulse width
- Pulse-width accuracy maintained at duty cycles approaching 100%

#### ASTABLE MULTIVIBRATOR FEATURES

- Free-running or gatable operating modes
- 50% duty cycle
- Oscillator output available
- Good astable frequency stability  
typical =  $\pm 2\% + 0.03\%/^{\circ}\text{C}$  @ 100 kHz  
frequency =  $\pm 0.5\% + 0.015\%/^{\circ}\text{C}$  @ 10 kHz  
deviation (circuits trimmed to frequency  $V_{DD} = 10V \pm 10\%$ )

#### Applications

- Frequency discriminators
- Timing circuits
- Time-delay applications
- Envelope detection
- Frequency multiplication
- Frequency division

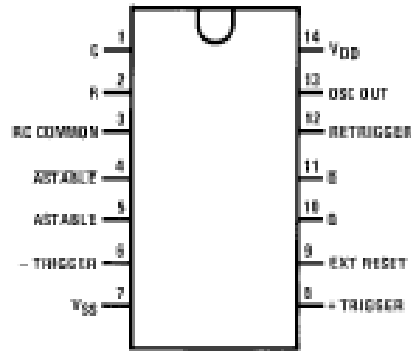
#### Ordering Code:

Order Number	Package Number	Package Description
CD4047BCM	M14A	14-Lead Small Outline Integrated Circuit (SOIC), JEDEC MS-120, 0.150" Narrow
CD4047BCN	N14A	14-Lead Plastic Dual-In-Line Package (PDIP), JEDEC MS-001, 0.300" Wide

Devices also available in Tape and Reel. Specify by appending the suffix letter "X" to the ordering code.

## Connection Diagram

Pin Assignments for SOIC and DIP



Top View

## Function Table

Function	Terminal Connections			Output Pulse From	Typical Output Period or Pulse Width
	To $V_{DD}$	To $V_{SS}$	Input Pulse To		
<b>Astable Multivibrator</b>					
Free-Running	4, 5, 6, 14	7, 8, 9, 12		10, 11, 13	$t_A(10, 11) = 4.40 RC$
True Gating	4, 6, 14	7, 8, 9, 12	5	10, 11, 13	$t_A(13) = 2.20 RC$
Complement Gating	6, 14	5, 7, 8, 9, 12	4	10, 11, 13	
<b>Monostable Multivibrator</b>					
Positive-Edge Trigger	4, 14	5, 6, 7, 9, 12	8	10, 11	
Negative-Edge Trigger	4, 8, 14	5, 7, 9, 12	6	10, 11	$t_M(10, 11) = 2.48 RC$
Retriggerable	4, 14	5, 6, 7, 9	8, 12	10, 11	
External Countdown (Note 1)	14	5, 6, 7, 8, 9, 12	Figure 1	Figure 1	Figure 1

Note 1: External resistor between terminals 2 and 3. External capacitor between terminals 1 and 3.

## Typical Implementation of External Countdown Option

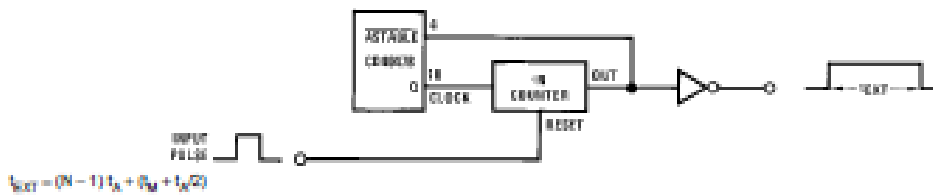


FIGURE 1.

$$t_{EXT} = (N - 1)t_A + t_M + t_{tr}(C)$$

## FEATURES

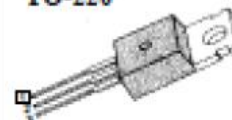
- ◆ Avalanche Rugged Technology
- ◆ Rugged Gate Oxide Technology
- ◆ Lower Input Capacitance
- ◆ Improved Gate Charge
- ◆ Extended Safe Operating Area
- ◆ Lower Leakage Current: 10 $\mu$ A (Max.) @  $V_{DS} = 400V$
- ◆ Lower  $R_{DS(on)}$ : 0.437 $\Omega$  (Typ.)

$$BV_{DSS} = 400 V$$

$$R_{DS(on)} = 0.55\Omega$$

$$I_D = 10 A$$

TO-220



1. Gate 2. Drain 3. Source

## Absolute Maximum Ratings

Symbol	Characteristic	Value	Units
$V_{DSS}$	Drain-to-Source Voltage	400	V
$I_D$	Continuous Drain Current ( $T_C=25^\circ C$ )	10	A
	Continuous Drain Current ( $T_C=100^\circ C$ )	6.3	
$I_{DM}$	Drain Current-Pulsed (1)	40	A
$V_{GS}$	Gate-to-Source Voltage	$\pm 30$	V
$E_{AS}$	Single Pulsed Avalanche Energy (2)	457	mJ
$I_{AR}$	Avalanche Current (1)	10	A
$E_{AR}$	Repetitive Avalanche Energy (1)	13.4	mJ
dv/dt	Peak Diode Recovery dv/dt (3)	4.0	V/ns
$P_D$	Total Power Dissipation ( $T_C=25^\circ C$ )	134	W
	Linear Derating Factor	1.08	
$T_J, T_{STG}$	Operating Junction and Storage Temperature Range	- 55 to +150	$^\circ C$
$T_L$	Maximum Lead Temp. for Soldering Purposes, 1/8, from case for 5-seconds	300	

## Thermal Resistance

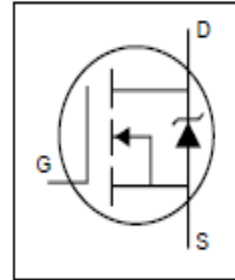
Symbol	Characteristic	Typ.	Max.	Units
$R_{\theta JC}$	Junction-to-Case	-	0.93	$^\circ C/W$
$R_{\theta CS}$	Case-to-Sink	0.5	-	
$R_{\theta JA}$	Junction-to-Ambient	-	62.5	

Rev. B

# IRF3205

HEXFET® Power MOSFET

- Advanced Process Technology
- Ultra Low On-Resistance
- Dynamic dv/dt Rating
- 175°C Operating Temperature
- Fast Switching
- Fully Avalanche Rated



$V_{DSS} = 55V$
$R_{DS(on)} = 8.0m\Omega$
$I_D = 110A^{\text{①}}$

## Description

Advanced HEXFET® Power MOSFETs from International Rectifier utilize advanced processing techniques to achieve extremely low on-resistance per silicon area. This benefit, combined with the fast switching speed and ruggedized device design that HEXFET power MOSFETs are well known for, provides the designer with an extremely efficient and reliable device for use in a wide variety of applications.

The TO-220 package is universally preferred for all commercial-industrial applications at power dissipation levels to approximately 50 watts. The low thermal resistance and low package cost of the TO-220 contribute to its wide acceptance throughout the industry.



TO-220AB

## Absolute Maximum Ratings


	Parameter	Max.	Units	
$I_D @ T_C = 25^\circ C$	Continuous Drain Current, $V_{GS} @ 10V$	110 ①	A	
$I_D @ T_C = 100^\circ C$	Continuous Drain Current, $V_{GS} @ 10V$	80		
$I_{DM}$	Pulsed Drain Current ①	390		
$P_D @ T_C = 25^\circ C$	Power Dissipation	200	W	
	Linear Derating Factor	1.3	W/°C	
$V_{GS}$	Gate-to-Source Voltage	$\pm 20$	V	
$I_{AR}$	Avalanche Current ①	62	A	
$E_{AR}$	Repetitive Avalanche Energy ①	20	mJ	
dv/dt	Peak Diode Recovery dv/dt ①	5.0	V/ns	
$T_J$	Operating Junction and Storage Temperature Range	-55 to +175	°C	
$T_{STG}$		Soldering Temperature, for 10 seconds		300 (1.8mm from case )
		Mounting torque, 6-32 or M3 screw		10 lbf·in (1.1N·m)

## Thermal Resistance


	Parameter	Typ.	Max.	Units
$R_{\theta JC}$	Junction-to-Case	—	0.75	°C/W
$R_{\theta CS}$	Case-to-Sink, Flat, Greased Surface	0.50	—	
$R_{\theta JA}$	Junction-to-Ambient	—	62	

# IRF3205

## Electrical Characteristics @ $T_J = 25^\circ\text{C}$ (unless otherwise specified)

	Parameter	Min.	Typ.	Max.	Units	Conditions
$V_{(BR)DSS}$	Drain-to-Source Breakdown Voltage	55	—	—	V	$V_{GS} = 0V, I_D = 250\mu A$
$\Delta V_{(BR)DSS}/\Delta T_J$	Breakdown Voltage Temp. Coefficient	—	0.057	—	V/°C	Reference to $25^\circ\text{C}, I_D = 1mA$
$R_{DS(on)}$	Static Drain-to-Source On-Resistance	—	—	8.0	m $\Omega$	$V_{GS} = 10V, I_D = 62A$ ①
$V_{GS(th)}$	Gate Threshold Voltage	2.0	—	4.0	V	$V_{DS} = V_{GS}, I_D = 250\mu A$
$g_{fs}$	Forward Transconductance	44	—	—	S	$V_{DS} = 25V, I_D = 62A$ ②
$I_{DSS}$	Drain-to-Source Leakage Current	—	—	25	$\mu A$	$V_{DS} = 55V, V_{GS} = 0V$
		—	—	250		$V_{DS} = 44V, V_{GS} = 0V, T_J = 150^\circ\text{C}$
$I_{GSS}$	Gate-to-Source Forward Leakage	—	—	100	nA	$V_{GS} = 20V$
	Gate-to-Source Reverse Leakage	—	—	-100		$V_{GS} = -20V$
$Q_g$	Total Gate Charge	—	—	146	nC	$I_D = 62A$
$Q_{gs}$	Gate-to-Source Charge	—	—	35		$V_{DS} = 44V$
$Q_{gd}$	Gate-to-Drain ("Miller") Charge	—	—	54		$V_{GS} = 10V$ , See Fig. 6 and 13
$t_{d(on)}$	Turn-On Delay Time	—	14	—	ns	$V_{DD} = 28V$
$t_r$	Rise Time	—	101	—		$I_D = 62A$
$t_{d(off)}$	Turn-Off Delay Time	—	50	—		$R_G = 4.5\Omega$
$t_f$	Fall Time	—	65	—		$V_{GS} = 10V$ , See Fig. 10 ③
$L_D$	Internal Drain Inductance	—	4.5	—	nH	Between lead, 6mm (0.25in.) from package and center of die contact 
$L_S$	Internal Source Inductance	—	7.5	—		
$C_{iss}$	Input Capacitance	—	3247	—	pF	$V_{GS} = 0V$
$C_{oss}$	Output Capacitance	—	781	—		$V_{DS} = 25V$
$C_{riss}$	Reverse Transfer Capacitance	—	211	—		$f = 1.0MHz$ , See Fig. 5
$E_{AS}$	Single Pulse Avalanche Energy ④	—	1050 ⑤	264 ⑥	mJ	$I_{AS} = 62A, L = 138\mu H$

## Source-Drain Ratings and Characteristics

	Parameter	Min.	Typ.	Max.	Units	Conditions
$I_S$	Continuous Source Current (Body Diode)	—	—	110	A	MOSFET symbol showing the integral reverse p-n junction diode. 
$I_{SM}$	Pulsed Source Current (Body Diode) ①	—	—	390		
$V_{SD}$	Diode Forward Voltage	—	—	1.3	V	$T_J = 25^\circ\text{C}, I_S = 62A, V_{GS} = 0V$ ②
$t_{rr}$	Reverse Recovery Time	—	69	104	ns	$T_J = 25^\circ\text{C}, I_F = 62A$
$Q_{rr}$	Reverse Recovery Charge	—	143	215	nC	$di/dt = 100A/\mu s$ ③
$t_{on}$	Forward Turn-On Time	Intrinsic turn-on time is negligible (turn-on is dominated by $L_S + L_D$ )				

### Notes:

- ① Repetitive rating; pulse width limited by max. junction temperature. ( See fig. 11 )
- ② Starting  $T_J = 25^\circ\text{C}, L = 138\mu H$   
 $R_G = 25\Omega, I_{AS} = 62A$ . (See Figure 12)
- ③  $I_{SD} \leq 62A, di/dt \leq 207A/\mu s, V_{DD} \leq V_{(BR)DSS}, T_J \leq 175^\circ\text{C}$
- ④ Pulse width  $\leq 400\mu s$ ; duty cycle  $\leq 2\%$ .
- ⑤ Calculated continuous current based on maximum allowable junction temperature. Package limitation current is 75A.
- ⑥ This is a typical value at device destruction and represents operation outside rated limits.
- ⑦ This is a calculated value limited to  $T_J = 175^\circ\text{C}$ .

# LM324, LM324A, LM224, LM2902, LM2902V, NCV2902

## Single Supply Quad Operational Amplifiers

The LM324 series are low-cost, quad operational amplifiers with true differential inputs. They have several distinct advantages over standard operational amplifier types in single supply applications. The quad amplifier can operate at supply voltages as low as 3.0 V or as high as 32 V with quiescent currents about one-fifth of those associated with the MC1741 (on a per amplifier basis). The common mode input range includes the negative supply, thereby eliminating the necessity for external biasing components in many applications. The output voltage range also includes the negative power supply voltage.

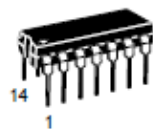
### Features

- Short Circuited Protected Outputs
- True Differential Input Stage
- Single Supply Operation: 3.0 V to 32 V
- Low Input Bias Currents: 100 nA Maximum (LM324A)
- Four Amplifiers Per Package
- Internally Compensated
- Common Mode Range Extends to Negative Supply
- Industry Standard Pinouts
- ESD Clamps on the Inputs Increase Ruggedness without Affecting Device Operation
- Pb-Free Packages are Available\*
- NCV Prefix for Automotive and Other Applications Requiring Site and Control Changes



**ON Semiconductor®**

<http://onsemi.com>



PDIP-14  
N SUFFIX  
CASE 646

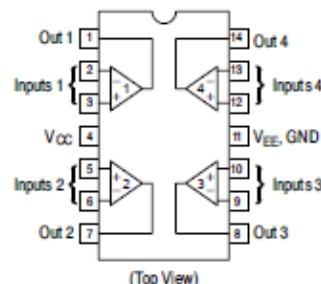


SOIC-14  
D SUFFIX  
CASE 751A



TSSOP-14  
DTB SUFFIX  
CASE 948G

### PIN CONNECTIONS



### ORDERING INFORMATION

See detailed ordering and shipping information in the package dimensions section on page 10 of this data sheet.

### DEVICE MARKING INFORMATION

See general marking information in the device marking section on page 12 of this data sheet.

\*For additional information on our Pb-Free strategy and soldering details, please download the ON Semiconductor Soldering and Mounting Techniques Reference Manual, SOLDERRM/D.



## IR2110(S)/IR2113(S) & (PbF)

### HIGH AND LOW SIDE DRIVER

#### Features

- Floating channel designed for bootstrap operation  
Fully operational to +500V or +600V  
Tolerant to negative transient voltage  
dV/dt immune
- Gate drive supply range from 10 to 20V
- Undervoltage lockout for both channels
- 3.3V logic compatible  
Separate logic supply range from 3.3V to 20V  
Logic and power ground  $\pm 5V$  offset
- CMOS Schmitt-triggered inputs with pull-down
- Cycle by cycle edge-triggered shutdown logic
- Matched propagation delay for both channels
- Outputs in phase with inputs
- Also available LEAD-FREE

#### Description

The IR2110/IR2113 are high voltage, high speed power MOSFET and IGBT drivers with independent high and low side referenced output channels. Proprietary HVIC and latch immune CMOS technologies enable ruggedized monolithic construction. Logic inputs are compatible with standard CMOS or LSTTL output, down to 3.3V logic. The output drivers feature a high pulse current buffer stage designed for minimum driver cross-conduction. Propagation delays are matched to simplify use in high frequency applications. The floating channel can be used to drive an N-channel power MOSFET or IGBT in the high side configuration which operates up to 500 or 600 volts.

#### Product Summary

$V_{\text{OFFSET}}$ (IR2110)	500V max.
(IR2113)	600V max.
$I_{\text{O+/-}}$	2A / 2A
$V_{\text{OUT}}$	10 - 20V
$t_{\text{on/off}}$ (typ.)	120 & 94 ns
Delay Matching (IR2110)	10 ns max.
(IR2113)	20ns max.

#### Packages

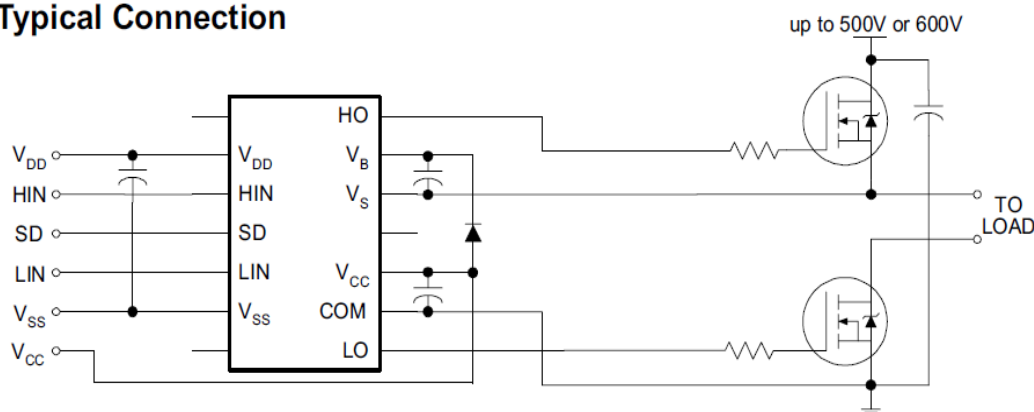


14-Lead PDIP  
IR2110/IR2113



16-Lead SOIC  
IR2110S/IR2113S  
(Also available  
LEAD-FREE (PbF))

#### Typical Connection



(Refer to Lead Assignments for correct pin configuration). This/These diagram(s) show electrical connections only. Please refer to our Application Notes and DesignTips for proper circuit board layout.

# IR2110(s)/IR2113(S) & (PbF)

International  
IR Rectifier

## Absolute Maximum Ratings

Absolute maximum ratings indicate sustained limits beyond which damage to the device may occur. All voltage parameters are absolute voltages referenced to COM. The thermal resistance and power dissipation ratings are measured under board mounted and still air conditions. Additional information is shown in Figures 28 through 35.

Symbol	Definition	Min.	Max.	Units	
V <sub>B</sub>	High side floating supply voltage (IR2110)	-0.3	525	V	
	(IR2113)	-0.3	625		
V <sub>S</sub>	High side floating supply offset voltage	V <sub>B</sub> - 25	V <sub>B</sub> + 0.3		
V <sub>HO</sub>	High side floating output voltage	V <sub>S</sub> - 0.3	V <sub>B</sub> + 0.3		
V <sub>CC</sub>	Low side fixed supply voltage	-0.3	25		
V <sub>LO</sub>	Low side output voltage	-0.3	V <sub>CC</sub> + 0.3		
V <sub>DD</sub>	Logic supply voltage	-0.3	V <sub>SS</sub> + 25		
V <sub>SS</sub>	Logic supply offset voltage	V <sub>CC</sub> - 25	V <sub>CC</sub> + 0.3		
V <sub>IN</sub>	Logic input voltage (HIN, LIN & SD)	V <sub>SS</sub> - 0.3	V <sub>DD</sub> + 0.3		
dV <sub>S</sub> /dt	Allowable offset supply voltage transient (figure 2)	—	50		V/ns
P <sub>D</sub>	Package power dissipation @ T <sub>A</sub> ≤ +25°C	(14 lead DIP)	—	1.6	W
		(16 lead SOIC)	—	1.25	
R <sub>THJA</sub>	Thermal resistance, junction to ambient	(14 lead DIP)	—	75	°C/W
		(16 lead SOIC)	—	100	
T <sub>J</sub>	Junction temperature	—	150	°C	
T <sub>S</sub>	Storage temperature	-55	150		
T <sub>L</sub>	Lead temperature (soldering, 10 seconds)	—	300		

## Recommended Operating Conditions

The input/output logic timing diagram is shown in figure 1. For proper operation the device should be used within the recommended conditions. The V<sub>S</sub> and V<sub>SS</sub> offset ratings are tested with all supplies biased at 15V differential. Typical ratings at other bias conditions are shown in figures 36 and 37.

Symbol	Definition	Min.	Max.	Units
V <sub>B</sub>	High side floating supply absolute voltage	V <sub>S</sub> + 10	V <sub>S</sub> + 20	V
V <sub>S</sub>	High side floating supply offset voltage (IR2110)	Note 1	500	
	(IR2113)	Note 1	600	
V <sub>HO</sub>	High side floating output voltage	V <sub>S</sub>	V <sub>B</sub>	
V <sub>CC</sub>	Low side fixed supply voltage	10	20	
V <sub>LO</sub>	Low side output voltage	0	V <sub>CC</sub>	
V <sub>DD</sub>	Logic supply voltage	V <sub>SS</sub> + 3	V <sub>SS</sub> + 20	
V <sub>SS</sub>	Logic supply offset voltage	-5 (Note 2)	5	
V <sub>IN</sub>	Logic input voltage (HIN, LIN & SD)	V <sub>SS</sub>	V <sub>DD</sub>	
T <sub>A</sub>	Ambient temperature	-40	125	

Note 1: Logic operational for V<sub>S</sub> of -4 to +500V. Logic state held for V<sub>S</sub> of -4V to -V<sub>BS</sub>. (Please refer to the Design Tip DT97-3 for more details).

Note 2: When V<sub>DD</sub> < 5V, the minimum V<sub>SS</sub> offset is limited to -V<sub>DD</sub>.



## Appendix (B)

### Details of Hardware Implementation

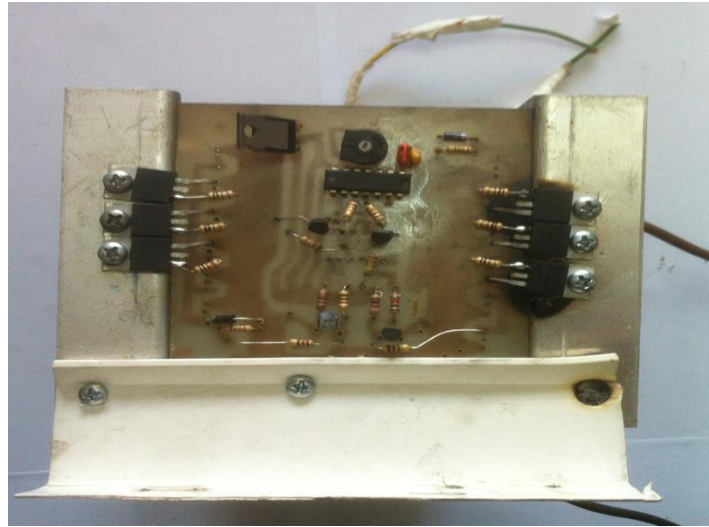


Figure c1

Figure c1 illustrate the push pull converter circuit which have six MOSFEET IRF3205 with heting skins also, IC CD4047 is used to generate square pulses.



Figure c2

Figure c2 demonstrate the center tap of transformer which having (13 0 13) volt in primary and 360 V in secondary, the core of transformer is (40mm\*80mm)

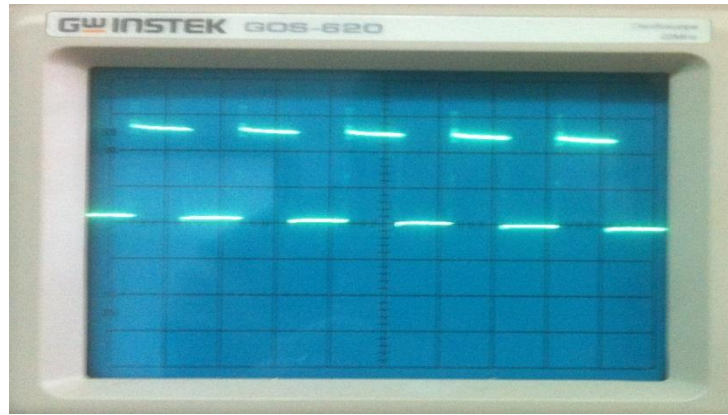


Figure c3

Figure c3 shows the square pulses generated by CD4047 for push pull converter using oscilloscope.

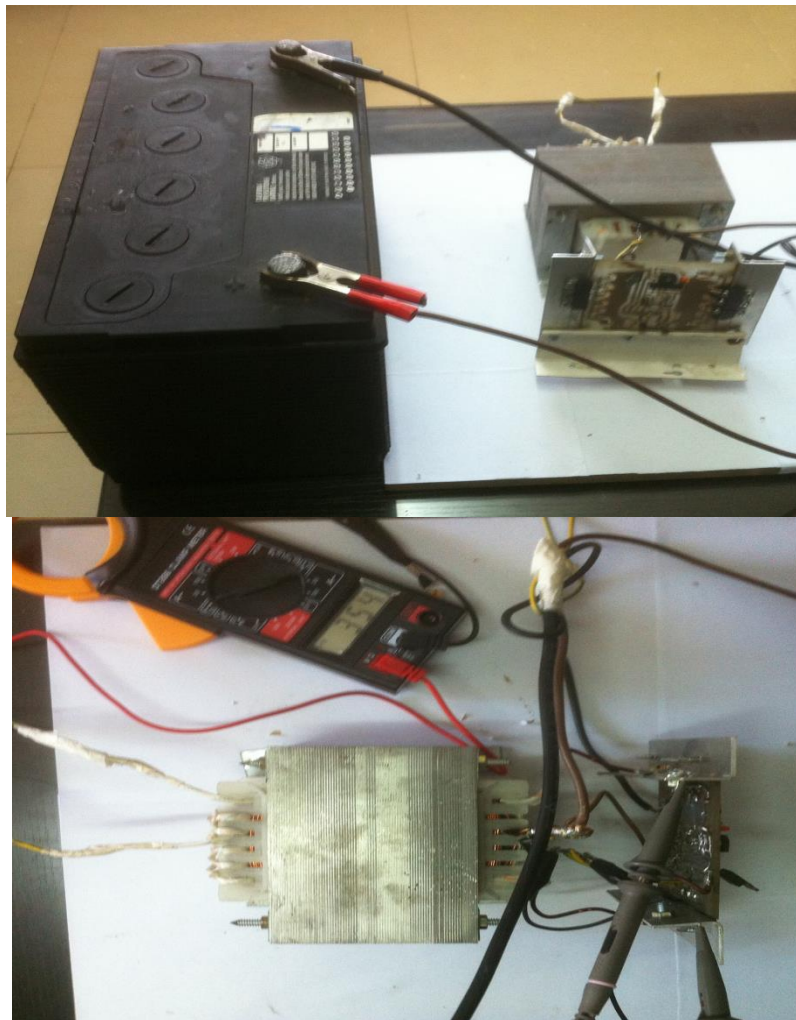


Figure c4 : Testing of push pull converter

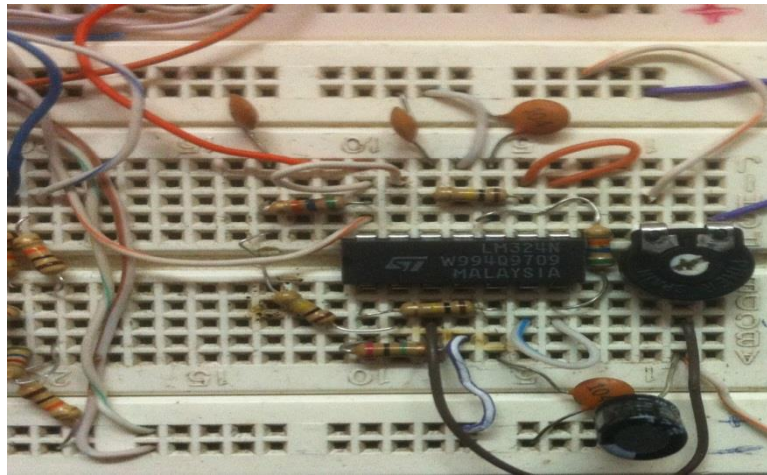


Figure c5 :Bubba oscillator

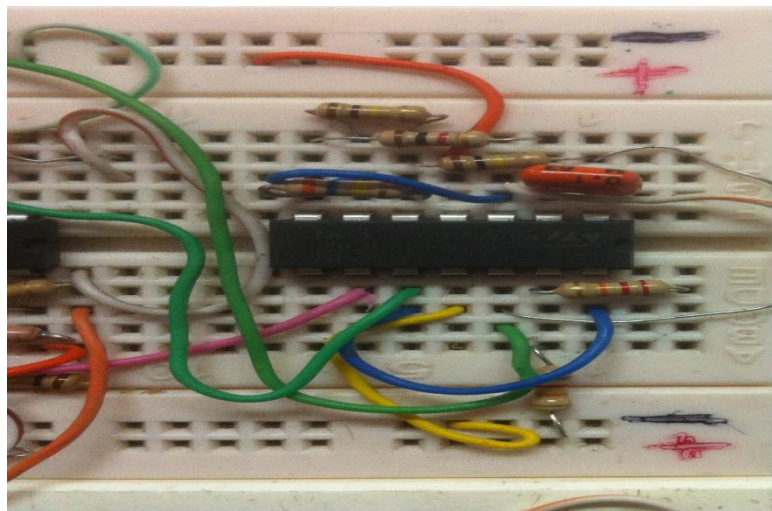


Figure c6: Traingulatre carrier generator

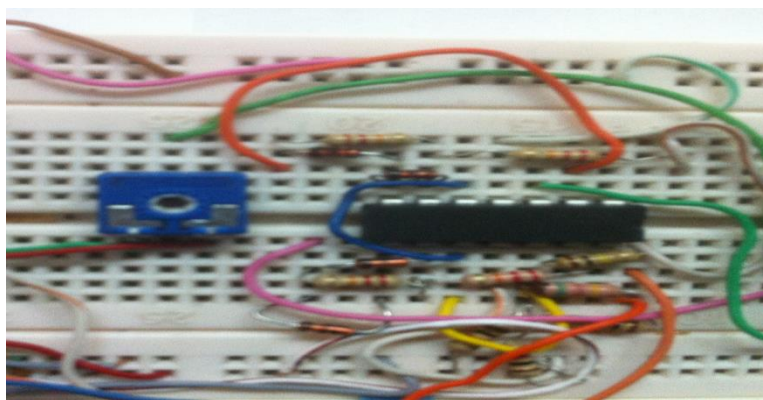


Figure c7: comparator circuit for reference and carrier signal



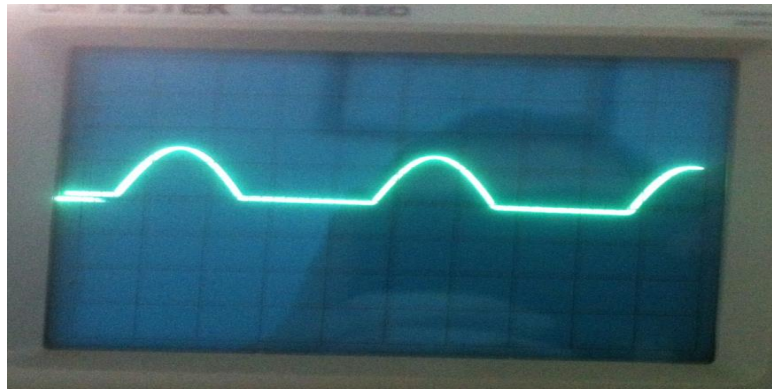


Figure c8: Half wave of reference signal

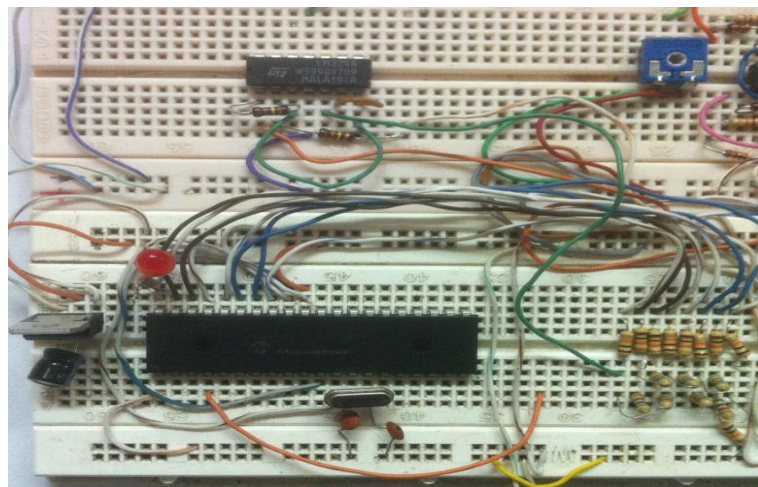


Figure c9: The controller circuit using PIC16F877A

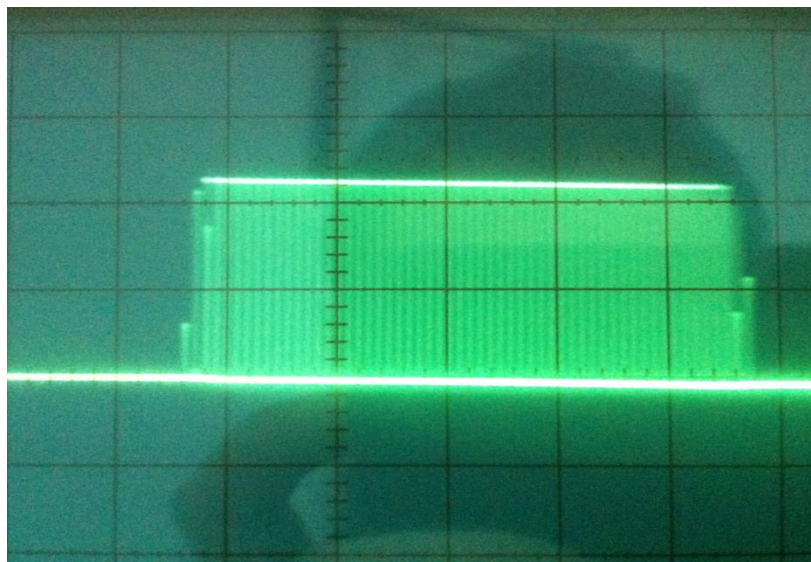


Figure c10: The output pulses generated by PWM generator